



EUROPEAN  
COMMISSION

European  
Research Area

# Prediction and monitoring of subsidence hazards above coal mines (Presidence)



Research Fund  
for Coal & Steel

## Interested in European research?

**RTD info** is our quarterly magazine keeping you in touch with main developments (results, programmes, events, etc.). It is available in English, French and German. A free sample copy or free subscription can be obtained from:

Directorate-General for Research and Innovation  
Information and Communication Unit  
European Commission  
1049 Bruxelles/Brussel  
BELGIQUE/BELGIË  
Fax +32 229-58220  
E-mail: [research@ec.europa.eu](mailto:research@ec.europa.eu)  
Internet: <http://ec.europa.eu/research/rtdinfo.html>

EUROPEAN COMMISSION  
Directorate-General for Research and Innovation  
Research Fund for Coal and Steel Unit

*Contact: RFCS publications*

*Address: European Commission, CDMA 0/178, 1049 Bruxelles/Brussel, BELGIQUE/BELGIË*

*Fax +32 229-65987; e-mail: [rtd-steel-coal@ec.europa.eu](mailto:rtd-steel-coal@ec.europa.eu)*

# Research Fund for Coal and Steel

## Prediction and monitoring of subsidence hazards above coal mines (Presidence)

C. Herrero, A. Muñoz

**Geocontrol**

Cristóbal Bordiú 19–21, 5º, 28003 Madrid, SPAIN

J. C. Catalina

**Aitemin**

Margarita Salas 14, Parque Leganés Tecnológico, Leganés, 28919 Madrid, SPAIN

F. Hadj-Hassen

**Armines**

Boulevard Saint Michel 60, 75272 Paris, FRANCE

R. Kuchenbecker

**DMT**

Am Technologiepark 1, 45307 Essen, GERMANY

V. Spreckels

**RAG AG**

Shamrockring 1, 44623 Herne, GERMANY

J. Juzwa

**Instytut Technik Innowacyjnych EMAG**

Ulica Leopolda 31, 40-189, Katowice, POLAND

S. Bennett, M. Purvis

**Mines Rescue Service Ltd**

Leeming Lane South, Mansfield Woodhouse, Mansfield, NG19 9AQ, UNITED KINGDOM

D. Bigby

**Golder Associates UK Ltd**

Attenborough House, Browns Lane Business Park, Stanton on the Wolds, NG12 5BL, UNITED KINGDOM

D. Moore

**UK Coal Mining Ltd**

Blyth Road, Harworth, Doncaster, DN11 8DB, UNITED KINGDOM

Contract No RFCR-CT-2007-00004

1 July 2007 to 30 June 2010

**Final report**

Directorate-General for Research and Innovation

## LEGAL NOTICE

Neither the European Commission nor any person acting on behalf of the Commission is responsible for the use which might be made of the following information.

***Europe Direct is a service to help you find answers  
to your questions about the European Union***

**Freephone number (\*):  
00 800 6 7 8 9 10 11**

(\* Certain mobile telephone operators do not allow access to 00 800 numbers or these calls may be billed.

A great deal of additional information on the European Union is available on the Internet. It can be accessed through the Europa server (<http://europa.eu>).

Cataloguing data can be found at the end of this publication.

Luxembourg: Publications Office of the European Union, 2012

ISBN 978-92-79-22246-7

doi:10.2777/3356

ISSN 1831-9424

© European Union, 2012

Reproduction is authorised provided the source is acknowledged.

*Printed in Luxembourg*

PRINTED ON WHITE CHLORINE-FREE PAPER

# TABLE OF CONTENTS

<b>1.</b>	<b>FINAL SUMMARY .....</b>	<b>5</b>
1.1.	PREDICTION OF SURFACE AND SUBSURFACE SUBSIDENCE.WP1.....	5
1.1.1.	<i>Prediction of subsidence caused by coal exploitations. WP1.1.....</i>	5
1.1.2.	<i>Prediction of subsidence caused by underground infrastructures. WP1.2.....</i>	5
1.2.	MONITORING AND CONTROL OF SUBSIDENCE EFFECTS ON SURFACE. WP2. ....	7
1.2.1.	<i>Geometrical monitoring tools.....</i>	7
1.2.2.	<i>Seismic and GPS monitoring tools .....</i>	7
1.2.3.	<i>Surface monitoring of shafts stability.....</i>	8
1.3.	RISK MANAGEMENT OF SUBSIDENCE HAZARDS ON SURFACE. WP3 .....	8
1.3.1.	<i>Integrated monitoring at surface.....</i>	8
1.3.2.	<i>Detection of hazardous areas at surface .....</i>	9
1.3.3.	<i>Validation and verification of results .....</i>	9
1.4.	PROJECT ASSESSMENT AND CONCLUSIONS. WP4 .....	10
1.4.1.	<i>Review of all techniques in the light of mining experience.....</i>	10
1.4.2.	<i>Evaluation and application of techniques to other areas .....</i>	10
<b>2.</b>	<b>SCIENTIFIC AND TECHNICAL DESCRIPTION OF THE RESULTS .....</b>	<b>11</b>
2.1.	OBJECTIVES OF THE PROJECT .....	11
2.2.	COMPARISON OF INITIALLY PLANNED ACTIVITIES AND WORK ACCOMPLISHED .....	11
2.2.1.	<i>Bar chart comparing actual situation with initial planning .....</i>	11
2.2.2.	<i>Major Deviations and their effects in the project.....</i>	12
2.3.	DESCRIPTION OF ACTIVITIES AND DISCUSSION .....	15
2.3.1.	<i>Prediction of surface and subsurface subsidence. WP1.....</i>	15
2.3.2.	<i>Monitoring and control of subsidence effects on surface. WP2. ....</i>	59
2.3.3.	<i>Risk Management of subsidence hazards on surface. WP3.....</i>	80
2.3.4.	<i>Project assessment and conclusions WP4.....</i>	95
2.4.	CONCLUSIONS .....	114
2.4.1.	<i>Prediction of surface and subsurface subsidence WP1.....</i>	114
2.4.2.	<i>Monitoring and control of subsidence effects on surface WP2. ....</i>	115
2.4.3.	<i>Risk management of subsidence hazards on surface WP 3. ....</i>	116
2.4.4.	<i>Project Assessment and conclusions WP 4.....</i>	117
2.2.	EXPLOITATION AND IMPACT OF THE RESEARCH RESULTS.....	117
<b>3.</b>	<b>LIST OF FIGURES AND LIST OF TABLES.....</b>	<b>117</b>
<b>4.</b>	<b>LIST OF REFERENCES .....</b>	<b>121</b>
<b>2.</b>	<b>GLOSSARY .....</b>	<b>126</b>
2.1.	ABBREVIATIONS.....	126
2.2.	SYMBOLS USED IN EQUATIONS.....	126
<b>6.</b>	<b>APPENDICES .....</b>	<b>128</b>
6.1.	MONITORING AND CONTROL OF SUBSIDENCE EFFECTS ON SURFACE.WP2 .....	128
6.1.1.	<i>Geometrical monitoring tools.....</i>	128
6.1.2.	<i>Seismicity monitoring tools .....</i>	128
6.1.3.	<i>Field trials of shaft fill stability sensor.....</i>	128



## **1. FINAL SUMMARY**

### **1.1. PREDICTION OF SURFACE AND SUBSURFACE SUBSIDENCE.WP1**

#### **1.1.1. *Prediction of subsidence caused by coal exploitations. WP1.1***

##### **1.1.1.1. Prediction of surface deformation**

###### **Prediction of surface deformation**

A comprehensive data base of 669 subsidence case histories from the UK and worldwide was produced. Analysis showed geology to be a major factor in surface subsidence. Empirical predictions, such as the Subsidence Engineers Handbook (SEH) and its computerised version (MULPAN), are inaccurate where experience is lacking and geology unusual. Geomechanical subsidence models, using FLAC 2D, were built and tested against two case histories from the Selby coalfield. They successfully predicted maximum subsidence taking account of inter-burden geology but were not able accurately to reproduce the measured subsidence profile using the constitutive models available without predefinition of subsided and non subsided strata.. Work under a later Task showed that anisotropic models are required if the subsidence profiles are to be reproduced.

###### **Influence of water in surface and sub-surface subsidence problems**

A detailed analysis of the surface subsidence due to mining and subsequent reactivation on flooding followed by minor uplift was undertaken for several coalfields including the recently closed Lorraine coalfield in France. Uplift after flooding was shown to be a real phenomenon but it is unlikely to result in surface damage. Previous to the laboratory testing of the effect of water on the geomechanical properties of argillaceous rocks was reviewed for incorporation into subsidence models. A coupled geomechanical-hydrological model was developed which could simulate a full subsidence history through mining, potential reactivation on flooding and subsequent uplift due to swelling and pore pressure. It was concluded that a simplified, non-coupled approach is adequate for most cases.

Statistical analysis of recent and historical UK case studies of water inflows to working longwalls. These studies provided a good prediction function based upon the maximum aggregate tensile strain at the base of the potential water source according to the 1966 Subsidence Engineer's Handbook (Disturbance index) and the panel width to height ratio.

Large scale modelling can also be useful. Limiting panel width to comply with the prediction function was shown to be effective in avoiding water inflows provided the potential water sources can be accurately identified.

###### **Prediction of sub-subsurface deformation**

Analysis of a range of case studies of recent experience with locating longwall panels above old workings indicated that previous guidelines were inappropriate for rockbolted gate roadways and face lines. New guidelines were developed and are described in Deliverable 1.1.6. A combination of three dimensional boundary element (MAP3D) for stress analysis and detailed three dimensional finite difference (FLAC3D) roadway models for reinforcement design, employing the Hoek Brow rockfailure and the GSI to account for rock condition depending upon roadway location within the subsidence trough, can be used for analysing such problems. A series of models was developed for UK coal seams where such workings are planned and these will now be applied for detailed layout and support design.

#### **1.1.2. *Prediction of subsidence caused by underground infrastructures. WP1.2***

##### **Shafts survey using innovative geophysical tools**

This task focussed on survey techniques such as dynamic laser, inertial measurement techniques and telemetry instrumentation, considering the existing difficulties in the access to the shaft walls.

A system to investigate telemetry and data-logging in the context of a remote monitoring system for disused mineshafts with a view to obtaining a warning of surface subsidence events based on the principles of reduced power consumption and GPRS data transmission was developed for use with a specially designed shaft-fill stability (SFS) sensor. The overall system design objectives concentrated on providing a simple but robust monitor of shaft-fill stability, combined with a scalable, web-based transmission system capable of interrogating a large number of potential shaft sites.

An initial scoping exercise relative to development of effective techniques for use in water-filled abandoned shafts with potentially turbid media determined the areas for further research. Many of the techniques reviewed were discounted on technical and high cost. A programme of experimental work, based on the most promising technologies consistent with sufficiently low cost for adoption in the field designed to establish incremental improvements to optical imaging was not able to demonstrate any appreciable benefits over the current generation of CCTV equipment. Even the best combinations of techniques were generally not capable of providing an acceptable optical image over a range of much more than a metre even in only slightly turbid water.

At the beginning a survey campaign of shaft, Lohberg 1', using a 3D-Laserscanner was carried out. The work undertaken shows the feasibility of shaft measurement by laserscanning in accessible shafts with guided hoist cages, using a 3D-scanner and a 'Stop & Go'- measurement strategy. Considering that future shaft measurements partially can only be performed in non-accessible shafts with explosive atmosphere, the aim modified to develop a new kinematic measurement system integrating a 2D-Laserscanner ('Profiler'), an inertial measurement unit and other sensor units.

Current monitoring tools and infrastructure for shaft monitoring have been reviewed. The proper motions of a carriage system for a laser scanner have been determined with a survey campaign. Additional sensors for collision detection and online supervisory have been identified. Work on the laserscanner system included necessary construction details on the components of the system including the profiler, the inertial measurement unit, the power supply, data storage, interfaces, data processing and control unit.

Careful consideration had to be given to fulfil the requirements of explosion-proofness. The design process, especially the mechanical and electrical construction has to be accompanied by German regulatory authorities, hence resulting in a time consuming iterative process until certification. Interactions between profiler and the other system components have to be synchronised and coordinated. In parallel the setup and test of internal components has been carried on.

### **Roadway survey using innovative geophysical tools**

In this task the research that was carried out was relative to the development of an inspection methodology based on visual inspection of roadways. Also a review of the applicable geophysical non destructive methods was done with special dedication to laser-scanner techniques (Ground Penetrating Radar, Sonic Methods, Geoelectrical methods and Tunnel Scanner), and a review of its capabilities was done in relation with an inspection carried out in a tunnel.

In particular the following tools are presented:

#### **GPR-3D**

The GPR Works by emitting into the ground an electromagnetic pulse and picking up through an antenna the rebound from the emitted signal when it reaches an anomaly in the dielectric properties of the medium in which it travels.

This system allows to detect anomalies in the filling of he tunnels or in the ground where they have been excavated.

In order to verify the advantages of this method, they have been carried out in the Tunnel of Archidona (Malaga, Spain), through 3D technology, which has revealed that the results provided by the GPR-3D system are more precise than the traditional GPR, providing high reliability for the detection of existing

voids in the ground until a depth of about 10m.

### **Effect of mine water on concrete, reinforced concrete and fill materials**

This task provided further information for shaft surveys as it aimed to identify the adverse effects of mine water. As a complement to Tasks 1.2.1 and 1.2.3, the effect of water in concrete and fill material and its influence in shaft and roadway collapses was analysed. This included a study of the adverse effects of mine water pollutants on fill materials and supports; including lab tests and other one about the methods to neutralise the adverse effects of mine water pollutants on fill and infrastructure.

Analysis of historic data relative to mine shaft collapse in the United Kingdom indicates over 80% of incidents relate to mine shafts abandoned in excess of 50 years ago and are less than 100m depth.

Long term immersion tests indicate degradation to both construction and shaft fill materials from aggressive mine waters which could reduce the competency of the shaft lining material and reduce the volume of fill in the shaft so as to create a void with potential for collapse.

Following prolonged immersion in an aggressive mine water concrete samples treated with available waterproofing solutions resulted in both water penetration and pitting to the surface of the samples. Material losses from the samples averaged 4 – 6.3%. Research has indicated the potential for alternative and innovation solutions to cementations grouting and use of admixtures in producing dense, impermeable and durable concrete along with non steel reinforcement reducing potential for degradation and corrosion to permanent shaft capping structures.

A “flash fill” material suitable for the stabilisation of shaft fill material, especially in cases involving thick unconsolidated superficial deposits was engineered from coarse and fine coal mining waste products.

## **1.2. MONITORING AND CONTROL OF SUBSIDENCE EFFECTS ON SURFACE. WP2.**

### **1.2.1. *Geometrical monitoring tools***

The work was focused on the use of two different tools to monitor the surface condition.

The goal of Aitemin’s work was to develop ground deformation control by high-resolution digital photogrammetry based on a prototype of computer vision system integrating modern high-resolution digital cameras

The performance of that prototype needed first to find appropriate hardware components that meet the assumed requirements for such a system. After selecting the hardware components and completing the designed system prototype, a series of experiments to obtain a digital terrain model derived from analysis of images from two digital cameras have been carried out. Learned and adopted techniques and algorithms for image analysis was used to produce maps of disparity and digital terrain model based on pairs of images and a set of pairs of images.

The goal of EMAG’s work consisted in the analysis of pairs of images distant in time of the area monitored in the task 2.2, derived from satellite interferometry technique, to assess the usefulness of this technique as a tool to support observation of the subsidence process. Seven scenes of surface above the monitored longwall have been acquired: three from time before the selected longwall excavation and four from time of the mining progress. On the base of carried out analysis, the conclusions regarding the usefulness of this technique for observing subsidence in mining areas have been reached.

### **1.2.2. *Seismic and GPS monitoring tools***

The work was focused on the development and implementation of a prototype system allowing for a comprehensive assessment of hazards on surface caused by geodetic and seismic processes. The assumed measurements at the selected research area were foreseen to examine the usefulness of developed tools and applied methods.

The effect of the accomplished work is the prototype of the system for monitoring hazards on surface based on constant measurements of positions and seismic signals of vibrations, recorded by GPS receivers and 3D vibration acceleration sensors, collected at local surface data concentrators, The measurements are supplemented by periodical surveys of position at other points increasing density of the measurement network covering the observed area. The system, except the monitoring function, enables - on the basis of developed mathematical models, prediction of surface behaviour and hazards that may arise in effect of mining activity. Implementation of the system in a selected area of research permitted for about 10 months of the testing period. Analysis of data collected under the real conditions proved the usefulness of the developed system for its use by mines and owners of grounds located in mining areas.

The work performed in the task included also search for the expected relationship between geodetic and seismic processes observed on surface as the result of mining. Due to the very small amount of seismic data, the obtained results should be considered as hypotheses encouraging to further work in that matter with the use of a more modern new generation equipment.

### **1.2.3. *Surface monitoring of shafts stability***

This task aimed to determine the effectiveness of the techniques studied in tasks 1.2.1 and 1.2.3. The two main aims were to carry out field trials with the developed monitoring and telemetry instrumentation, and to develop effective techniques in water filled shafts with potentially turbid media, investigating the use of high resolution pulse-echo ultrasonic imaging.

The initial field trials of the shaft fill monitor and associated custom-designed low-power data logger and a GPRS transmitter telemetry system have not indicated any serious problems. The trials have indicated that a ‘twin’ set of LiFeS<sub>2</sub> cells should last for 15 years and use of standard antennas would be adequate to achieve the coverage required. The overall design concept was based on minimisation of risks from corrosion and biological activity although in practical terms some issues would not become apparent for some time.

Research and on-site evaluation has indicated that Ultrasonic scanning provides a means of inspecting the linings of mine shafts, flooded with turbid water, in which optical inspection is often ineffective. Although the Ultrasonic Scanning evaluation was successful as a proof of concept, several peripheral aspects will require addressing before this can be considered a practical solution for deployment in the field. Whilst the resolution of the system is adequate to detect salient features it is often not possible to unambiguously identify a feature in a scan. Therefore, except in the case of severe deterioration of the lining, which will often be clearly obvious, it is probably better to consider ultrasonic scanning as a tool for detecting changes in the condition of a shaft by comparing the results with those obtained on a previous occasion.

## **1.3. RISK MANAGEMENT OF SUBSIDENCE HAZARDS ON SURFACE. WP3**

### **1.3.1. *Integrated monitoring at surface***

RAG’s runs the GeoMon Database (GeoMon-DB) in day-to-day business and continues the maintenance, updating and special analysis of terrestrial and remote sensing data.

Data from project partners like DMT, EMAG and AITEMIN have successfully been integrated into the GeoMon-DB. For instance for DMT the laserscanner data of a shaft measurement could be attached to the shaft coordinates as a “BLOB” (Binary Large Object). EMAG selected and prepared point measurements of terrestrial GPS campaigns for RAG’s GeoMon-DB that could successfully be integrated. The integration of EMAG’s seismic data was non-scheduled. AITEMIN provided stereo-photogrammetric point measurements (matched points and derived grid points) from two measurement campaigns of AITEMIN’s laboratory test site.

The suitability and the limitations for the use of SAR interferometric methods DInSAR and PSI have

been determined for the satellites ENVISAT, ALOS and TerraSAR-X. All results gained by the comparison of terrestrial and remote sensing radar data sources will be described in the following chapters.

### **1.3.2. *Detection of hazardous areas at surface***

RAG was able to confirm ground movements detected by terrestrial measurements with movements derived from remote sensing data by comparison in RAG's GeoMon-DB. Damages caused by active mining beneath a discontinuity could be separated from notifications of claim from beyond this discontinuity. An area with up to then unknown uplifts due to the flooding of an abandoned mine out of RAG's responsibility has been detected and verified.

To quantify the hazardous areas at surface MRSLS has focused on the evaluation of the potential risks that present the abandoned mineshaft; while ARMINES, EMAG and GEOCONTROL have worked on methods to defined and evaluate the hazardous areas at surface.

The first part of the studies carried out has justified the need of adopting control measures in the areas of abandoned mines.

Factors other than construction / fill related contributing to mine shaft collapse are considered to be:

- Depth of Workings <100m – 86% on incidents
- Time from abandonment >50years – 80% of incidents >100years 40%
- Unconsolidated Superficial deposits >20%
- Changes in Ground Temperature / Rainfall.

In a complementary manner, this study provides a risk scale to assess the probability of surface damage, in order to allow intervention strategies in mining areas.

A very important factor related to hazards in mining areas is estimation of a damage occurrence risk due to surface deformation.

The chosen method of measuring risk value depends on a type of the analysed risk. The damage is estimated by:

- probable damage value,
- maximum damage value.

A determination of probability seismic event occurrence primarily depends on the analysis of similar past cases of damages and refers to:

- number of preceding events, which were followed by a damage – historical data,
- a damage as result of risk,
- determination of distribution's quantile empiric value for adequate confidence level.

The second part of the studies carried out, have allowed to develop a calculation methodology based on geomechanical models, aimed to establish a prevision of surface subsidence caused by mining galleries or in general underground works, including a specific study of the evolution in time of abandoned mines susceptible of flooding.

The performed works have allowed to establish application criteria to quantify the damage caused by subsidence in buildings located in hazards areas, confirming that methodology with a practical example based on the analysis of subsidence in a stretch of the Tunnel of Elche (Alicante, Spain).

### **1.3.3. *Validation and verification of results***

By comparing different measurement methods in the GeoMon-DB it is possible to make reliable

statements about the inner accuracy as well as checks and balances of the used systems to state their applicability. When the measurement intervals are densely enough the natural movement behaviour of the earth surface can be assessed and separated from mining or flooding induced ground movements.

In order to verify the validity of the methodology based on 3D models to estimate the subsidence caused by the roadways and tunnels excavated near the surface an exercise was performed in a stretch of the Tunnel of Archidona (Malaga, Spain), focusing the exposure on a section excavated in Marl with low overburden (less than 15 m) in which there was a limitation of vertical moments on the surface to prevent the affection to a tower of high voltage power line.

The ground on which the excavation was going to take place is made of marl, which are very weathered in the proximity of the surface.

To perform this study it was considered important to consider that these grounds correspond to the so-called “soft rock” type, which is characterized for losing an important part of their resistance in the post-break phase, i.e. when the strain they undergo exceeds their maximum resistance. In terms of numerical modelling this behaviour of the ground makes necessary to change the classical constitutive model “Mohr-Coulomb” for a “Strain-Softening” type, which takes into account the modifications in the terrain resistance as they increase their deformations.

In this case, it was also considered essential to make variations depending on the terrain deformation and therefore a specific routine was established, integrated into the FLAC 3D software.

In surface, coinciding with the axis of the tunnel, five milestones were placed for the topographic control of the ground movements.

With the assumptions made, the displacements estimated with the calculation model, reached a maximum deviation of 18,2 % from the values measured during the excavation of the Tunnel on the milestones set in surface, this confirms the validity of the calculation methodology of subsidence developed at this point.

#### **1.4. PROJECT ASSESSMENT AND CONCLUSIONS. WP4.**

##### **1.4.1. Review of all techniques in the light of mining experience.**

In chapter 2.3.4.1 of this Final Report, the review of all techniques developed in this project, has been completed. The review includes project assessments and conclusions of the whole project. Taking into account that summarizes a summary probably has non sense and to avoid duplication of text, the content of this task is completed in the chapter before mentioned.

##### **1.4.2. Evaluation and application of techniques to other areas.**

In chapter 2.3.4.2 of this Final Report, the evaluation and application of techniques to other areas, has been completed. The evaluation includes project assessments of the whole project and a very graphic table which includes the possible applications for the methods developed in the project. To avoid duplication of text, the content of this task is completed in the chapter before mentioned.

## **2. SCIENTIFIC AND TECHNICAL DESCRIPTION OF THE RESULTS**

### **2.1. OBJECTIVES OF THE PROJECT**

There are three main general objectives in this research:

- i) to improve the understanding of the mechanics of mining subsidence regarding the prediction of its occurrence.
- ii) To apply innovative tools in the monitoring of surface subsidence.
- iii) To use the results of the predictions and monitoring of mining subsidence as a tool for a better, safe and accurate land management above closed mines or following active coal mining.

These general objectives were achieved because the following specific objectives were reached:

- i) For subsidence prediction
  - to develop improved tools for predicting the effects of subsidence on rock matrix itself, using 2D and 3D numerical modelling,
  - to develop a methodology for assuring surface deformation due to water rebound in mines,
  - to develop innovative and cost effective techniques for roadways support surveying and its influence in subsidence,
  - to develop innovative techniques for shaft surveying and modelling and a methodology for the prediction of shaft movements,
  - to develop a method to neutralise adverse effects of mine water on mine fill and support, and finally,
  - to develop and implement a shaft and gallery collapse prevention methodology.
- ii) For subsidence monitoring
  - to built a prototype for ground deformation control combining the surveying and photogrammetric techniques by processing images captured from digital cameras attached to motorised theodolites,
  - to register all the 3D movements induced by mining at surface in an uniform fashion, supported by a multisensor concept,
  - to develop an advance measuring system for seismicity and deformation at surface, including traixial sensors synchronized with GPS and INSAR data, and
  - to develop a cost effective in situ shaft monitoring and telemetry system.
- iii) For land management
  - to create an information system for mantenining the raw data and the results of GIS-supported analysis and evaluation of subsidence, and
  - to create an information system for interpretation of subsidence monitoring data, including deformation, INSAR and seismicity data.

### **2.2. COMPARISON OF INITIALLY PLANNED ACTIVITIES AND WORK ACCOMPLISHED**

#### **2.2.1. Bar chart comparing actual situation with initial planning**

PROGRAMME BAR CHART (TASK, PARTNER, DELIVERABLES, MILESTONE)														
Work Packages	Work Packages ' title	Deliverables	1st Year				2nd Year				3rd Year			
			I	II	III	IV	I	II	III	IV	I	II	III	IV
<b>WP 0</b>	Co-ordination, reporting and dissemination													
Task 0.1	Project co-ordination	-												
Task 0.2	Project management and control	D.0.1/D.0.3												
Task 0.3	Communication and dissemination	D.0.2												
<b>WP 1</b>	Prediction of surface and subsurface subsidence													
WP 1.1	Caused by coal exploitations													
Task 1.1.1	Prediction of surface deformation	D.1.1.1												
Task 1.1.2	Prediction of surface deformation due to water rebound	D.1.1.2 / D.1.1.3 / D.1.1.4												
Task 1.1.3	Prediction of subsurface deformation	D.1.1.5 / D.1.1.6												
WP 1.2	Caused by underground infrastructures													
Task 1.2.1	Shafts survey using innovative geophysical tools													
Task 1.2.2	Roadway survey using innovative geophysical tools	D.1.2.3 / D.1.2.4												
Task 1.2.3	Effect of mine water on concrete, reinforced concrete and fill materials	D.1.2.5												
<b>WP 2</b>	Monitoring and control of subsidence effects on surface													
Task 2.1	Geometrical monitoring tools	D.2.1												
Task 2.2	Seismic and GPS monitoring tools	D.2.2												
Task 2.3	Surface monitoring of shafts stability	D.2.3 / D.2.4												
<b>WP 3</b>	Risk management of subsidence hazards on surface													
Task 3.1	Integrated monitoring at surface	D.3.1												
Task 3.2	Detection of hazardous areas at surface	D.3.2												
Task 3.3	Validation and verification of results	D.3.3												
<b>WP 4</b>	Project assesment and conclusions													
Task 4.1	Review of all techniques in the light of mining experience	D.4.1												
Task 4.2	Evaluation and application of techniques to other	D.4.2												
Task 4.3	Final Report	D.4.3												

Planned   
Done 

Reporting Period (01/07/07 - 30/06/10) 

## 2.2.2. Major Deviations and their effects in the project

### 2.2.2.1. WP1. Prediction of surface and subsurface subsidence

#### WP1.1. Prediction of Surface and subsurface subsidence caused by coal exploitations

The surface subsidence modelling under Task 1.1.1 was delayed for approximately 6 months due to the time taken to set up a subcontract with Nottingham University to undertake this work. This did not interfere with progress on the other Tasks. Based on the advice of the TGC1 Committee, following the

first six monthly report, the originally planned laboratory testing of the effects of water on the geomechanical properties of argillaceous strata for Task 1.1.2 was not undertaken by ARMINES. Instead they assessed previous work and concentrated their resources on a more comprehensive analysis of the subsidence history of the Lorraine coalfield pre and post mining.

The FLAC modelling and case study statistical analyses undertaken for water inflows to longwalls under Task 1.1.2 took considerably longer than originally expected, due to the complexity of the data and difficulties in identifying the required variables from the more historic case studies. Eventually the detailed statistical analyses had to be undertaken on only the more recent case studies where better data was available. This resulted in more man power resources being used than had been planned. Similarly the analysis of data and the FLAC3D back analysis of the experiences of working above old goafs at Welbeck colliery took longer than expected. This meant that there was insufficient time or resources to undertake the intended modelling of the planned Thoresby Deep Soft workings using the models developed from the Welbeck back analysis. This work is currently being undertaken outside the framework of the Project.

### **WP1.2. Prediction of Surface and subsurface subsidence caused by underground infrastructures**

- **Shafts survey using innovative geophysical tools**

The activities undertaken by MRSL proceeded as planned and fulfilled the Task Objectives. There were no deviations that affected the project.

DMT carried out a laser scanner survey campaign with existing static 3d-technique in a disused shaft. The results gave useful hints for the new dynamic survey system that DMT has developed in this project. Also the data will be used as reference for future surveys. For the development of a shaft laser scanner two design concepts were elaborated. Results of investigations at the beginning of the project have shown that the quality of the final laser scanner results is fundamentally dependent on the prevention or measurement and processing of the occurring carrier system's proper motions. As the motion dynamics of the whole system cannot fully be predicted by simulations, DMT carried out a campaign of pre-examinations for estimating the magnitude of the motion components which have an effect to the system. Therefore, a shuttle system to carry all the needed sensor components was designed and manufactured. Also the electronics for online surveying and control were built and adapted. The results are used for the dimensioning of the inertial measurement system and for the possibly necessary gyroscopic stabilisation. The results from this survey together with the experience from the laser scanner survey set the basis for the detailed design of a shaft laser scanner. The equipment used in the test, which was performed in a hard coal mining shaft, was subject to permission of the mining authorities, causing a delay of several months. DMT tried to compensate this delay by reorganisation of the foreseen work plan. Consequently Task 2.3 suffered a delay too, because the field trials foreseen require the shaft scanning system in operable state. Another difficulty arose due to unforeseeable lacks in development capacities on side of the chosen profiler manufacturer, leading to delays of several months. Alternatives regarding the profiler manufacturer had to be studied. As a research didn't show satisfying alternatives, the strategy in the cooperation with the profiler manufacturer had to be changed. To minimize the dependence on the manufacturer's development capacities, DMT acquired necessary profiler components to be able to finalize the profiler design and continue the development of the measurement system.

- **Roadways survey using innovative geophysical tools**

The activities undertaken by GEOCONTROL proceeded as planned and fulfilled the Task Objectives. There were minor deviations with the duration of the task that did not affect the the project results.

- **Effect of mine water on concrete, reinforce concrete and fill materials**

The activities undertaken by MRSL proceeded as planned and fulfilled the Task Objectives. There were no deviations that affected the project, except a reasonable delay at the beginning.

#### **2.2.2.2. WP2. Monitoring and control of subsidence effects on surface**

- **Geometrical monitoring tools**

The work undertaken by Aitemin and EMAG was accomplished in accordance to the assumed plan without deviations.

- **Seismic and GPS monitoring tools**

The work undertaken by EMAG proceeded generally according to the foreseen plan. The delay in start of the research area observation due to postponement of the start of the longwall no 10 excavation in 2009, had no influence on the final results of the task. No deviations affected the task termination.

- **Surface monitoring of shafts stability**

The activities undertaken by MRSL and DMT proceeded fulfilled the Task Objectives. There were a delay that has been explained in WP 1.2 that did not affect the the project results.

#### **2.2.2.3. WP3. Risk Management of subsidence hazards on surface**

- **Integrated monitoring at surface**

The work undertaken by DSK, Aitemin and EMAG proceeded as planned and fulfilled the Task Objectives. There were not important deviations that affected the project.

- **Detection of hazardous areas at surface**

The work undertaken in this task proceeded as planned and fulfilled the Task Objectives. There were not important deviations that affected the project.

- **Validation and verification of results**

The work undertaken in this task proceeded as planned and fulfilled the Task Objectives. There were not important deviations that affected the project.

#### **2.2.2.4. WP4. Project assessment and conclusions**

- **Review of all techniques in the light of mining experience**

The work undertaken in this task proceeded as planned and fulfilled the Task Objectives. There were no major deviations that affected the project.

- **Evaluation and application of techniques to other areas**

The work undertaken in this task proceeded as planned and fulfilled the Task Objectives. There were no major deviations that affected the project.

- **Final report**

The present final report has been submitted on time.

## 2.3. DESCRIPTION OF ACTIVITIES AND DISCUSSION

### 2.3.1. Prediction of surface and subsurface subsidence. WP1.

#### 2.3.1.1. Prediction of Surface and subsurface subsidence caused by coal exploitations. WP1.1.

##### 2.3.1.1.1. Task 1.1.1. Prediction of surface deformation

At the outset of the Project, current surface subsidence prediction tools were based upon empirical data through look up tables and simple analytic tools, such as the UK's Subsidence Engineers Handbook (SEH), or the use of influence functions; UKCoal's current tool included a computer program (MULPAN) based upon look up tables derived from the SEH supplemented by alternative empirical data where appropriate. This Task was aimed at investigating the effects of geology on subsidence and whether geotechnical numerical modelling may have the potential to improve upon these empirical methods. Deliverable 1.1.1 provides a full report on the work done and results for this task. It takes the form of a report and electronic database. Incorporation of hydrogeology was addressed in Task 1.1.2.

##### Historic Subsidence Database

The first aspect of the work was to recover, supplement and analyse a database of surface subsidence measurement data from the UK and worldwide. It now comprises 669 cases, with data about. Source Author, Country, Coalfield, Goaf treatment, Seam, No worked faces, Depth  $h$  (m), Width  $w$  (m),  $w/h$  Ratio, Extraction  $m$  (m), Subsidence  $S$  (m),  $S/m$  Ratio, Geological Index (%), Surface Geology,  $E$  Tens (mm/m),  $E$  Comp (mm/m), SEH Case No, Geological comments.

The most complete data set is  $w/h$  ratio and  $S/m$  ratio cases. The least complete data concerns surface maximum strains. The database is available as part of Deliverable 1.1.1 in printed and electronic form.

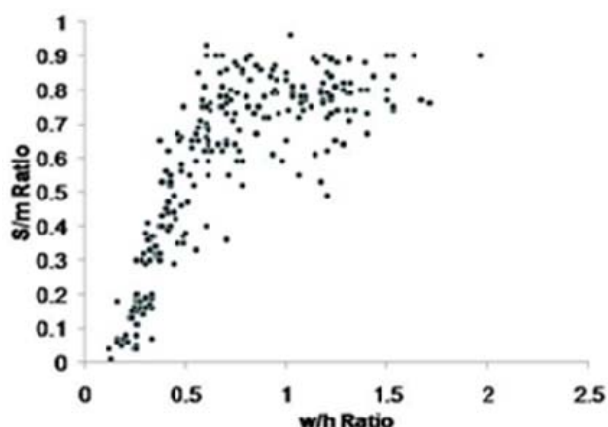


*Figure 2.3.1.1.1-1 w/h ratio against S/m ratio, all UK data*

(Figure 2.3.1.1.1-1) shows a plot of the normalised maximum subsidence ( $S/m$ ) against panel width to depth ratio ( $w/h$ ) for all the UK data set. This shows a broad spread with a general increase in subsidence with  $w/h$  ratio up to a value of  $w/h$  of around 1.0; thereafter subsidence remains fairly constant at a high value. The data is well spread with a maximum error of perhaps  $\pm 30\%$  of  $S/m$ .

##### Numerical modelling of surface subsidence

Previous research was carried out at the University of Nottingham in this field (Reddish 1984, Yao 1992 & Benbia 1995).

The research under this Project includes comparison of numerically calculated subsidence profiles with measured data. UK Coal prepared three detailed case studies comprising data from levelling surveys over recent UK longwall mining operations. Nottingham University developed numerical models of surface subsidence for two of these. The first was taken from above the Barnsley seam at Naburn in North Yorkshire.

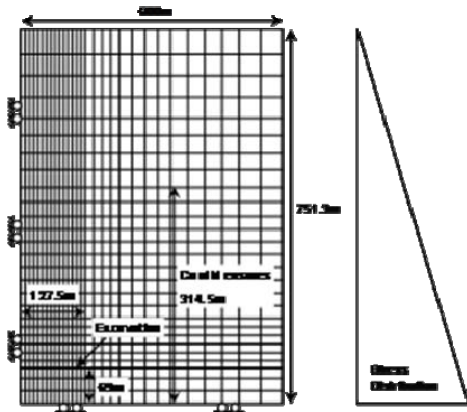


Figure 2.3.1.1.1-2 Schematic of Nabura Model

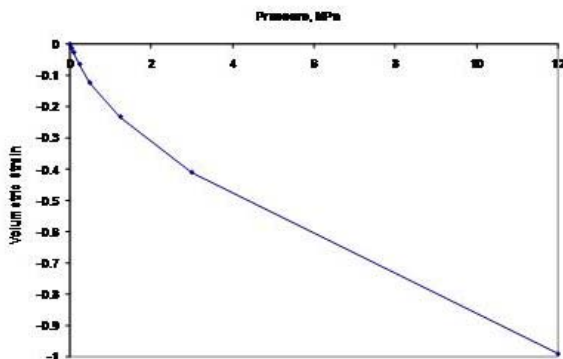


Figure 2.3.1.1.1-3 Pressure/Volumetric Strain Goaf Properties Schematic of Nabura Model

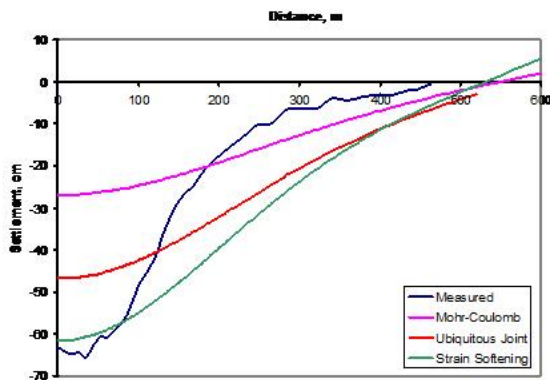


Figure 2.3.1.1.1-4 Surface Settlement Half-Profile

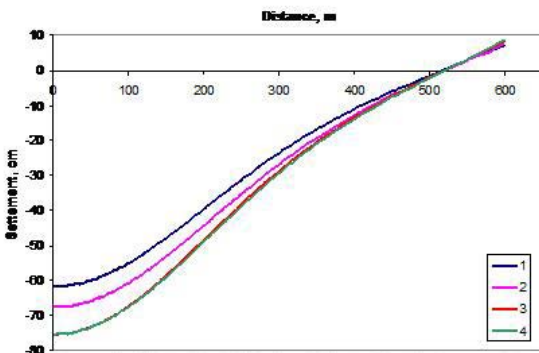


Figure 2.3.1.1.1-5 The Effect of Strain Softening on the Subsidence Profile

A plane strain model and symmetry were used to reduce the size of the rock domain to 600 metres wide and 751.3 metres deep (Figure 2.3.1.1.1-2).

Hydrostatic stress was imposed both on the mesh and the free boundary before excavation. Excavation was simulated by replacing the coal face and a volume of rock directly above the excavation with goaf; the goaf being 3 times excavation height.

Various elasto-plastic failure criteria were used to describe rock behaviour, each being linear elastic (except for that used for goaf). The goaf was modelled using a double yield material. The volumetric-compression goaf properties were constant throughout, as shown in the (Figure 2.3.1.1.1-3). A check showed these caused the goaf height to reduce by 2.5m, approx. 90% excavation height; hence they appear satisfactory.

### Choice of Failure Model

To investigate failure model influence, the deformation and failure parameters were fixed while different failure models were used in the analysis. The failure parameters were decided using the Rock Mass Rating (RMR) system. Based on work by Lloyd et al (1997), the linear relationship between RMR and depth, shown in Equation (2.3.1.1.1-1) and Lloyd et al's modified Serafim and Pereira equation (2.3.1.1.1-2) were used to determine the elastic stiffness used in the model for any given depth.

$$2.3.1.1.1-1 \quad RMR = 4.7143 + 0.0779 \cdot \text{Depth}$$

$$2.3.1.1.1-2 \quad E = 10^{\frac{RMR-10}{40}} - 0.562$$

The results are shown in (Figure 2.3.1.1.1-4). Distance zero corresponds to the excavation centre line and zero gradient across the face is assumed. It can be seen that the strain softening model was able to achieve the measured settlement. Neither the Mohr-Coulomb nor the Ubiquitous Joint models gave a deep enough trough. The widths of the subsidence profiles are much wider than observed. The version of FLAC used in this model series did not allow the combination of both strain softening and ubiquitous joints.

### The Effect of Strain Softening on Surface Subsidence

To investigate the effect of strain softening on the subsidence profile, a number of post failure strength-strain relationships were tested. (Figure 2.3.1.1.1-5) shows the resulting surface settlement profiles. This shows that the rate of post failure softening does not have an effect on the width of the surface subsidence trough. This investigation showed a clear trend between the rate of softening and the depth of the settlement trough particularly at strains of less than 1%.

In these models, the height of the area of plastic deformation was 270 metres above the floor of the excavation (i.e.400 metres below the surface). Also the lateral extension of the plastic zone only affected the depth of the subsidence profile and not its shape.

Further model runs showed that an increase in Poisson’s ratio resulted in a deeper surface subsidence trough but did not affect the width of the surface subsidence profile.

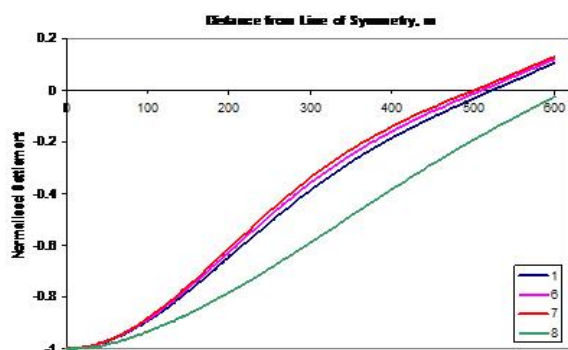


**Figure 2.3.1.1.1-6 Normal Subsidence Profiles**

### Elastic Stiffness

A number of relationships between stiffness and depth were investigated. It was confirmed that this has an effect on the subsidence profile and a linear depth-RMR relationship, as used in the base model, was the most likely to have the ability to achieve the desired trough width without predicting excessive heave. Four linear depth-RMR relationships with varying gradients, including zero, were used to investigate their influence on the subsidence profile. The normalised results are shown in (Figure 2.3.1.1.1-6) which allows investigation of their influence of subsidence trough

width. This shows that increasing the gradient of the depth-RMR relationship for the purposes of calculating the elastic stiffness results in a narrower settlement profile but with increased surface heave.

### A63 Leeds Road FLAC case history

A second subsidence case history, A63 Leeds Road, was modelled using essentially the same methodology as for the Naburn model. The major differences were in the model geometry and use of a later version of FLAC which allowed ubiquitous joints to be incorporated into the strain softening model, giving a better representation of stratified rock. This case was a short longwall face at a shallower depth but within a similar geological environment to Naburn.

The H156 panel modelled was one of a sequence of 12 narrow panel single entry workings undertaken in the Selby coalfield. A plan of the survey line and survey results is included in the appendices to deliverable D1.1.1. The monitored subsidence trough was wider than normally anticipated due to adjacent panels resettling a little after being disturbed by the new working.

In this model, the rock domain was 600 metres wide and 484 metres deep, discretised into a mesh 172 elements wide and 336 elements deep. Three basic model types were compared, Mohr Coulomb, Strain Softening and Strain Softening with Ubiquitous Joint (Subiquitous). All models included stiffness modification with depth and geological layers as appropriate from boreholes. They also include the extended modified goaf region.

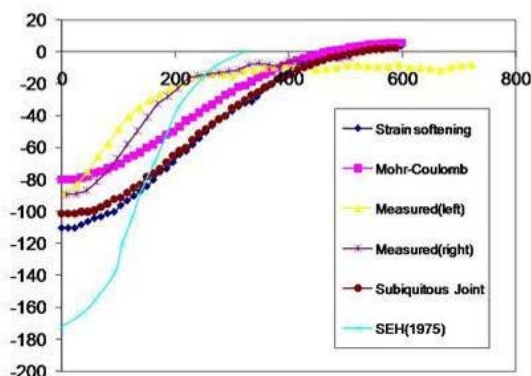


**Figure 2.3.1.1.1-7 Comparison of model subsidence with monitoring**

(Figure 2.3.1.1.1-7) shows the 2 measured half subsidence troughs compared to the 3 chosen models and a Subsidence Engineers Handbook (1975) prediction. The Mohr Coulomb model is close in maximum subsidence but is rather flat in profile and includes heave areas at its margins. The Strain Softening model has a better shape but generally overestimates the subsidence. It also still heaves at its margins as found with case study one. The Subiquitous model has slightly less maximum subsidence than the Strain Softening and has an improved profile at the margin with minimal heave. It is interesting to note the difference in the two measured half profiles plus the extended draw on the left profile as commented on earlier. The Subsidence Engineers Handbook (SEH) prediction overestimates subsidence by a factor of 2 and produces a

significantly narrower profile than measured or predicted. The presence of a strong non Coal Measures layer in the overburden is the main reason for the Subsidence Engineers Handbooks overestimation of Subsidence.

Analysis of the areas of yield in the models confirmed that the narrower face has encouraged early bridging in this circumstance when compared to the previous wider face at Naburn. Also the Strain Softening and Subiquitous models have increased areas of yield over the Mohr Coulomb models due to the introduction of greater weakness through the strain softening action and the introduction of horizontal planes of weakness. In all models, vertical stress shows clear areas of stress relief over the goaf and the building of stress abutments over the solid edges. Horizontal stress patterns are similar but more greatly influence by immediate overburden geology.

### **Conclusions on FLAC modelling**

The models used were relatively sophisticated utilising special techniques to simulate the goaf and altering stiffness properties with depth and strain during yield. The general modelling of the situations was satisfactory with the maximum subsidence of model and monitoring similar, but the measured surface profile was narrower than the modelled profiles.

The introduction of anisotropy to the stiffness of the overburden in modelling by others has been shown to be effective for improving subsidence profile shape. However this can upset the balance between vertical and horizontal ground movements, a good subsidence fit being at the cost of poor horizontal displacement and strain prediction. Also, it is not currently possible to include strain softening and elastic anisotropy for the same elements in a FLAC model, though a mixture of such elements in a model is possible. Thus, the likelihood of an element failing would need to be predetermined when constructing the model, which is undesirable. The basic continuum nature of FLAC appears to extend the subsidence laterally with angles of draw significantly wider than generally reported from the field. The introduction of further structure into the rock mass possibly with strong directional weaknesses would appear to be the best approach to improving the ability to model surface subsidence further. This work has confirmed that sub-surface geology plays a strong role in surface subsidence and that current tools are inadequate in dealing with this. Geotechnical numerical modelling provides a means to account for geology and is better than current empirical methods at determining maximum subsidence in non typical geology. However further development is required to obtain reliable subsidence profiles and no account of the influence of water has been taken in this FLAC modelling approach.

#### **2.3.1.1.2. Task 1.1.2. Influence of water in surface and subsurface subsidence problems**

The first aspect of this task aimed at understanding the mechanisms governing the behaviour of the surface when closing and flooding coal mines in order to establish comprehensive models and rules for prediction and safe post-mining management. This part of the work programme had four main phases as set out below (also showing the relevant Project Deliverables):

1. Analysis of flooded European sites in order to identify the phenomena and the parameters governing the behaviour of the surface **(D1.1.2)**.
2. Reviewing the experimental and theoretical work on the effect of water on the mechanical behaviour of argillaceous rocks which are commonly encountered in coal mines **(D1.1.3)**.
3. Elaborating a comprehensive approach capable of describing the behaviour of the surface of a caved coal mine during the different stages of its life **(D1.1.4)**.
4. Application and validation of the developed approach on a selected site and definition of rules and guidelines for the assessment of the surface behaviour **(D1.1.4)**.

### **Review of the European flooded colliery basins**

Longwall mechanics were reviewed in order to understand the movements of the surface during the mining operations and the behaviour during water rebound. Suitable laws were selected to assess the

extension of the caved zone as well as the maximum subsidence and its profile. These laws were used to evaluate the residual porosity after subsidence stabilisation and before the beginning of flooding.

Four European sites of closed and flooded coal mines were selected in order to study the behaviour of the surface during and after the flooding phase: Limburg in Netherlands, Zwickau-Oelsnitz in Germany, Blanzky and Faulquemont in France. The most important points can be summarised as follows:

- All cases indicated heave after flooding. Other cases are quoted in the literature with the same phenomenon (Liege basin, Belgium, Rhur basin, Germany). No surface damage was observed.
- The main feature of all sites was argillaceous rock in the seam overburden (shales/mudstones).
- No reference mentioned reactivation of subsidence during flooding.
- The profile of ground level uplift is virtually congruent with that of subsidence, the point of maximum uplift correlating with the point of maximum subsidence. The uplift was 3 to 4% of subsidence. Uplift continued to occur beyond the flooding phase but with very low amplitude.
- Subsidence due to coal mining is relatively rapid. It occurs at a speed of several centimetres per day. However, uplift, due to rising mine water, has a large radius of curvature with slow, weak amplitude. This considerable difference in rate has a crucial impact on the severity of damage.

In conclusion, all the analysed sites showed that uplift is a governing phenomenon of the surface behaviour during flooding.

### **The Lorraine colliery basin**

The Lorraine colliery basin can be divided into three major sectors: the West sector defined by la Houve, the Central sector defined by Reumaux and Vouters and the East sector defined by Simon and Wendel. Unlike the flat areas exploited with longwall mining, the Vouters area corresponds to steep coal seams which have been mined by the cut and fill method. Flooding of the basin was carried out in several phases. At the beginning (November 2001), only the workings below 500m from the surface in the West sector (Vernejoul field) were flooded. Pumping continued until 2006 when the decision was taken to flood the whole basin.

The most important conclusions derived can be described as follows:

- Subsidence reactivation during flooding is a real phenomenon occurring when the water table reaches the caved area. It is mainly due to the rocks' sensitivity to water and rearrangement of the equilibrium found after residual settlement. The amount of reactivated subsidence is very low (few percent of the initial settlement) and presents no risk to surface stability.
- If caving did not occur properly during the mining phase, flooding may reactivate the process and may lead to higher values of subsidence (e.g. for panels 15 and 7 of the sector West, nearly 11.5 and 16 % of maximum subsidence respectively).
- Resettlement is followed by an uplift phase, due to dilation of the caved rock reservoir under pore water pressure. The surface uplift appears to increase with the water table rise.
- As for the reactivated subsidence, the uplift is small and has no effect on surface stability. (see Figure. 2.3.1.1.2-1).
- Where levelling frequency is limited, resettlement may be hidden by the uplift. (Figure 2.3.1.1.2-2) shows an illustration of this situation.
- No resettlement was observed above cut and fill panels; only a slight uplift was recorded.
- Due to the geological conditions and the depth of mining in the Lorraine colliery basin, swelling of shaly rocks had no effect on the behaviour of the surface.
- The different phases of surface behaviour of a longwall during its life can be summarised as follows: subsidence due to mining, residual subsidence, reactivated subsidence, uplift induced by

water table rise, uplift induced by swelling in special conditions.

The trend of reactivation of subsidence shown in (Figure 2.3.1.1.2-1), which began before the official flooding, was due to a non controlled intrusion of water in the mined area.

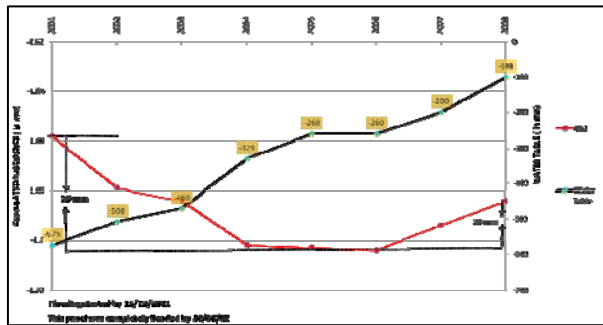


*Figure 2.3.1.1.2-1 General behaviour of surface after flooding; resettlement followed by uplift (panel 12, Vernenjoul field, sector West)*

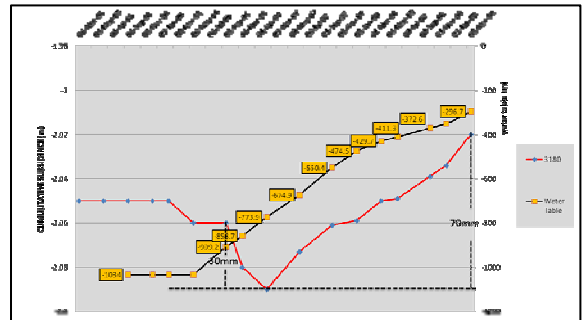


*Figure 2.3.1.1.2-2 Uplift may hide the reactivated subsidence in case of low measurement frequency (panel Cocheren Sud 1, Cocheren field, sector Centre)*

### **Review of experimental and theoretical work on the effect of water on the mechanical behaviour of argillaceous rocks.**

Within the ECSC contract N° 7220-PR-136, Armines conducted a large testing programme on different samples of shale from the French Lorraine coal mines and German Saar mines (La Houve, Merlebach and Luisenthal).

The tests on intact samples showed that the mechanical properties of argillaceous rocks are strongly affected by water (drop of 60 to 80 %) and that these rocks can undergo swelling or creep depending on the applied stress with regard to the swelling pressure. The results of the tests allowed establishment of a new viscoplastic rheological law able to describe the anisotropic swelling of argillaceous rocks with the effect of water. This law was integrated in the Armines software and validated on several examples.

To approach the conditions of a flooded caved longwall, large scale laboratory tests were developed. The objective of these tests was to take into account the caving (assemblage of blocks) and to try to understand and separate the different mechanisms which could affect the behaviour of the surface.

The main results derived from the large scale tests can be summarised as follows:

- The compaction phase, simulating subsidence, was well described by an exponential law.
- During flooding, the phase corresponding to water filling of the goaf induces a reactivation of settlement.
- The magnitude of resettlement measured in the laboratory was overestimated due to simulation factors linked mainly to the representation of the blocks.
- Swelling was not measured because the applied stress was higher than the swelling pressure.
- Uplift induced by the dilation of the caved rock under a pore pressure was identified but its magnitude was not quantified due to friction between the piston and the cell.
- The reservoir to be dilated under the water pressure should comprise not only the caved rocks of the immediate roof but also the fractures contained in the main roof.

### **Modelling the surface behaviour including hydrogeological effects**

Based on the results obtained and the observations made, it was proposed to develop a numerical modelling approach to simulate the surface behaviour of a caved longwall through all the episodes of its life and to take account of the different mechanisms which could affect the movement of the surface;

resettlement due a reduction of the mechanical properties, uplift induced by swelling of argillaceous rocks in contact of water and uplift brought by dilation of a reservoir under pore pressure induced by water table rise.

As a first stage, a very simple numerical model was developed to study separately the effect of each phenomenon.

The effect of flooding was described by a reduction of 50% of the mechanical properties and, in a first approach, swelling was considered to be equivalent to a thermal dilation. Pore pressure was only applied in the caved area and was considered to be equal to the weight of the total water head.

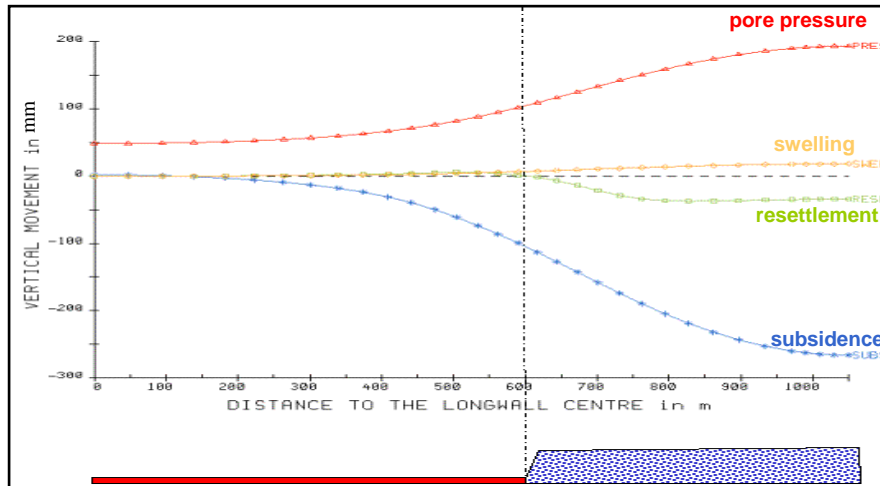


(Figure 2.3.1.1.2-3)

summarises the results obtained; settlement due to mining, reactivation of settlement due to the reduction of the mechanical properties during flooding, uplift due to swelling simulated by a thermal dilation and uplift caused by pore pressure within the reservoir constituted by the caved rocks.

**Figure 2.3.1.1.2-3 Separate simulation separately of the different phenomena that could affect the surface of a caved longwall during the mining and the flooding**

In the second stage of modelling, all the rocks were assumed to have an elastic behaviour and

swelling was neglected as the average weight of the overburden generally exceeds the swelling pressure. Only the caved area (reservoir) was subjected to pore pressure and its hydraulic properties were not taken into account. The following steps were considered:

- Excavation of the longwall and subsidence of the surface: the mechanical properties of the rocks were adjusted (mainly caving) to obtain a maximum settlement of the surface equal to around 80 % of the coal seam thickness.
- Flooding the caved area and reduction of the mechanical properties of the caving by around 60%: a reactivation of settlement is observed with a very low magnitude (around 2cm).
- Rise of water table to reach the top of the caved area: a small uplift is observed.
- Rise of the water table to 200 m on top of the caved area : uplift is dominating the behaviour but the magnitude is too high (unrealistic). The same tendency is confirmed with a higher water table level (600 m).

The main results which could be derived from these numerical simulations were :

- the subsidence phase was properly reproduced,
- the reactivation of settlement induced by weakening of the mechanical properties had a limited magnitude.
- pore pressure governs the longwall behaviour during the flooding phase and resettlement could be easily masked by the uplift induced by dilation of the reservoir with water table rise,

The magnitude of uplift obtained was assessed to be too high and completely unrealistic (non justified by site observations). The sensitivity analysis conducted to study the parameters affecting this

magnitude pointed to the role of the effective pore pressure (Biot's coefficient less than 1), the stiffness of the overburden and the location of the reservoir.

A new model, similar in principle to the previous one, was established by considering two separate zones in the overburden; a first zone affected directly by caving and situated on top of the longwall with a caving angle around  $14^\circ$ , and a second zone corresponding to the rest of the overburden. This separation allowed the location of the reservoir to be extended into the fractured area of the overburden when modelling the flooding phase (Figure 2.3.1.1.2-4).

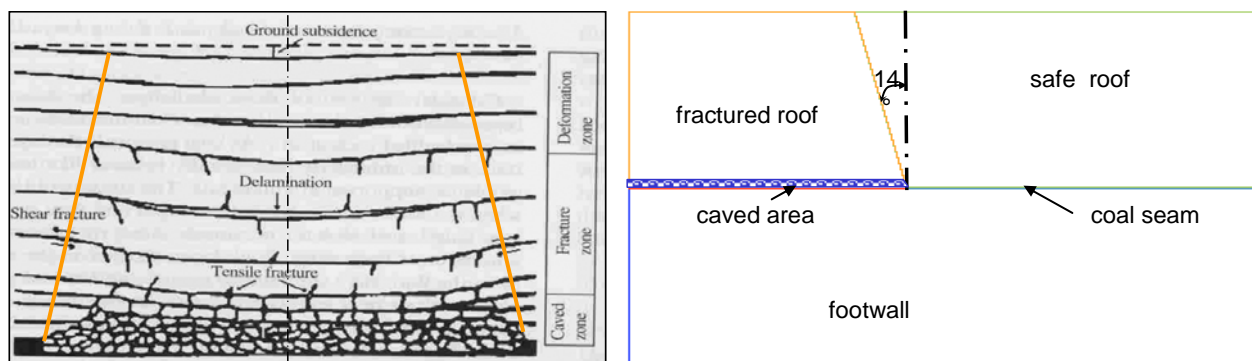


*Figure 2.3.1.1.2-4 New model of caved longwall*

Further to this difference linked to the geometrical conditions, the modelling also integrated more precise laws to describe the behaviour of the rocks (viscoplastic laws deduced from the laboratory results) and large displacement calculations. A Biot's coefficient equal to 0.15 was applied to the pore pressure. The value of this coefficient was determined according to available data on shales and argillaceous rocks.

The magnitude of uplift calculated with these conditions was around 15 cm and corresponded to approximately 5% of the maximum subsidence. This value is very reasonable and is coherent with all the measurements made on the flooded sites and presented in deliverable D1.1.2. (Figure 2.3.1.1.2-5) gives the surface behaviour for the two situations where the water table is respectively 500 m above the coal seam and 800 m (total flood).

The modelling approach presented above is very simplified because the water pressure is introduced only within the goaf to dilate it. The next improvement made consisted of developing a hydraulic model capable of describing the behaviour of the longwall from mining to closure and flooding. This new model is based on the following hypotheses (Figure 2.3.1.1.2-6);

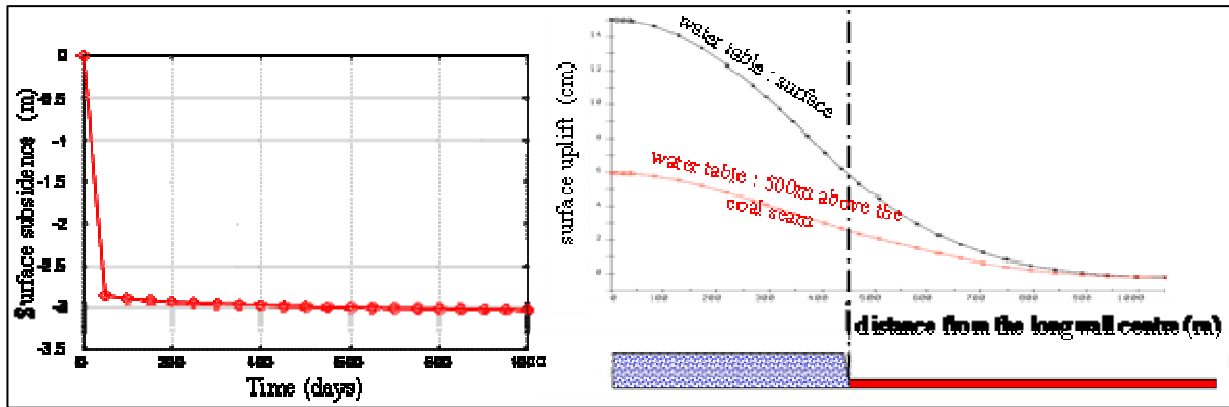


Figure 2.3.1.1.2-5 Showing the effect of time on subsidence and water table rise on uplift

- Only a single seam was considered at a depth of 1000 m, its average thickness was 4m and the height of caving was assumed to be 4 times the coal seam thickness.

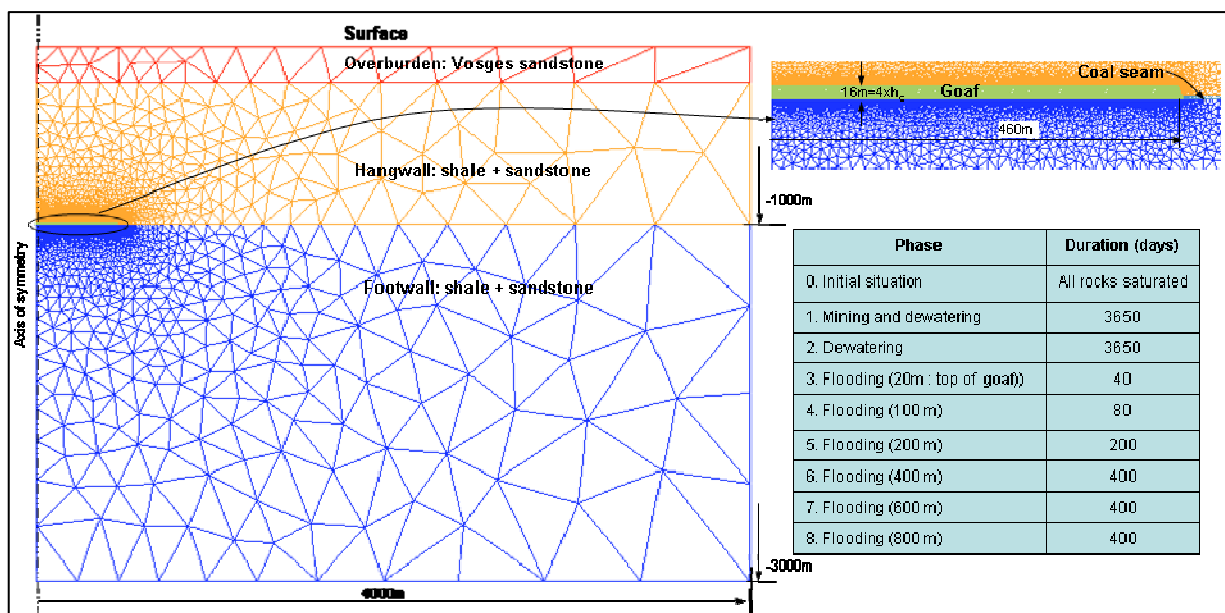


Figure 2.3.1.1.2-6 Features of the new numerical model developed to couple the hydraulic and the mechanical behaviour)

- An axis of symmetry was taken in the middle of the longwall and the problem analysed in plain strain conditions, the total mined width was 920 m, corresponding to approximately 4 longwalls without intermediate pillars.
- The footwall was considered to be homogenous and the hanging wall comprised two main layers; very permeable sandstones at the top (from the surface to a depth of 200 m) and an equivalent roof of shales and sandstone (model inspired from the French Lorraine basin).
- Due to the sensitivity of the flow problem, the limits of the numerical model were extended to 4000 m horizontally and 3000 m deep, all the simulations were performed in a transient regime.
- In the same way, the hydraulic properties of the different materials were assessed from available data recovered from the Lorraine colliery basin (porosity, horizontal and vertical permeabilities, storing coefficient).

- Before mining, the rocks were considered to be fully saturated. The hydraulic scenario simulated was as following : mining the different longwalls in 10 years and dewatering, a stand by period of 10 years where dewatering was maintained, flooding with a pore pressure rising progressively within the goaf from 0 to the whole water column, different steps were thus reproduced with an average water table rise of 0.5 m/day.

The main conclusions which can be drawn from all the analyses conducted on the surface behaviour of a longwall coal mine during the different episodes of its life can be summarised as follows:

- The modelling approach developed allows account to be taken of all the observed phenomena of surface behaviour; mining subsidence, residual subsidence, reactivated subsidence due to water effect, uplift induced by swelling and uplift induced by pore pressure
- This modelling approach could be used to assess the hazards and the risks when flooding caved coal mines.
- Caved rocks and overburden govern the mechanics of subsidence when flooding coal mines; effect of water, swelling, creep behaviour of overburden
- Swelling is governed by the swelling pressure and is therefore linked to the mining depth.
- Swelling is a rapid process and continuous swelling is due mainly to the presence of argillaceous materials in the overburden.
- Pore pressures are not totally active and a Biot's coefficient is required to weight their effect.
- Uplift is governed by the dilation of a reservoir comprising the caved rocks under the effect of pore pressure; the contribution of swelling on this phenomenon being very limited.

#### **Water inflows to underground longwall workings**

The second area of work under this Task examined the risks of water inflows into active longwall workings at coal mines through mining subsidence induced fractures and increased permeability. Potential water sources include surface water, the seabed, underground aquifers and other mine workings. Data was obtained from the UK Northumberland and Durham coalfields, pre 1980, and more recent case studies from the Selby coalfield, NW Leicestershire and Northumberland.

(Table 2.3.1.1.2-1) shows international criteria for working beneath the sea and bodies of water. Many countries have used criteria of minimum cover and limiting tensile strain at the base of the water body, but few have taken into account specific geological criteria. In Durham it was recommended to limit the tensile strain at the base of the Permian aquifer to 6mm/m (calculated according to the 1975 edition of the SEH). In the geometries involved this is actually a very similar criterion to the 10mm/m for seabed cover, calculated according to the 1966 edition of the SEH, included in the British Coal Production Instruction. The SEH was not intended to calculate subsurface tensile strains and such calculations may be called a Subsurface Disturbance Index.

During its 20 year life 2 further longwall faces, H52 (130m wide) and H706 (120m wide), at wistow colliery suffered water inflow problems. Here, a coal measures sandstone aquifer (the Woolley Edge Rock) which incropped to the Permian, is thought to have been the water source, separation to the aquifer being 130m. In each case the wet face was the second of the series in the mining area, the first at similar dimensions having been worked without incident. The key parameters for all the wet faces and some dry faces at Wistow are given in (Table 2.3.1.1.2-2).

Country	Minimum cover (m)	Minimum carboniferous strata (m)	Limiting tensile strain (mm/m)	Remarks
Australia	120	-	-	For panel and pillar method the panel width does not exceed D/3 and pillar width is not less than D/5 where D is the cover thickness. Cover should be at least 60m for partial extraction
Canada	213	-	6	-
Chile	150	Only 15m in one worked area	5	-
India	-	-	3	If, in an area, the percentage of shale > 35%, a higher limit of strain may be considered.
Japan	60	-	8	Coal mine safety regulations apply to drilling 8m advance of mining and various other aspects of undersea mining
Turkey	160	-	-	-
UK (Seabed)	105* (M<1.7m) 60**	60* 45**	10 (1966 SEH)	BC production instruction - *Limits for longwall extraction **Limits for room and pillar extraction
UK (Aquifer)	45	-	- 6 (1975 SEH)	Precautions Against Inrushes Regulations Local practice NE area (recommended by Garrity 1980)
USA	18.3M	-	8.75	M: thickness of extraction

**Table 2.3.1.1.2-1 International criteria for working beneath sea and bodies of water (after Allonby, Bicer and Tomlin – 1985 with additions)**

Panel	Length (m)	Width (m)	Seam height (m)	Extraction (m)	Cover to aquifer (m)	Approx depth to surface (m)	Max tensile strain at base of aquifer 1966 SEH (mm/m)		Presumed aquifer
							Individual panels	Aggregates	
H01AW	475	140	2.8	2.29	85	328	12.4	12.4	Permian
H02AW	290	130	2.8	2.13	80	320	12.3	12.3	Permian
H31AW	940	45	2.9	2.45	81	320	11.8	13.2	Dry
H32AW	930	45	2.9	2.41	82	320	11.3	12.6	Dry
H41AW	1030	45	2.9	2.77	85	320	12.2	14.3	Permian
H42AW	1010	45	2.9	2.72	87	320	10.4	12.9	Permian
H02BW	500	47	2.8	2.46	91	342	8.7	8.7	Dry
H52	445	130	2.8	2.49	130	420	10.0	10.6	WER
H706	310	120	2.9	2.80	130	436	11.2	11.2	WER

**Table 2.3.1.1.2-2 Sample of Wistow colliery longwalls (wet and dry)**

A table of key geometry and disturbance indices for Ellington and Lynemouth colliery Brass Thill panels where flooding either occurred or is known to have been a potential due to overlying flooded workings is shown in (Table 2.3.1.1.2-3). This includes the “Disturbance Indices” at the base of potential water source calculated according to the 1966 and 1975 SEH. Comparison shows little difference for standard width panels but significantly greater values from the 1966 version where the panels are narrow.

Panel	Width (m)	Extr. min (m)	Extr. max (m)	Cover to Yard (m)	Cover to Main (m)	Cover to Ashford (m)	Yard seam		Main seam		Ashford sandstone	
							E (mm/m) (1966)	E (mm/m) (1975)	E (mm/m) (1966)	E (mm/m) (1975)	E (mm/m) (1966)	E (mm/m) (1975)
K21	220	1.07	1.52	66	73	-	9.5 -13.5	9.5 -13.5	8.6 -12.2	8.6 -12.2	-	-
K214	255	1.02	1.02	70.7	-	-	8.4	8.4	-	-	-	-
K220	240	1.4	1.73	64.6	71.9	-	12.7 -15.7	12.7 -15.7	11.4 -14.1	11.4 -14.1	-	-
KS32	255	1.52	1.8	-	70.1	-	-	-	12.7 -15.0	12.7 -15.0	-	-
KS311	255	1.88	2.39	62.5	76.2	-	17.6 -22.4	17.6 -22.4	14.4 -18.3	14.4 -18.3	-	-
KS35	255	1.52	1.8	59	72.5	127	15.1 -17.8	15.1 -17.8	12.3 -14.5	12.3 -14.5	7.0 -8.3	7.0 -8.3
KS36	60	1.68	1.83	62	74	130	14.5 -15.8	12.7 -13.8	10.9 -11.8	9.2 -10.0	4.2 -4.6	3.2 -3.4
KS36(n.w.)	255	1.68	1.83	62	74	130	15.9 -17.3	15.9 -17.3	13.3 -14.5	13.3 -14.5	7.6 -8.2	7.6 -8.2

**Table 2.3.1.1.2-3. Disturbance indices for Ellington Brass Thill panels (1980-2004)**

### Statistical analysis of water inflow data

Possible approaches for statistical analysis of water inflow with the independent variables such as face width, cover and disturbance index (tensile strain) were examined. Conventional statistical methods such as multiple regression would require the flow rate values to be normally distributed and the independent variables to be not correlated with each other. These assumptions were not met by the pre 1980 Durham and Northumberland data and consequently Garritty used a non parametric statistical technique to test for significant relationships.

Since Garritty undertook his work, logistic multiple regression has been developed (Swanson et al) which could potentially be used. For Wistow, we have 135 records, 6 wet faces and 129 dry, but the small proportion of wet faces means that the variable sample number criterion is not met, so for the Wistow data we are limited to using non parametric rank tests.

The North East data comprises a larger number of cases and in principle it would be possible to perform logistic regression analysis. Unfortunately the full data sets are not available and data points have been derived from illustrated graphs. For a relatively large number of cases where a zero or non unique flow rate is recorded it is not possible to pair up the corresponding values and this limits the analysis. Also the tensile strains were calculated using the 1975SEH, whereas the Wistow data was generated by MULPAN using the 1966 method. Without the original data it is not possible to convert the tensile strains for a direct comparison. These restrictions reduced the number of available data sets and independent variables, ruling out logistic regression analysis.

The Wilcoxon Mann Whitney U signed rank test has the advantage that the two data sets do not need to have the same number of observations although they are assumed to have the same form. It can be used to compare sets of parameters from wet and dry faces for significant differences at the 95% level. In this way independent variables correlated with the dependent condition (wet or dry) can be confirmed and their relative importance examined.

The parameters examined for Wistow are listed in (Table 2.3.1.1.2-4). As expected the probability of a wet face is increased as the panel width increases and the cover to the aquifer decreases, but these parameters are only significant if they are combined as the w/h ratio (>99% probability). The extraction height only varied within a narrow range and within this it does not have any effect. Face length does have a significant effect, with shorter face runs more likely to be wet, but this is probably because wet faces tend to be shortened or stopped.

Parameter	R	Z value and sig level	Comment
Width (w)	517	1.16 not significant	But wider more likely to be wet
Extraction height (m)	385	-0.025 not significant	No effect on its own
Face length (l)	64	-3.67 significant at 1%	Shorter face runs more likely to be wet probably because stopped
Cover to aquifer (h)	299	-1.16 not significant	But less cover more likely
w/h	678	2.88 significant at 1%	Higher ratio more likely
Max subsidence (s)	649	2.50 significant at 5%	Greater subsidence more likely
S/m	671	2.81 significant at 1%	Higher ratio more likely
Tensile strain (single panel) d	779	3.96 significant at 1%	Higher strain more likely—good predictor
Most likely aggregate strain D	774	3.91 significant at 1%	Higher strain more likely-good predictor
w*m/h	693	3.04 significant at 1%	Higher ratio more likely-better predictor than w/h
D*w/h	774	3.91 significant at 1%	Higher ratio more likely –no better than single panel tensile strain
D*wm/h	778	3.95 significant at 1%	Higher ratio more likely - no better than single panel tensile strain
D/(15-4.44w/h)	789	4.06 significant at 1%	Values > 1 predict wet panel-best predictor

*Table 2.3.1.1.2-4. Wistow data analysis results –Wilcoxon Mann Witney U tes*

The maximum calculated subsidence is significant at the 5% level and this is increased to 1% using the ratio of s/m. However the disturbance parameters are in general the most effective prediction parameters. Single panel tensile strain and aggregate strain are significant at the 1% level suggesting the primary role of apparent strain magnitude at the aquifer base as the water inflow trigger. The parameter w\*m/h is also highly significant confirming that the cross section extracted in relation to distance to water source is very important. Again this will be linked to the level of apparent strains at the aquifer base. Further combinations of D\*w/h, D\*wm/h proved no better than single panel strain.

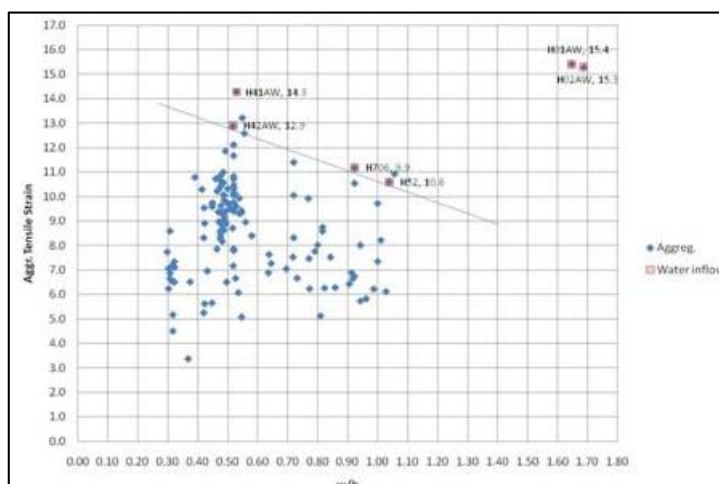


*Figure 2.3.1.1.2-7 Wistow panels – Aggregate tensile strain against width to height ratio*

(Figure 2.3.1.1.2-7) shows the relation between w/h ratio and aggregate tensile strain. The wet panels show relatively high values for both parameters with very little overlap with dry face data points. This suggests a combination of these parameters is an effective predictor of water inflow. The line separating wet and dry faces has the equation aggregate tensile strain (mm/m) = 15-4.44w/h. Consequently the parameter, aggregate tensile strain / (15-4.44w/h) > 1 predicts that the face will suffer a water inflow.

(Table 2.3.1.1.2-5) summarises the data for the 4 Asfordby faces. The width/height ratios of the two wider panels were beyond the Wistow data range, but the computed strains place the faces well above the extended criterion line, whereas the narrow panels are below it.

Thus, the Wistow criterion could have a more general application as a predictive tool for longwall water inflow.

Face	w	h	w/h	Strain (base of aquifer) 1975 SEH	Strain 1966 SEH	Outcome	Wistow criterion prediction
101 face	250m	90m	2.77	14mm/m	14.3mm/m	Wet-weightings	Wet
102b, c	60m	90m	0.66	11mm/m	11.3mm/m	Dry-no weightings	Dry
101c	120m	80m	1.50	14.7mm/m	16.1mm/m	Weightings	Wet

*Table 2.3.1.1.2-5 Asfordby water inflow data*

In view of these findings, the pre 1980 water inflow data for the North East of England coal mines were re-examined to compare the relationships between w/h ratio and aggregate strain with that derived in the Wistow analysis. The flow rates vary from over 30l/s in a few cases to zero in a much larger number. For the latter group it is not possible to link the corresponding w/h ratio and aggregate tensile strain for each case.

Analysis of the more recent KS36s inflow at Ellington concluded that the water source was flooded Yard Seam workings 60m above. The face had retreated 60m when the inflow occurred so the effective w/h ratio was 1 and the calculated tensile strain at the base of the Yard Seam workings (1966 SEH) was approximately 14.5-12.8 mm/m. This significantly exceeds the Wistow criterion and it would be expected to be wet. The preceding face, K35s, was not overworked in the Yard Seam and was dry, although the strain at the base of the worked Main seam further above again exceeded the Wistow criterion. It is not known if these Main Seam workings were flooded. An earlier Brass Thill longwall, KS311s in 2002-3, also suffered an inflow, the source presumed to be flooded Yard seam workings where the strain was again well in excess of the Wistow criterion (> 20mm/m). Two other faces with lower Yard seam strains, (Yard thought to be flooded) were dry. These strains varied, from 10-16mm/m (1966 SEH). The Wistow criterion line indicates that these faces should also have been wet, although the w/h ratios exceeded 3 and so are outside the Wistow data range.

A notable feature of these results is that the calculated strains affecting the flooded workings are of the expected magnitudes, whereas previous data, where the water source was assumed to be the sea or the Permian, resulted in most strain values being much lower. These more recent incidents suggest that the Wistow criterion is potentially applicable more widely providing the water source is correctly identified, and also suggest that failure to identify the correct water source is the main reason why the earlier North East data is so inconsistent.

To allow wider application, the Wistow criterion needs to be extended to cover greater w/h ratios. It is clearly not applicable at large w/h ratios because the resulting critical strain level would be extremely small or even negative. Unfortunately there is only limited reliable data available for cases with larger w/h ratios. These cases, from Asfordby and Ellington, are described above. The data points are plotted together with those from Wistow.

The available data suggest that the critical level of aggregate tensile strain does not continue to reduce as w/h increases beyond 1. It is illogical to expect that it increases again as w/h increases beyond 1. It will either continue to decrease or remain approximately constant if the w/h ratio no longer has an important influence. The data fits with it remaining constant at around 10mm/m, which accords with past experience.

The Wilcoxon Mann Whitney U analysis was repeated to include all the available data. As the additional data is less comprehensive than the Wistow data the number of parameters examined had to be reduced, but the proposed criteria were included. The results are given in (Table 2.3.1.1.2-6).

Parameter	R value	Z value and sig level	Comment
Width (w)	989	2.07 significant at 5%	wider more likely to be wet
Extraction height m	739	.011 not significant	no effect on its own
Cover to aquifer (h)	441	-2.23 significant at 5%	Less cover more likely to be wet
w/h	1239	4.03 significant at 1%	higher ratio more likely
Most likely aggregate strain D	1350	4.9 significant at 1%	Higher strain more likely-good predictor
D*w/h	1328	4.73 significant at 1%	No better than aggregate strain
D/(15-4.44w/h) for w/h<1, D/10.5 for w/h≥1	1368	2.05 significant at 1%	Values>1 predict wet panel-best predictor
D/(9.5+h/w)	1363	2.01 significant at 1%	Values>1 predict wet panel- continuous function alternative for best predictor

**Table 2.3.1.1.2-6 All Data Analysis Results –Wilcoxon Mann Witney U Test**

The analysis was performed with 134 dry face results (128 Wistow, 4 Ellington, 2 Asfordby) and 10 wet face results (6 Wistow, 2 Ellington, 2 Asfordby).

The additional data results in both face width and height now being significantly related to risk of water inflow and the w/h ratio and aggregate strain both have a greater significance (increased z value) compared with the Wistow data alone. The analysis indicates that the selected criteria (which combine the aggregate strain and w/h ratio) are equally effective as prediction tools, having a very significant influence on the risk of water inflow. They are the best available parameters for predicting water inflow over the extended data range. Both criteria successfully predict all 10 wet cases, and only 6 dry cases out of 134 are wrongly classified as wet.

However in view of the limited data covering the higher values of w/h, the prediction tools should be applied with some caution at w/h values >1 until confirmed by additional data.

#### **Modelling of Wistow water inflow case studies**

The use of a FLAC2D transverse model to examine strata disturbance and thus propensity for water inflow from overlying aquifers to the longwalls at Wistow colliery was also explored. Similar modelling of the 700s panel area was previously undertaken and reported under ECSC Project 7220 PR052. A series of models was constructed for the three separate “blocks” of the mine where water inflows occurred (H01A, H52 and H706). In each of these “blocks” some panels were wet and others dry. Each model represented the positions of the aquifer (either Lower Magnesian Limestone/Basal Sands or the Woolley Edge Rock sandstone) and other major geological units, such that the effects on the intervening strata of extracting each series of parallel longwall panels in sequence could be examined. The effects of varying the geomechanical input parameters and the best output parameters for indicating water inflow were studied.

Five alternative sets of strata properties were compared (1 being the weakest and 5 being the strongest) and the results were examined in the form of both indicated plastic and volumetric strain above the panels at the base of the inferred water source (Permian limestone or Woolley Edge Rock). (Figure 2.3.1.1.2-8) shows the calculated strains at the aquifer for the series of panels modelled for property set 2 which gave the best match with actual experience. It can be seen that the 3 wet panels, H01AW, H52 and H706 showed the highest strain values for both strain types. It was concluded that the correlation with plastic strain was probably the closest. It can be seen that this approach can be used to identify a water path to the aquifer provided appropriate strata properties are available and the panel layout can be reasonably approximated to a two dimensional transverse cross section. It also appears that the aggregate strain effect, due to a series of adjacent panels, is greater using this method than is derived from using the SEH to obtain a Disturbance Index based on calculated aggregate tensile strain.

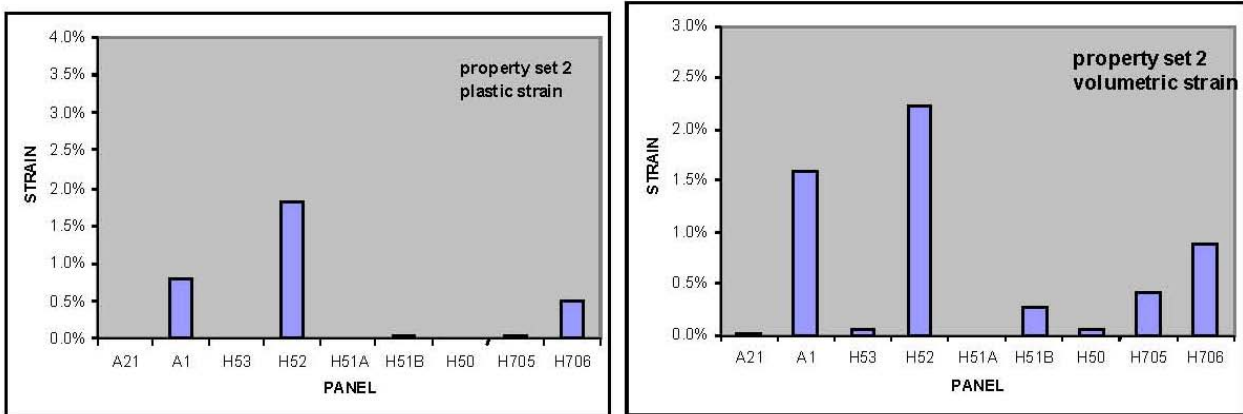


*Figure 2.3.1.1.2-8 FLAC 2D modelling of Wistow case history panels, plastic and numeric strains*

### 2.3.1.1.3. Task 1.1.3. Prediction of subsurface deformation

The aim of this Task was to develop improved techniques for predicting stress distributions and roadway support requirements where seams are worked above or vertically between previous areas of coal extraction. A set of guidelines has been produced (Deliverable 1.1.6).

The state of the art in 1972 was described by a UK NCB working party. They suggested that gate roadways should be stepped into the shadow of an underlying goaf by “about 15 feet” or placed at least 0.03depth and preferably more to the solid side of a pillar edge. The “15 feet” recommendation made no reference to separation between the worked seams. This results in a “Pyramid Layout” (Haycocks and Zhou, 1990) with successive panels becoming narrower as they become shallower. Today, such a layout is considered uneconomic, with trends to increase panel widths and maximise extraction ratios.

An important factor, in addition to stress distribution, is the condition of the rock around the roadway. The 1972 Working Party sat prior to adoption of rockbolting as primary support.

**Case Study 1, Manton Colliery, Flockton Seam.** Here, the Parkgate seam panels, 40m below, had been worked 40 years earlier. The Flockton panels were approximately 900m deep. The immediate roof was generally medium to strong, but roof control problems occurred where the overlying Chavery seam approached within 6-8m. PT12 panel was laid out conventionally with the gates offset 10m into the goaf.

The rock stress was measured by overcoring 2.8m and 2.5m away from the goaf and solid sides of the main gate respectively, giving vertical stresses of 7 MPa on the goaf side and 16 MPa on the solid side. Horizontal ribside borehole core logging showed significant fracturing 3m beyond a point directly above the pillar edge as well as within the first few metres of ribside, with no significant fracturing deeper into the goaf side.

**Case Study 2, Point of Ayr Colliery, Three Yard and Two Yard Seams.** Final production from Point of Ayr was from rockbolted room and pillar workings using place changing continuous miners and Fletcher bolters in the shallow Three Yard seam only 210-250m below the surface/seabed and the Two Yard seam some 36m below. The Hard Five Quarter edges had the most effect, although furthest below the Three Yard, as it was the first worked, with the intervening seams having been subsequently extracted in its subsidence zone. Roof conditions in the areas of gradient change were often poor with up to 3m cavities forming prior to bolting. Roof softening extended to 2.4m in places. Remedial long tendon cable bolting was often required in these areas. In the Two Yard room and pillar workings, there were no visible inflections observed in association with the Hard Five Quarter workings alone. In general, inflections above the Durbog and Durbog/Stone Coal panel edges occurred within a few metres of the goaf side edge while over the Stone Coal panel edges alone this occurred approximately 10-15m

from the goaf edge. Again roof overbreak or, at worst, cavities in excess of 2m tended to occur in the inflection areas.

**Case study 3, Easington Colliery, G40.** Extensive measurements were undertaken here in association with introduction of rockbolt support. The 1.2m thick G seam lay 460m below sea level. The roadway roof comprised relatively weak mudstone grading to stronger siltstones some 3m up. Rock stress measurements indicated a near isotropic horizontal stress field.

Roof conditions were good in the areas above solid and worse in the areas above goaf, with particularly high rockbolt loads measured at about 12m into the goaf and particularly high rib movements measured in the solid. The roof remained stable in all cases though additional remedial rockbolting was employed in the goaf area. Support conditions directly over goaf edge appear favourable with low roof and rib movement and acceptable bolt loads... Approximately 10m over goaf, however, roof condition deteriorates, bolt loads increase and water flows may occur.

**Case study 4. Ellington and Lynemouth Collieries, Main seam.** Tubby and Farmer described the effects of a series of longwalls under-working an existing superjacent room and pillar system. Borehole extensometers were placed in down holes between the 2.4m-4m thick Main seam room and pillar workings and the 1.6m Brass Thill seam, to be extracted by longwalls, 75m below. (Figure 2.3.1.1.3-1) shows the measured vertical borehole displacements as bay strain contours across the goaf/rib side section. Vertical strain contour sections for other sites leading to similar conclusions were presented in a 1981 final report under ECSC Research Project 7220-AC806. Another useful data set from this work is the subsurface subsidence profiles shown in (Figure 2.3.1.1.3-2), which could be interpreted as indicating that the zone of increased disturbance extended some 50-60m into the goaf-side from the underlying pillar edge.

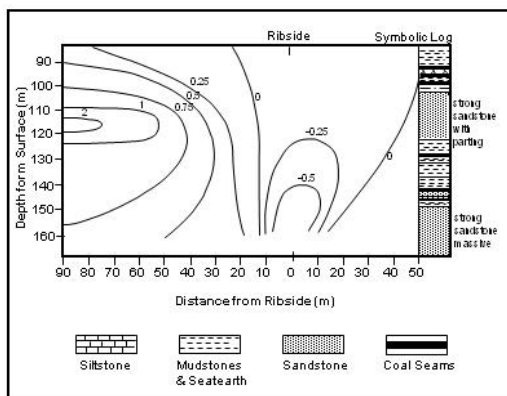


**Figure 2.3.1.1.3-1** Bay strain contours across goaf-rib side section, Ellington/ Lynemouth collieries

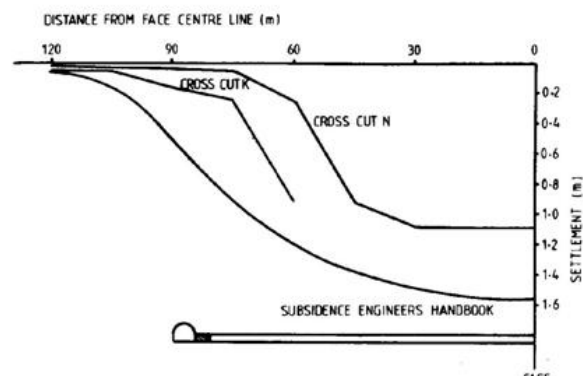


**Figure 2.3.1.1.3-2** Settlement profiles measured in Main seam above Brass Thill longwall

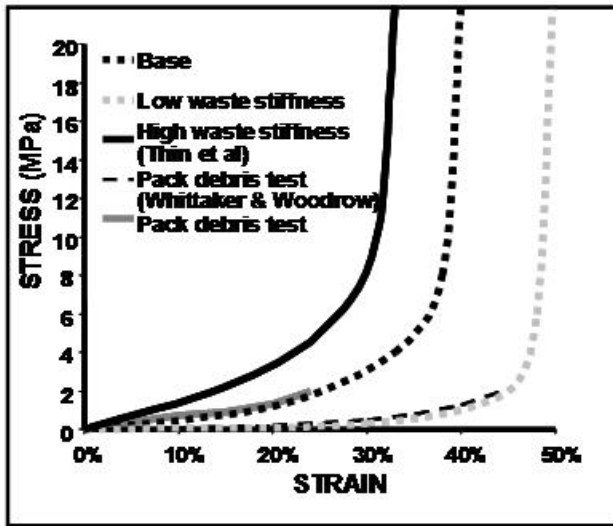


Figure 2.3.1.1.3-3 Compaction properties used to model bulked waste material

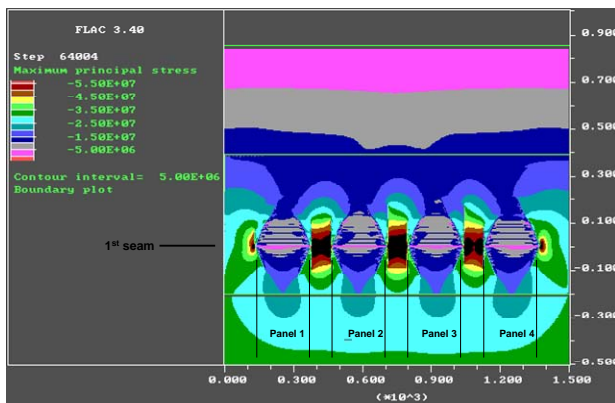


Figure 2.3.1.1.3-4 Influence of underlying panels. Principal stress contours around sequence of panels, Riccall Colliery

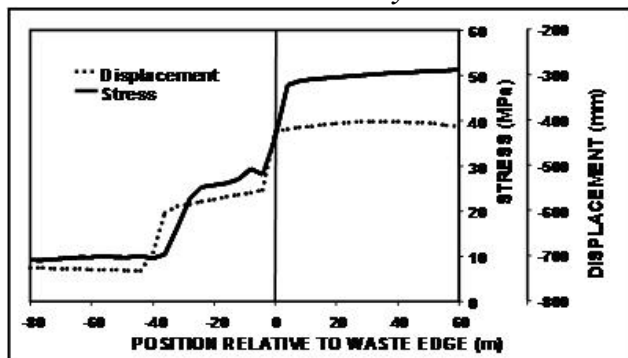


Figure 2.3.1.1.3-5 Stress and displacement across waste edge at 70m above

stress relief is contained within these bands. Sensitivity analyses showed the results were most sensitive to variations in the waste properties and the friction angle of the rock. The angle of friction controlled the angle at which the shear bands propagated into the roof and so the distance in from the waste edge that full stress relief may be obtained. The recommendations, made on a basis of this modelling, combined with the experience gained from other case studies, were that, if gates are to be placed in the area close to a pillar/goaf edge, they should be 8m inside the underlying Parkgate goaf edge.

**Case Study 5, Riccall Colliery, Stanley Main seam (from ECSC Project 7220/PR055).** Barnsley seam longwalls with stable “finger” pillars were worked at Riccall at a depth of 800-900m. The next seam, the Stanley Main, 60-70m above, was also to be worked by retreat longwalling with rockbolt supported gate and main access roadways. RMT applied computer modelling to investigate the interaction effects, the most appropriate positions for gateroads and the likely support conditions. The first stage was to analyse the effects of extracting the Barnsley seam. The process was similar to that described for the surface subsidence modelling under Task 1.1.1 and the water inflow modelling under Task 1.1.2, with double yield material representing the goaf. The goaf properties were obtained from tests on debris packs and published data (Figure 2.3.1.1.3-3). (Figure 2.3.1.1.3-4) shows stress contours for a sequence of four panels illustrating the destressed zones above the panels and high stresses above pillars. (Figure 2.3.1.1.3-5) shows stress and displacement or subsidence profiles across a pillar edge. Above pillars indicated stresses of 50MPa were indicated.

**Case Study 6. Welbeck Colliery, Deep Soft.** Extensive FLAC2D and MAP3D modelling of the complex interaction geometries and support options for a series of three Deep Soft panels (244, 242 and 240, Figure 2.3.1.1.3-6) was undertaken under the RFCS Project GEOMOD. A large variety of alternative layouts was considered. Several important issues were highlighted including stress redistribution above “skin to skin” panels and problems produced by vertical “stress windows”.

(Figure 2.3.1.1.3-7) shows shear strain contour output from a FLAC model of the strata around a single Parkgate panel, indicating bands of high strain running away from the waste edge. The most prominent of these run upwards into the roof above the waste. The region of greatest

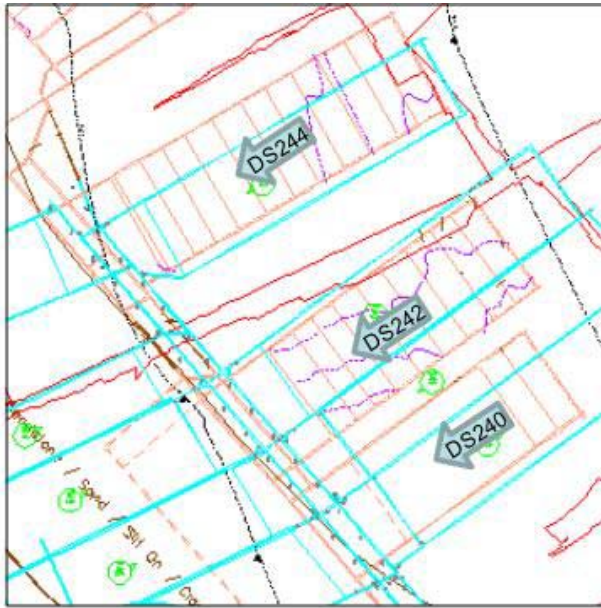


**Figure 2.3.1.1.3-6 Plan illustrating interaction for Deep Soft seam. Welbeck colliery**

Results from 53 roof extensometers showed minimal roof movement and softening for development with no clear difference between above waste and above solid. A summary of total roof extensometer displacement after 100 days for all 6 gate roads plus 244 face line (over solid, beneath Top Hard pillar, poor direction) and the main trunk roadways (also over solid) is shown in (Figure 2.3.1.1.3-8). Two roadways suffered poor conditions (244 Face Line and 242 LH gate).

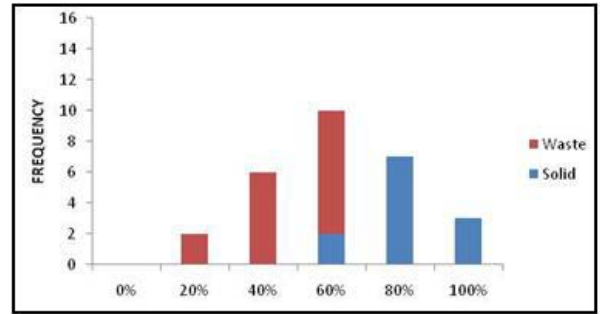


**Figure 2.3.1.1.3-7 FLAC model showing shear strains surrounding single panel in the Parkgate seam at Welbeck colliery**

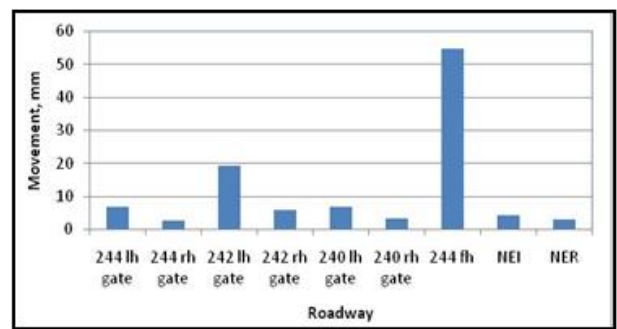


**Figure 2.3.1.1.3-8. Roof extensometer data at 100 days from Welbeck DS244, 242 and 240 gate roadways**

**Modelling of planned Deep Soft workings above Parkgate at Thoresby colliery.**

The retreat of two adjacent longwall panels, planned for the new Deep Soft area at Thoresby colliery, was first modelled using the MAP3D boundary element program. This is a highly complex interaction area. For most of their length the Deep Soft panels cross a large underlying goaf from previous “skin to skin” workings in the Parkgate seam some 40m below. At their inbye end they cross two parallel high stress concentrations on development and hard seam, 170 above, has also been extensively presented at various stages of retreat in 38 individual

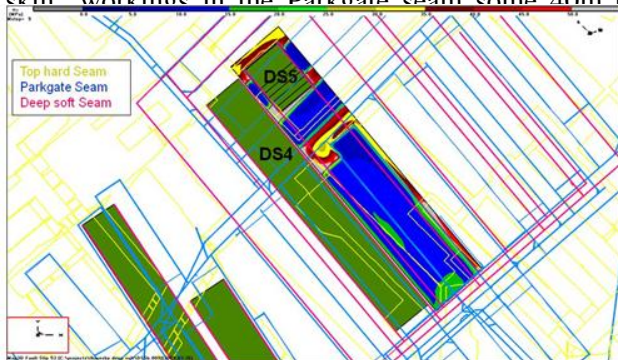


**Figure 2.3.1.1.3-9 Vertical stress contours during DS5 retreat**

(Figure 2.3.1.1.3-9) shows vertical stress contours for DS5 at 450m retreat where it crosses an underlying Parkgate pillar, resulting in extremely high stresses in the face end area of the left hand gate (beside DS4 goaf).

(Figure 2.3.1.1.3-10 a) shows a graph of the vertical stresses for each gate, 20m ahead of the retreating face and (Figure 2.3.1.1.3-10 b) shows the corresponding situation for DS2. It can be seen that extremely high vertical stresses were predicted in the stress window areas, particularly for DS4 right hand gate (>80MPa) and for DS5 left hand gate (almost 70MPa). The work indicated that the preferred

loader gates were DS4 left hand gate and DS5 RH gate. The faces were re-handed accordingly.

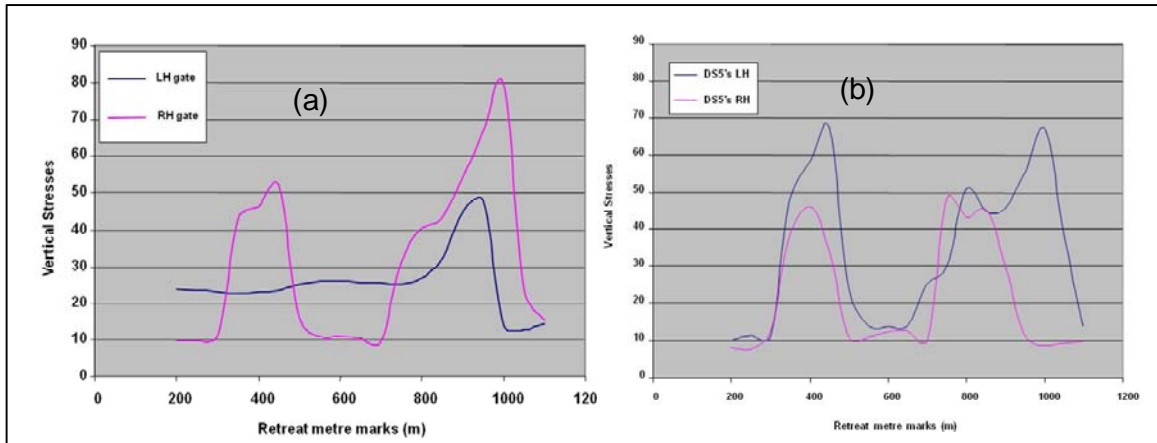


Figure 2.3.1.1.3-10 Vertical stress 20 m ahead of retreat Telltale data above ting face a)DS4, b)DS5

The previous detailed non-elastic models of gates driven above goafs used two dimensional programs such as FLAC. Under this Project, FLAC3D v3.1 models were developed for the Welbeck/Thoresby Deep Soft seam. Their predictions were checked against the previously verified FLAC 2D models of the Deep Soft at Welbeck. The models developed were for a short representative length of roadway (one support cycle). Translational symmetry was invoked on the front and rear planes of the model to simulate an infinitely repeating support cycle down an infinitely long length of the gate roadway. The mesh was graded such that the finite difference zones were very fine in the area of interest around the roadway, becoming much coarser further away where detail was not required. The Strain Softening Ubiquitous Joint material was used to represent the rock, enabling increasing strength with confinement, higher friction angles at low confinement, post failure strain-softening and reduced strength along bedding planes. Roof and rib bolts were represented using pile structural elements.

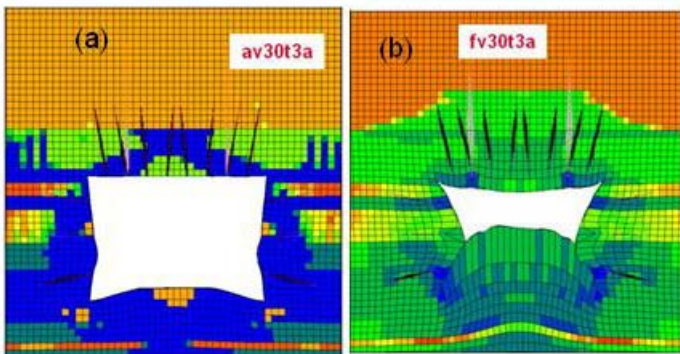


Figure 2.3.1.1.3-11 Vertical stress 30MPa, low lateral stress, support A – a) GSI 80, b) GSI 60

To examine support options in areas affected and not affected by subsidence disturbance, an approach similar to that used previously for FLAC2D involving modifying the rock properties according to the Hoek and Brown’s GSI was tried. A GSI of 80 represented undisturbed rock; 70 a more disturbed or jointed rock and 60 a highly disturbed rock mass. (Figure 2.3.1.1.3-11) shows the significant increase in rock failure (reduced

cohesion) for support pattern A for a GSI of 60 against a GSI of 80. (Figure 2.3.1.1.3-12) compares simulated roof extensometer results for the three support patterns for GSIs of 80 and 60 for the same ratios of lateral to vertical stress This suggest that a denser pattern of rockbolts without longer flexible bolts would provide better roof control in the undisturbed condition, but that a less dense rockbolt pattern supplemented by longer flexible bolts could be preferable in the disturbed ground.

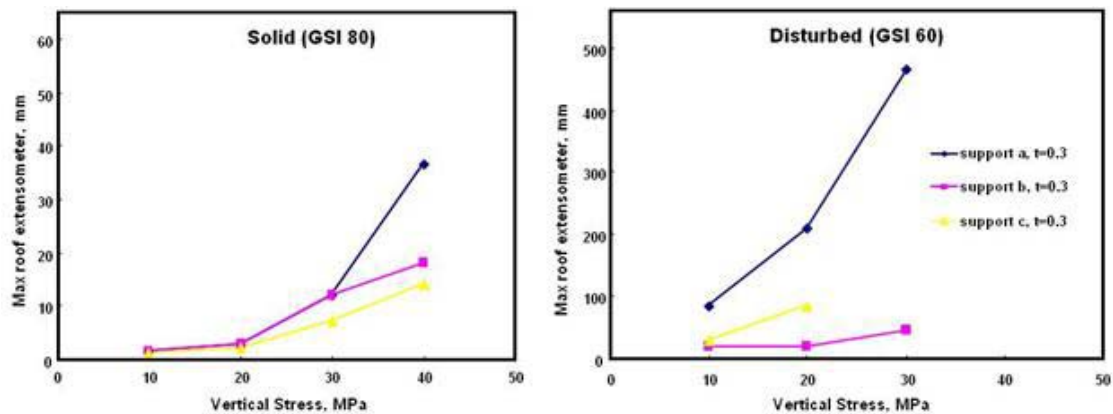


Figure 2.3.1.1.3-12 Simulated roof extensometer data for low lateral stress

### Back analysis of Welbeck experience using FLAC3D and GSI

Following the Deep Soft FLAC 3D model development and initial examination of applying GSI to the Thoresby gate roads, the model was used for detailed back analysis of the experience of mining the Welbeck Deep Soft panels and further examination of the use of GSI, particularly with regard for post failure residual rock strength and bedding plane properties. Full details of this work are provided in Deliverable 1.1.2. Three hypotheses for application of GSI to residual strengths were examined.

**Hypothesis 1** used the same residual strength for all GSIs with a bilinear fit directly to the rock test data. For lower values of GSI the residual strength exceeds original rock mass strength at higher confinement. Although unexpected, this is possible, implying strain hardening at higher confinement.

**Hypothesis 2** used a different residual strength for each GSI. The residual strength applied was the minimum of peak strength and measured residual strength.

**Hypothesis 3** was a compromise between Hypotheses 1 and 2. Here, the low confinement residual strength from the test data was maintained with the higher confinement using the minimum of GSI reduced peak and original laboratory residual strengths.

The results for hypothesis 3 (Figure 2.3.1.1.3-13) showed the best match to the range of conditions experienced. Above unworked Parkgate, a GSI of 80 showed minimal roof movement with some rib and floor movement for a stress range of 20-35MPa. This matches the experience in 244 LG well. Above Parkgate waste, the vertical stress was expected to be in the range 5-15MPa and the GSI to be lower than above unworked Parkgate. At locations away from the influence of any waste edges the gates experienced minimal roof movement and the rib and floor movement was less than above unworked Parkgate. Assuming a GSI of 60 provided the best match although the roof movements predicted by the model were larger than those actually experienced. Above Parkgate waste, where influenced by waste edges, the stress may be higher if full stress relief is not obtained and the GSI lower if on the edge of the subsidence trough. Using a GSI of 50 gave increased roof movement, matching the 50mm on A tell-tales with minimal B movement experienced in sections of 242 and 240 L/G.

This back analysis from Welbeck can now be applied to modelling the gate roadways being developed in similar interaction circumstances at the neighbouring Thoresby colliery. FLAC3D models for Harworth and Kellingley collieries were also completed and are now available for application to mine roadway support design using the principles outlined above for overworking previous longwall panels.

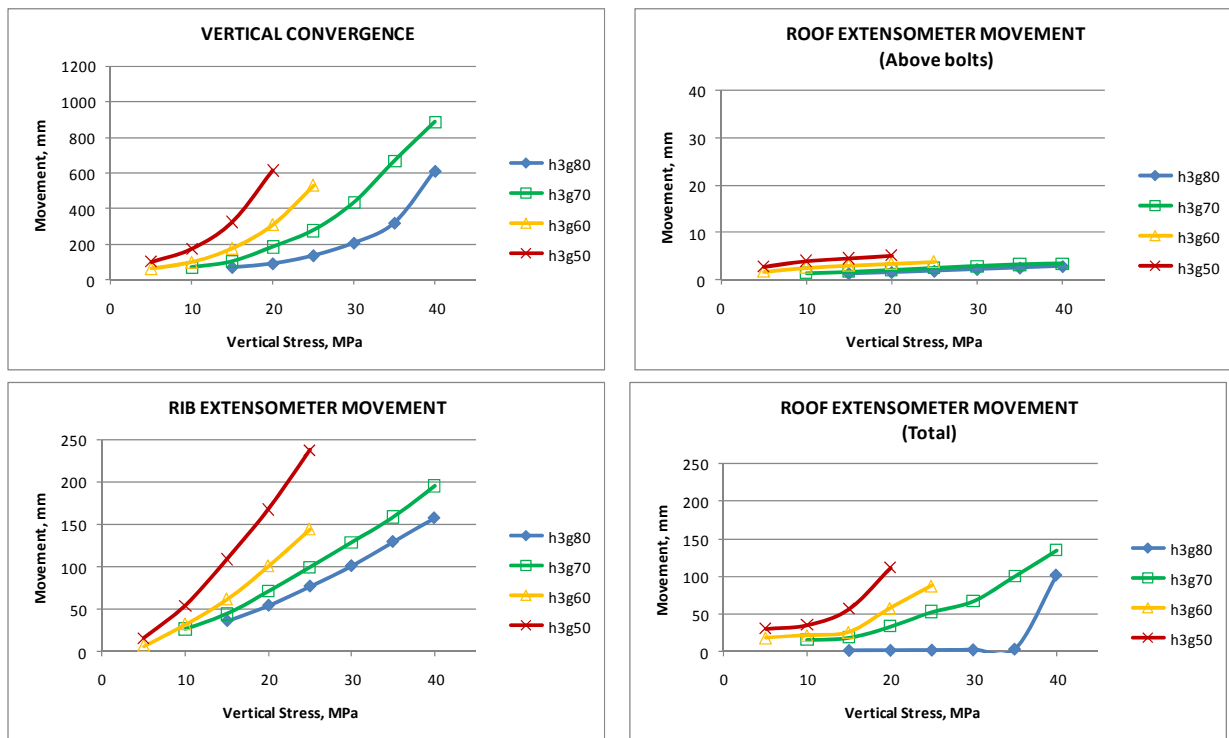


Figure 2.3.1.1.3-13 Summary of model results using properties H3

### Alternative modelling methods

Exeter University's study of alternative modelling methods for representing longwall caving produced a detailed 56 page report (Addendum to Deliverable 1.1.6). This includes a detailed table listing features, advantages and disadvantages of the following numerical approaches; Continuum - Boundary element, Finite-element and Finite-difference; Discontinuum -Discrete element; and Hybrid Codes incorporating intact rock fracture capability (Finite-discrete element). Codes used by the partners during the Project fall into the first two categories and the purpose of Exeter work was to determine whether significant benefit might be derived by moving to the latter type, in particular, Rockfield's ELFEN Code.

### 2.3.1.2. Prediction of Surface and subsurface subsidence caused by underground infrastructures. WP1.2.

#### 2.3.1.2.1. Task 1.2.1. Shafts survey using innovative geophysical tools

##### 1) Telemetry and Instrumentation for SFS monitor

The aim of this sub-task was to investigate telemetry and data-logging in the context of a remote monitoring system for disused mineshafts with a view to obtaining a warning of surface subsidence events. A system based on the principles of reduced power consumption and GPRS data transmission was developed for use with a specially designed shaft-fill stability (SFS) sensor. The overall system design objectives concentrated on providing a simple but robust monitor of shaft-fill stability, combined with a scalable, web-based transmission system capable of interrogating a large number of potential shaft sites. The initial study was used as the basis for design work in Task 1.2.3, and work then progressed to the field trial of a prototype system in Task 2.3. A summary of the system components is as follows.

##### a. Shaft-Fill Extensometer

A survey of commercial draw wire sensors was carried out. Included in this review were 33 products from seven manufacturers offering measurement ranges from 1.5 m to 15 m. Various custom designs were then considered, which provided only the features necessary for this application, and at a lower cost than commercially-available sensors. There was, importantly, also the potential to pursue a custom

design that addressed the environmental limitations of most of the commercial sensors reviewed, namely the ingress of water vapour giving rise to condensation and to the possibility of long-term corrosion inside these units. After appraising the key features of both approaches it was decided that a custom design was favoured.

An analysis indicated that limitations in the interface electronics might require the pay-out rate of the extensometer to be mechanically limited. Two designs were investigated; a frictional retarder and one based on a pawl and ratchet assembly. Several methods were investigated for sensing the rotation of the extensometer spool. Both designs addressed the issues of the long-term viability of the components in the presence of adverse biological and environmental conditions. Prototypes of both designs were constructed and were evaluated within the field trials of Task 2.3.

#### **b. Electronic Sensor**

The extensometer measures movement by detecting the rotation of the spool on which the draw wire resides. An electronic sensor reads the rotation and conveys the information to the data logger. Particular issues that were studied include the compatibility of the sensing method with the ultra-low power consumption that was required and the method of decoding the positional data from the spool.

Initially a standard form of optical shaft encoder was considered. The advantages being that the quadrature channel information gives unambiguous position information, the standby current is zero and the sensing time is very low – of the order of microseconds. However, an optical sensor needs to be protected against dust and biological activity and it was considered that a mechanically simpler design using magnetic sensors would therefore be preferable. Hall effect sensors were considered but it was decided that magnetic reed switches would be preferable due to the advantages of a lower standby power consumption.

#### **c. Data Logger**

The logger samples data from the sensor and stores it in a memory chip. A study of battery technologies lead to the conclusion that a ten-year operating life could be met by using lithium iron disulphide cells (Li/FeS<sub>2</sub>) which have an extremely low self-discharge of 5% in 15 years.

#### **d. Telemetry transmitter**

It was intended that the transmitter should use the same technology as a mobile phone; using the GPRS packet data service to send data to the Internet. Data (including a status report) would be transmitted daily or more frequently when needed. Software was therefore developed for a number of functions, namely...

- to permit the GPRS modem to communicate with a web server and to upload data
- to permit the web server to send commands to the remote logger to configure its options regarding frequency of reporting, etc
- to permit the modem to send SMS ‘flash’ messages. (See Technical specification for digital cellular telecommunications system (Phase 2+), GSM 03.38 version 7.0.0 Release 1998).

#### **e. Survey of Radio Signal Strengths**

A review was undertaken of the network coverage of various telecommunications operators in the UK, with a view to establishing whether GPRS network coverage was available in the areas where disused mineshafts needed to be monitored. For field trials, a preliminary list of suitable disused mineshafts in the UK was then drawn up. It was originally envisaged that, in the event that these proved to be in marginal or questionable coverage areas, field trials at representative sites would be carried out to determine what level of performance could be achieved using high gain antennas. However, the review indicated that the use of standard antennas would most likely be adequate and it was understood that the situation was broadly similar in other member states of the EU.

#### **f. Web server**

The operation of the web server was simulated with synthesised data. Programs running on one web server simulated the operation of the remote data-logger by sending daily HTTP requests containing small amounts of data to a second web server which stored these in a text file. A number of other database issues were addressed, which would allow the system to easily be scalable to a large number of sensors. The field trials in task 2.3 included simulations of such systems.

## 2) Shaft Imaging in Low Visibility Conditions

Within Task 1.2.1 (development of effective techniques for use in water-filled abandoned shafts with potentially turbid media) was considered. An initial scoping exercise with a view to recommending areas for further research and development work was undertaken. Many of the techniques reviewed (Table 2.3.1.2.1-1) were discounted on technical and high cost. A programme of experimental work, based on the most promising technologies consistent with sufficiently low cost for adoption in the field, was undertaken.

		Comments
<b>Standard Borehole and Shaft Optical Imaging Systems</b> , i.e. equipment currently used in shaft imaging and equivalent in other industries		Acceptable performance in air, poor in flooded shafts, especially in turbid water
<b>Incremental Improvements to Optical Imaging Systems</b>		Potential improvements include the use of monochromatic light (the exact colour of which might depend on the degree of turbidity), wide separation of lamps from camera, and perhaps the use of polarising filters.
<b>Advanced Optical Techniques</b>	Side illumination by scattering of laser light	This technique is offered only by one supplier. It appears to offer no advantage so long as the increased equipment width required for separating the lamps from the camera can be tolerated or a telescopic arm arrangement engineered.
	Gated cameras	Impressive performance has been demonstrated.
	Laser scanning	Impressive performance has been demonstrated
	Ultra-low light cameras	Based on discussion with manufacturers it appears that this technique, although useful in clear water, will show minimal benefit in turbid waters.
	Synthetic aperture Techniques	To date only academic studies have been carried out. The necessary arrays of mirrors would be difficult to 'ruggedise' for use in a hostile environment (i.e. a flooded shaft).
	Software solutions	A variety of techniques has been demonstrated. Most are at the research and development stage.
<b>Ultrasonic Techniques</b>	Shaft wall sonic signature	This technique doesn't actually produce an image. Beyond the scope of this project.
	Borehole Imaging Scanners	It is anticipated that borehole imaging scanners, while offering the ultimate in environmental protection, do not lend themselves to shaft imaging.
	Underwater Imaging Scanners	The presence of numerous products from a number of suppliers suggests this is a mature technique, despite the fact it is not generally employed for shaft imaging.
<b>Contact Methods</b>	Ultrasonic Methods	These techniques are considered supplementary to the main theme of shaft imaging in that they would be used for follow-up investigations in the event that one of the other methods revealed a potential failure. They are included for completeness but are not recommended for further research within this project.
	Impact Methods	

**Table 2.3.1.2.1-1 Summary of Survey Techniques Reviewed**

A programme of experimental work was carried out to determine the level of improvement that can be obtained by using various incremental improvements to the current generation of optical imaging equipment.

The test rig comprised a portable, above-ground, circular swimming pool with a maximum diameter of 4.6 m. Because the pool walls bulge out to the maximum diameter at a height of about 500mm, and because a brick wall had to be built in the pool to act as an imaging target, the maximum imaging range was 3.1m, equating to a maximum shaft diameter of 6.2m. A structure which allowed a CCTV camera and several lights to be fixed in position with respect to each other, and to the optical target, was immersed in the pool. Utilising information taken from a wide range of mine water samples turbidity was provided by an amount (16mg/l) of Fuller's Earth placed in the pool and agitated at the start of each test. (Figure 2.3.1.2.1-1).



*Complete Assembly for the Maximum 3.1m Imaging Range*



*Complete Optical Target*



*Filling the Pool*

*Figure 2.3.1.2.1-1 Optical Imaging Test*

The following techniques were used in various combinations for the two ranges (i.e. from the camera to the optical imaging target) of 1.1m and 3.1m:

- use of green and blue monochrome light, with white light for comparison,
- separation of the lights from the camera, with zero separation for comparison,
- the use of cross-polarised filters over the lights and camera, with no filters for comparison.

### 3) Laser Scanning of Shafts

Field trials of a commercial ultrasonic imaging device were conducted at Collins Green No 2 shaft in the U.K. The results of the field trials are reported under Task 2.3.

In this field, the objective is to develop an inspection methodology of shafts, in terms of nondestructive techniques, so an accurate evaluation of its long term stability can be performed. The first approach to perform a laser scanner survey campaign in a shaft was realized using the standard static 3d-technique. In November of 2007, a shaft measurement was carried out at the former mine 'Lohberg' (Diameter: 6.3 m) shortly before it was closed. The main aim of the survey campaign was to capture a maximum of shaft data with existing equipment while the shaft was still accessible. The data is to be used as reference for future surveys, then to be performed with a new dynamic survey system to be developed in the project.

#### Laserscanner Survey

Scanning the shaft, (Figure 2.3.1.2.1-2) could yet only be done in a static way, using the existing laser scanner 'Imager 5006' from Zoller + Fröhlich. The scanner was fixed at a bracket in a headover-position beneath the hoist cage, while all scanner control was done from within the cage.



*Figure 2.3.1.2.1-2 Scan image of reinforced shaft area*

### **Development of a Shaft Survey System**

As the situation for future logging shaft campaigns will be totally different, a new suitable shaft survey system, consisting of the following components is going to be developed:

#### **a. 2D-Laserscanner ('Profiler')**

Initially, the use of the 3D-Laserscanner 'Imager5006ex' was planned, which actually is being developed in cooperation with Zoller+Fröhlich. Due to new and higher requirements, instead of the 3D-Scanner a 2D-Scanner ('Profiler') will be considered.

The development of the 2D-Scanner will be based on components of existing laserscanners from Zoller+Fröhlich, which are able to fulfil the main technical requirements for the kinematic use (speed, range, precision).

#### **b. ISSM**

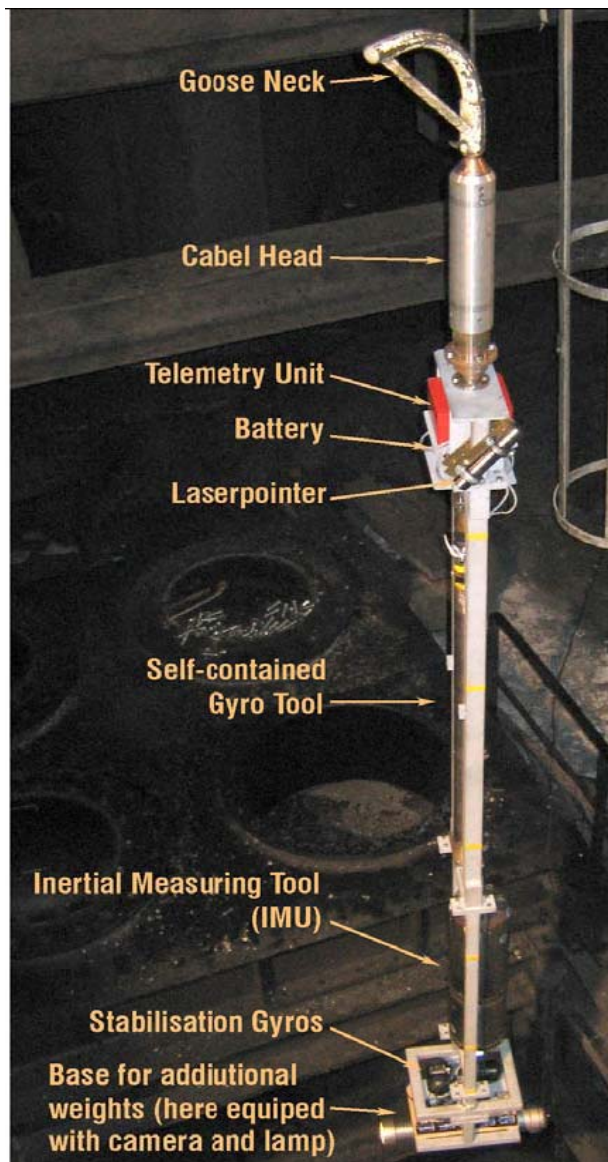
An inertial measurement system is essentially made up of three acceleration sensors and three rotational sensors (gyroscope), whose measurement axes are orthogonal to each other. An inertial surveying system for shaft applications has been developed, the ISSM (Inertial Shaft Surveying Mining).

### **Examinations for the measuring and processing of the carrier system's proper motions**

Earlier investigations have shown that the quality of the final laser scanner results is fundamentally dependent from the prevention or measuring and processing of the occurring carrier system's proper motions. As the motion dynamics of the whole system cannot fully be predicted by simulations, a campaign of pre-examinations for estimating the magnitude of the motion components which have an effect to the system was carried out. The results are used for the dimensioning of the inertial measurement system und for the possibly necessary gyroscopic stabilisation.

The investigations took place in shaft 'Lohberg2', which was put out of service shortly ago. To allow several combinations to be tested, a special frame was manufactured, (Figure 2.3.1.2.1-3). It consists of the following:

- 'Goose neck' to protect the cable, when straighten up / laying down the frame
- Rotary and lockable cable head
- Telemetric unit for signal conditioning for the cable and control of the stabilization gyros



- Battery supply for the stabilisation gyros
- Laser pointer for distance measuring to the shaft wall
- ‘Self-sustaining Gyro Tool’ for online monitoring of the frame behaviour
- ‘Inertial Measuring Unit’ (IMU) for logging
- Stabilisation gyros
- Base for additional weights
- Several logging runs were carried out with different speeds, different weights, with or without stabilisation gyros etc.

The Investigations of the carrier systems proper motions led to a lot of new information for the design of a shaft laser scanning system. The main statement regarding the dimensioning of the laser scanner unit is the fact, that the motion in x-direction can be properly detected by the depth measuring system included in the winch. The most distinctive motion is the rotation pendulum movement around the vertical axis.

Hence the gyroscope of the vertical axis has to be the most accurate. The design foresees to have a Ring Laser Gyroscope (RLG) for the vertical axis and two Fibre Optic Gyroscopes (FOG) for the vertical axes.

In the (Figure 2.3.1.2.1-4) the tool frame with sensor equipment is shown.

**Figure 2.3.1.2.1-3 Tool frame with sensor equipment**

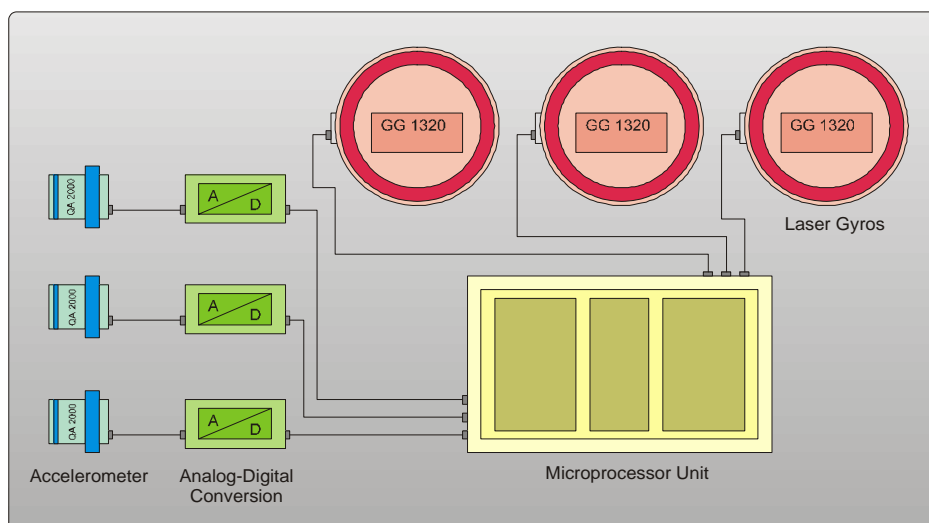


**Figure 2.3.1.2.1-4 Tool frame with sensor equipment**

The disadvantage of this design is, that a coning of the system significantly effects the drift of the Ring Laser Gyroscope. If then the accuracy of the Fiber Optic Gyroscopes will be sufficient to compensate that movement, has to be determined by intensive simulations. The savings that were expected with the implementation of two lower accuracy gyroscopes may then be compensated by the additional simulation work.

The profiler manufactured by Zoller + Fröhlich (ZF) matches the requirements best. ZF is already a partner of DMT in another laserscanner project and therefore contractual issues are well defined. RIEGL and Fraunhofer scanners have not been considered, partially due to higher costs or lack of cooperation interest.

In several discussions with the experts from Zoller + Fröhlich, the objective was to define the exact parameters. The demands of the decision table are to be fulfilled, but the requirements have to be reduced to a practicable minimum. Hence standard components should be used without the need for unnecessary additional development effort.

- Mirror speed: Current speed of the Imager5006 is 25Hz (50 Hz in profiler mode) -> No need for additional development effort
- Logging Rate: Max. Rate is currently 500kHz. For 10m shaft distance and a mirror speed of 25Hz the logging rate is app. 125kHz -> The logging rate is sufficient
- Logging Range: A range of 0 to 79m is technically possible. Currently it is reduced to larger than 0,5m due to laser safety reasons. -> A range of 15cm to more than 10m seems to be appropriate and achievable.
- Accuracy: defined to 3,5 mm (1 Sigma, 10m distance, 10% reflectivity) Temperature compensation is important. -> A calibration bolt, which temporarily moves into the laser beam is aspired. This would minimise the shadowing.
- Laser Power: Highest allowed laser class is 3B (max. 150mW). Visibility is not necessary. -> The laser class will be chosen due to safety and measurement aspects.
- Atmosphere: 0 to +40°C. Condensing atmosphere is generally not expected. -> No technical additions like air flushed windows/mirrors are planned. In worst case the tool can be heated prior to logging.

Due to unforeseeable lacks in development capacities, pronounced on side of ZF, alternatives had to be studied, thus resulting in a delay 6 months. As the research didn't show satisfying alternatives, the strategy in the cooperation with the profiler manufacturer had to be changed. To minimize the dependence on the manufacturer's development capacities, DMT acquired necessary standard profiler components to be able to finalize the profiler design and continue the development of the measurement system.

Based on the design of most existing laser scanners, the first design concept included a large hollow shaft for driving the external mirror. This shaft was the motor armature at the same time. The difficulty existed in the demands for the device to be operated in explosive atmosphere. A double protection is necessary as the device will be operated in shafts with permanent CH<sub>4</sub> atmosphere.

The general protection is a flameproof enclosure. Additionally the tube will be filled with an inert gas under overpressure. With the large hollow shaft it will be impossible to keep this overpressure. The solution was to plan an extra chamber and set up the motor as intrinsically safe or to extra mold it. This would mean a rather high effort in the examination process, apart from the difficulty to manufacture such a special motor.

### c. Carrier System / Probe

The carrier systems will have the appearance of a probe (cylindrical, edgeless) with the probe head connected to a cable. The system will be separated into several sections, which require different forms

of explosion-protection. Due to some requirements the probe should be able to reach a depth of 1000 meters. In terms of expected weight and dimensions, the probe might approach 200 kg and have 300 mm in diameter and 2 m in length. Hence the data cable must be of adequate length, which will – together with other cable parameters - affect the type of winch.

After the change in strategy of cooperation with the profiler manufacturer, DMT acquired necessary profiler components by Zoller+Fröhlich. At the same time the support of the DMT engineers by Z+F engineers was acknowledged, thus enabling DMT to proceed the development with its own development capabilities.

### Scanner Components

The main components provided by Zoller+Fröhlich, (Figure 2.3.1.2.1-5) are the following:

- Laser Generation Unit  
This unit generates the two laser beams of different wavelength for the phase difference measurement and detects the reflected beams
- “LARA”-Box  
The analogue signal from the laser generation unit is measured and digitized. It also controls the LGU in means of intensity and safety.
- Central Processing Unit  
All data from the LARA-Box is collected and stored with precise time information. All software runs on a real time operating system. This board represents the interface to the command pipe.
- Rotating mirror  
High precision mirror for converting the single dimensional beam into a two dimensional slice.

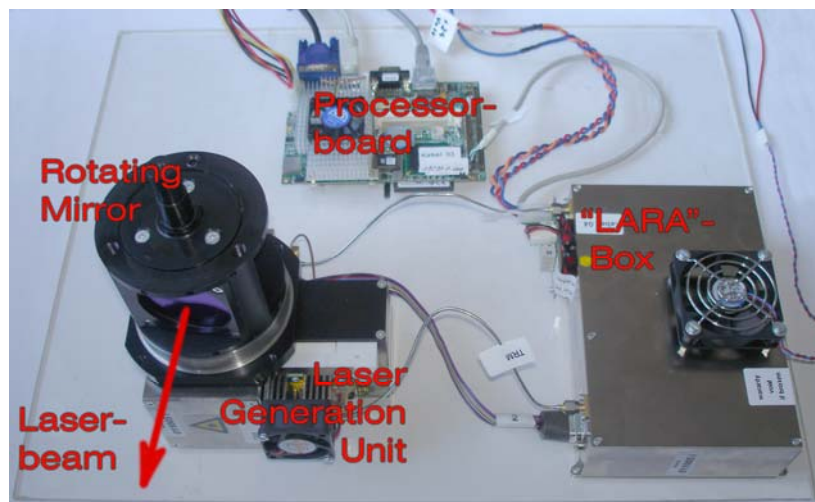


*Figure 2.3.1.2.1-5 Components of the Laser Scanner*

## Collision Detection

For collision detection it was decided to implement a SwissRanger SR4000, (Figure 2.3.1.2.1-6). This device doesn't only deliver images of the region ahead (below the scanner), it also gives information about the distance.

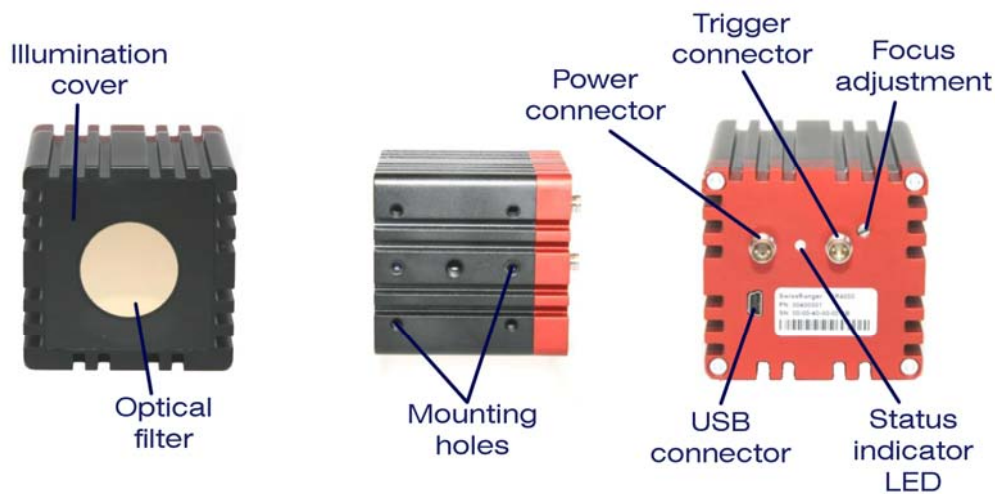


*Figure 2.3.1.2.1-6 SwissRanger SR4000 for collision detection*

The principle behind is quite similar to that of the laser scanner itself. A light source is modulated, and the back scattered light is sampled with a CCD sensor. Time of flight (TOF) and phase shift give information about the distance from the camera.

## Scanner Design

The most important key point in the design of the scanner is the strong coupling between the demands of the safety enclosure and the proper function of the rotating mirror.

The protection type of the scanner is a combination of pressurized and flameproof enclosure (as other combinations or intrinsic safety are not realizable). However the rotating mirror has to be placed outside the enclosure, resulting in the demand for a force transfer through the enclosure.

As a result from former considerations, a belt drive outside the housing and a thin shaft feed through were thought to be the best solution. However detailed design showed the difficulty to combine frictionless feed through and gas tightness. Hence another design concept was followed up:

The rotating mirror is bedded outside, and the laser beam will be feed through a flameproof glass window. The driver will totally stay inside, and the force will be transmitted via a strong magnetic coupling. The advantage of this concept is the totally tight enclosure for the price of much more effort in synchronisation of the mirror.

### 2.3.1.2.2. Task 1.2.2. Roadways survey using innovative geophysical tools

After analyzing the possibilities of the geophysical methods more common to assess the state of the roadway, the Ground Penetrating Radar (GPR) and the Tunnel Scanner have been chosen, as the most promising.

To evaluate the effectiveness of these two methods, two trials were performed in two different tunnels, with the following results presented here below.

Additionally in a final section a new experimental method called Capacitive Resistivity Imaging (CRI) is presented, which has good prospects for a near future.

## A.- GPR-3D

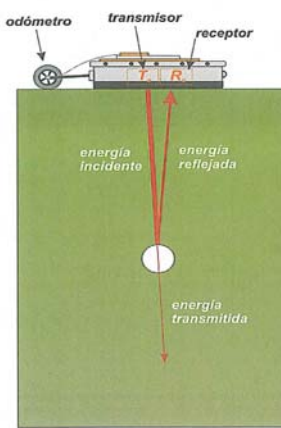


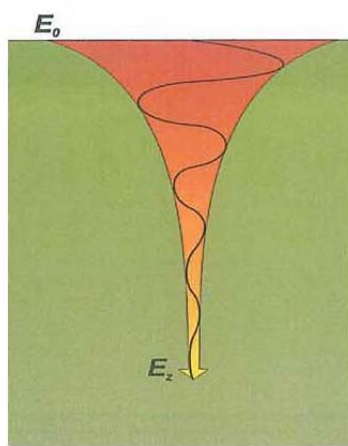
**Figure 2.3.1.2.2-1**  
**GPR Fundamentals**

The GPR Works by emitting into the ground an electromagnetic pulse and picking up through an antenna the rebound from the emitted signal when it gets to an anomaly in the dielectric properties of the medium in which it travels. In (Figure 2.3.1.2.2-1) this concept is exposed.

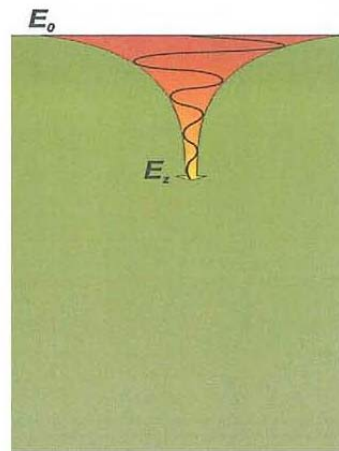
In the use of the GPR for detecting anomalies in the backfill of the tunnel or on the ground in which these tunnels are excavated must take into account the problem of the signal attenuation, depending on their frequency.

As shown in (Figure 2.3.1.2.2-2), the high frequency signals have a much higher attenuation than the low frequency, but it must be taken into account that high frequency signals have a lower resolution than high frequency

signals.



**I.- Low frequency signals**  
**Señal de baja frecuencia**



**II.- High frequency signals.**

**Figure 2.3.1.2.2-2 Attenuation of GPR signals.**

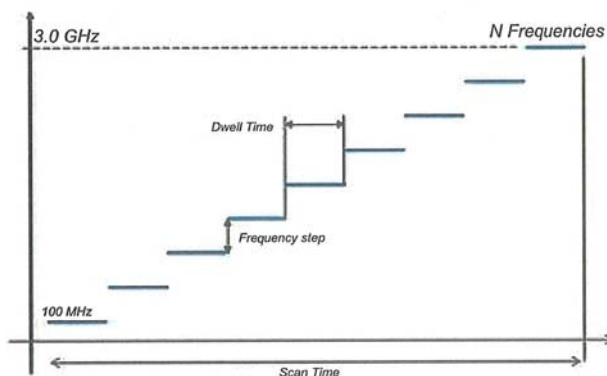


**Figure 2.3.1.2.2-3 Frequency variations**  
**in a three-dimensional antenna**

MHz to 3 GHz. This provides a high resolution in the surface layers and good depth of research as shown in (Figure 2.3.1.2.2-3).

The most innovative GPR's use so-called three-dimensional antennas, operating on different frequencies, which by combining different attenuations and resolutions, allow to obtain three-dimensional images from the inside of the ground.

In the application that has been performed of this technology in the Tunnel of Archidona (Malaga, Spain) a 3D antenna made of 29 individual elements spaced by 7,5 cm, has been used, so in each scan 29 simultaneous profiles are recorded from which the three-dimensional model is obtained, about 2,1 meters wide. The frequency range that this antenna can cover goes from 200



**Figure 2.3.1.2.2-4 View of a three-dimensional antenna, Step-frequency type and towed by a Vehicle during the works.**

To carry out the inspection, the equipment must include a sender and a receiver device, and it should be displaced at a relative constant speed, as shown in (Figure 2.3.1.2.2-4).

To check the effectiveness of the GPR with a 3D antenna, a data collection campaign was performed in the Tunnel of Archidona (Malaga, Spain).

In total there have been performed four multi-antenna sweeps over the ground's surface inside the excavation. Each sweep of the antenna provides a model of 2.1 meters width and the length of the sweeps has been of 360 meters. The sweeps of the antenna are parallel to each other, overlapping each other to facilitate the final

assembly of the corresponding models, obtaining as a result a total area of research of 6 x 360 meters.

The GPR data was recorded with a multichannel 16 bits equipment, using a frequency range between 100 and 800 MHz, with measurement intervals of 2,5 MHz. GPR reading were made every 7,5 cm, which were measured with a specific GPR odometry wheel.

Once the information of the GPR is processed a three-dimensional image of the surveyed ground is obtained, which, for a better understanding is cut in several horizontal planes. In (Figure 2.3.1.2.2-5) the planes levels at depths of 0,25 m, 1,8, 3,2 m and 3,8 m corresponding to a stretch of 120 m of the Tunnel of Archidona are shown.

The results obtained with the GPR-3D in the Tunnel of Archidona show that this innovative technique offers results much more accurate than the traditional GPR and allow to detect, with reliability, the existing voids in the ground to a depth of about 10m.

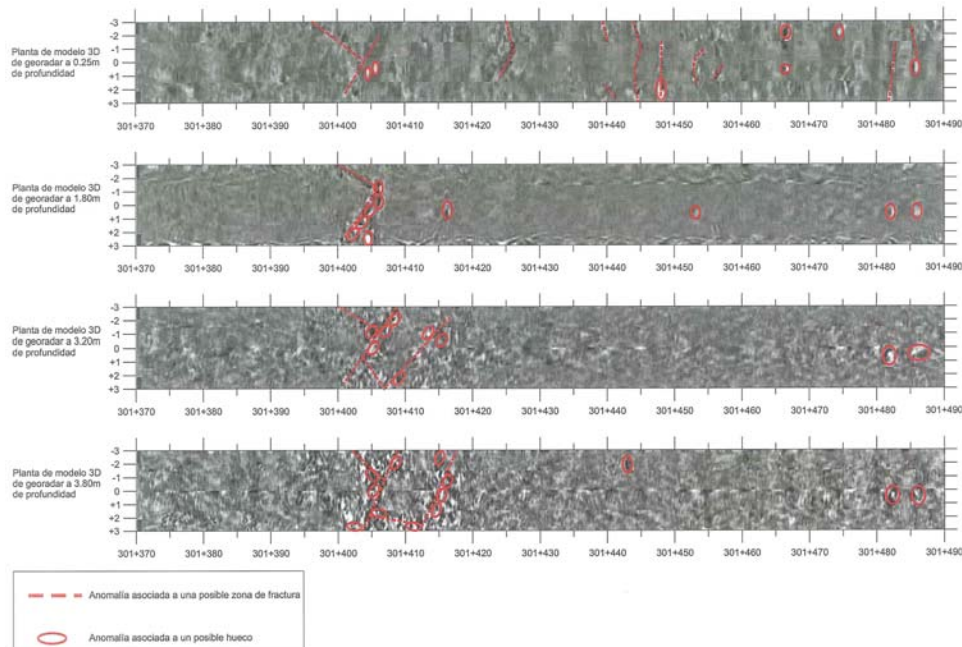


**Figure 2.3.1.2.2-5 Survey results with the GPR-3D.**

**B.- TUNNEL SCANNER TS-360**

The “Tunnel Scanner 360” system, developed by the German company Spacetec, allows to recognize the estate of roadways and tunnels and it’s geometry, in a Fast and accurate manner.

This system has the three following channels:

- VISUAL: Records real time image inside the tunnel.
- PROFILE: Provides a continuous profile of the tunnel.
- THERMOGRAPHY: By measuring the temperature variation on the outer surface of the tunnel lining, it is able of determining its state and the areas where there are anomalies in the backfill.

The two first channels, VISUAL and PROFILE use the laser technique, while the so-called THERMOGRAPHY uses the technique of temperature measurement by infrared rays.

The equipment to perform inspections for the TS-360 is composed of a trunk that is mounted in a Vehicle, as shown in (Figure 2.3.1.2.2-6).

The TS-360 has a laser emitter which through a rotation mirror, runs around the perimeter of the tunnel, and while the vehicle that supports the Tunnel Scanner moves forward a three-dimensional image of the perimeter of the excavation ton inspect is obtained.

In (Figure 2.3.1.2.2-7) the operation of the TS-360 is shown.



*Figure 2.3.1.2.2-6 Tunnel Scanner mounted on a wagon*

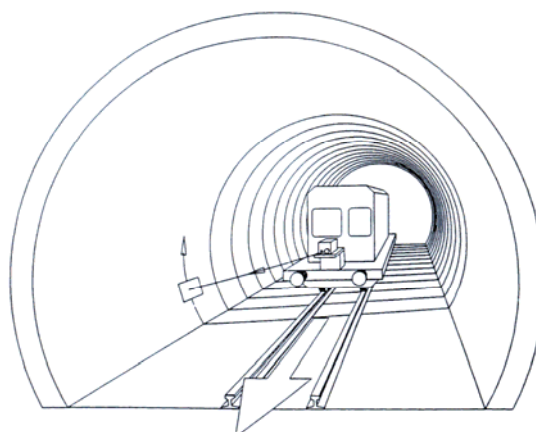


*Figure 2.3.1.2.2-7 Operating principle of the “Tunnel Scanner”*

The resolution of the TS-360 depends on the Lumber of pixels recorded in the equipments, on the Tunnel radius, and its translation velocity, as shown in (Table 2.3.1.2.2-1).

TUNNEL RADIUS (m)	RESOLUTION CHOSEN (Pixel)	TRASLATION VELOCITY (km/h)	RESOLUTION (cm)	
			TANGENTIAL	RADIAL
2	2.500	3,6	0,5	0,5
	2.000	1,8	0,25	0,25
4	2.500	7,2	1,0	1,0
	2.000	3,6	0,5	0,5
6	2.500	10,8	1,5	1,5
	2.000	5,4	0,75	0,75

*Table 2.3.1.2.2-1 Resolution of the TS-360.*

The TS-360 can operate with the three operating modes listed here below.

## **Visual mode**

Its operation is based on the radiation of a laser beam, sent abroad through a rotating mirror. This beam illuminates sequentially around the whole perimeter of the tunnel, capturing the same mirror image through photogrammetry the visual contour. The collected signal is sent to the internal processor that makes it digital, achieving an optimal contrast between points, fundamental for further interpretation.

The simultaneous collection of visual image and geometrical data provides a perfect location of each point, necessary for the correct interpretation of the information.

## **PROFILE CHANNEL**

This channel provides a high frequency modulator beam, which allows from the gap between the transmitted and received signals, to determine accurately the distance to each one of the registered points.

This information, combined with the one provided by the positioning system from the vehicle, provide a perfect three-dimensional representation of the tunnel thanks to:

- The 2.500/2.000 points taken in each revolution.
- The spacing between two successive profiles of less than 1 cm..

As it is easily seen, if the mirror rotates at 200 revolutions per second and in each round 2.500 points are recorded, 500.000 points are being recorded for each second of recognition, which gives an idea of the magnitude of the computer files generated.

## **THERMOGRAPHICAL CHANNEL**

The TS-360 incorporates an infrared camera that allows to measure the temperature of each point on the perimeter of the excavation with an accuracy of 0,1 °C. This manner, a thermal image can be obtained, which is associated with the presence of cracks in the perimeter of the tunnel, where the temperature is lower, as voids next to the wall of the tunnel and the presence of water in the ground.

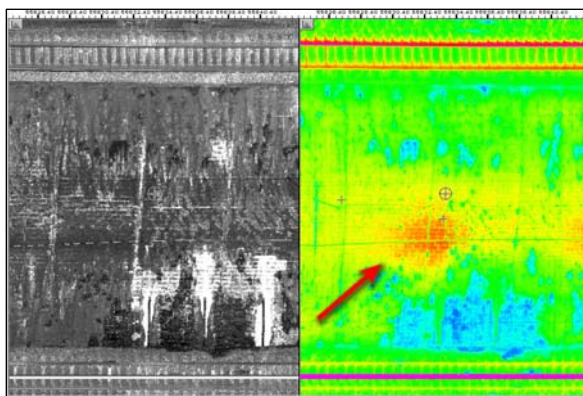


*Figure 2.3.1.2.2-8 Comparison between the visual channel and the thermographical channel where thermal anomalies in the backfill are seen in the backfill associated with the presence of voids.*

Through the software TUVIEW, of the TS-360 a comparison between the visual channel and the thermographical channel can be performed, thus being able to find voids in the backfill of the lining due to the generated air gradient in the void. In (Figure 2.3.1.2.2-8) an example of the comparison between the visual record and the thermographical record is shown.

In the Tunnel of Abdalajís (Malaga, Spain) a state inspection of the surface using the computer perimeter TS-360 was performed.

The inspection performed with the TS.360 has allowed to inventory all the points of upwelling water in the tunnel and also to locate the damage to the segments and to locate the existing crack on the surface of the tunnel perimeter.

In (Figure 2.3.1.2.2-9) one of the outputs of the TS-360 in the Tunnel of Abdalajís is shown.

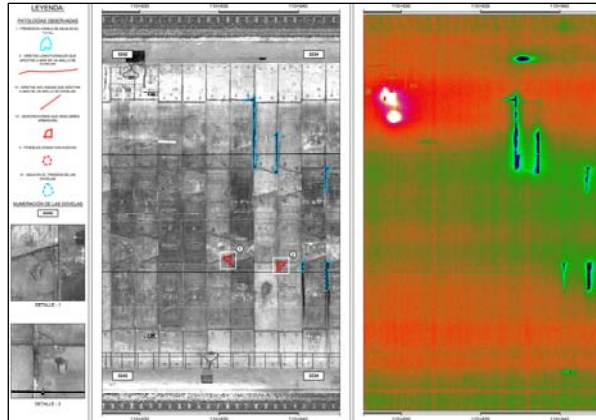


**Figure 2.3.1.2.2-9** The result of applying the TS-360 to the Tunnel of Abdalajís.

### C.- CRI

Capacitive Resistivity Imaging (CRI) is a technology that allows to obtain in a Fast manner an three-dimensional image from the subsurface with a resolution in the order of centimetres, through sensors with electrical resistivity capacity arranged in multiple dipole that do not require pre-ground anchor.

The physical basis of this technique is very similar to conventional electrical tomography, which principal is to deliver electric currents to the subsoil and to measure through electrodes the potential difference between them. Increasing the distance between the electrodes increases the depth of investigation.

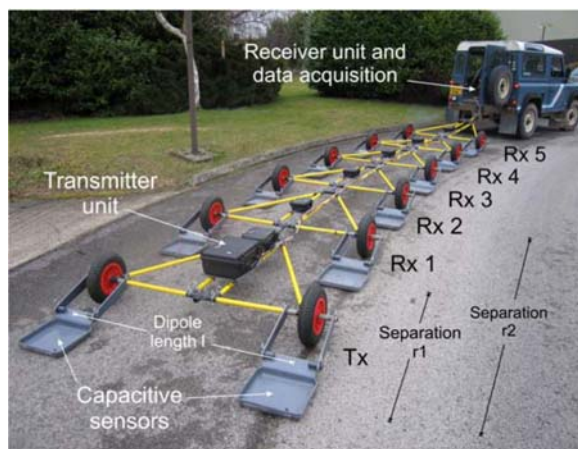


**Figure 2.3.1.2.2-10** Functional diagram and devices thar make up the CRI towed by a vehicle.

As shown in (Figure 2.3.1.2.2-10) the device can be attached to a mechanic vehicle, which allows to investigate large areas, in order of 150x25 m in one day of work.

The Data Unit controls all the time the position of the dipole through a GPS and records around 100.000 data points in a few hours. To process this vast amount of data and to generate images of resistivity, inversion methods of algorithms are used, similar to those developed for the conventional electrical tomography.

The CRI allows to recognize grounds with an electrical resistivity contrast, to a depth of 3-4 meters from the surface, especially suited to detect voids, areas of weakness, fracture zones, or stretches of

water input, in the backfill of underground works.

(Figure 2.3.1.2.2-11) shows as an example a plant resistivity's obtained by the CRI which allowed to detect the position of a mineshaft.

As shown in (Figure 2.3.1.2.2-12) it is possible to generate images at different depths, which allows to obtain a three-dimensional view of the underground resistivity's, showing in this case the geometry of the void.

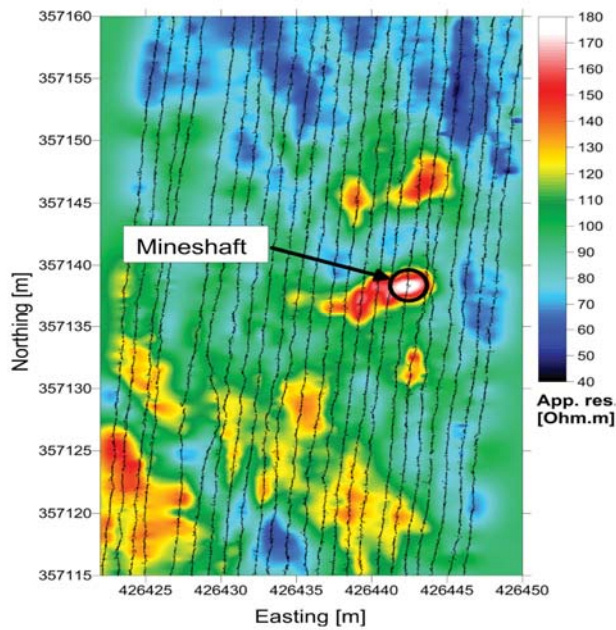


*Figure 2.3.1.2.2-11 Underground resistivity image obtained through CRI, which shows the position of a mineshaft.*

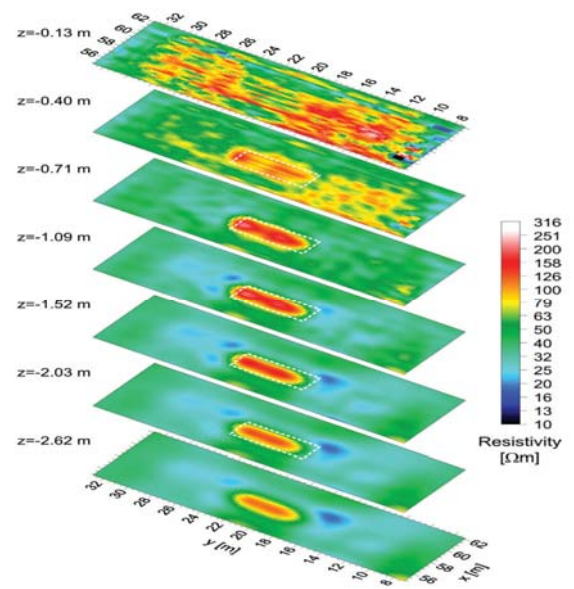


*Figure 2.3.1.2.2-12 Underground resistivity's sections at different depths obtained with the CRI. Geometry of a mineshaft detected.*

From the images provided by the CRI it was possible to locate a mineshaft, as shown in (Figure 2.3.1.2.2-13), whose section was 1 m wide by 4 m in length.



*Figure 2.3.1.2.2-13 Aspect of the mineshaft detected with the CRI.*

### 2.3.1.2.3. Task 1.2.3. Effect of mine water on concrete, reinforce concrete and fill materials

#### Adverse effects of mine water pollutants on fill materials

The objectives of Task 1.2.3 were to provide further information on the adverse effects of mine water to improve knowledge of the geochemical processes required to enable a more accurate monitoring and prediction of surface hazards relative to abandoned coal mine shafts. The following activities have been carried out within this sub Task:

- Evaluation of first response hazard data held my MRSL at the start of the project.
- Analysis of the components wich lead to the collapse of coal mine shafts and the rsultant subsidence problems.
- Study and quantification of the adverse effects of mine water pollutants on fill material types and

support, including laboratory test.

An evaluation of first response mining hazard data in the UK held my MRSLS was made at the beginning of the project. This research considered timing of collapse (month), superficial and solid geology, date of abandonment and depth of associated workings. The review of data indicated that, in general terms, most of the shafts (87%) that had become exposed are shallow in depth (<100m), with obscure or unknown information associated with them and abandoned for more than 50 years. (Figure 2.3.1.2.3-1) Over 20% were located within unstable superficial deposits. (Figure 2.3.1.2.3-2) The majority of incidents occurred in the early spring when the ground temperature and rainfall were both rising.

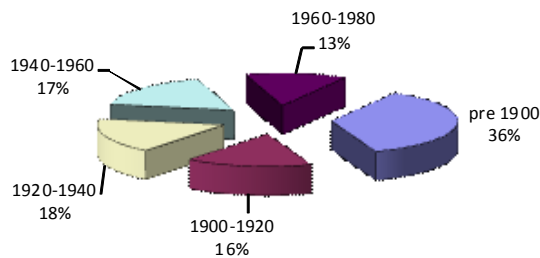


Figure 2.3.1.2.3-1 Age of last working

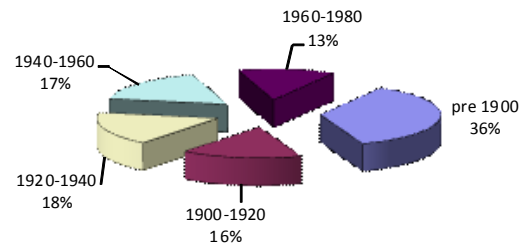


Figure 2.3.1.2.3-2 Superficial Conditions

An element of the quantification of the adverse effects of mine water pollutants was the study of the stresses existing around mine shafts. The mechanisms involving the collapse of a shaft are numerous and complex and the objective of this element of the research was to analyse components leading to the collapse of shafts and the resultant subsidence problems. Work carried out on the stress analysis of shaft linings dealt with the theoretical development of equations required to calculate stress build up within linings and effects of flooding with water.

From the work carried out in adaption of thick cylinder theory to mine shaft linings determinations of the following are possible:

- Distribution of radial and circumferential stresses in the lining.
- Longitudinal stress in the lining.
- Changes in the internal and external diameter of the lining.
- Changes in circumferential (hoop) and radial stresses in the event of the shaft flooding.

In order to show variations of stress in open and flooded shafts example calculation were made using Lamé's solution  $\delta_r = A - \frac{B}{r^2}$  and  $\delta_\theta = A + \frac{B}{r^2}$  to determine radial and hoop stresses at the outer and inner surface of shaft lining. (Table 2.3.1.2.3-1).

	Radial Stress MN/m <sup>2</sup>	Hoop Stress MN/m <sup>2</sup>
<b>Normal Mineshaft</b>		
Inner Surface	0	32.73
Outer Surface	5	27.73
<b>Water Filled Shaft</b>		
Inner Surface	2	21.64
Outer Surface	5	18.64

Table 2.3.1.2.3-1 Example Calculations showing changes in stress due to flooding

This work was applied to a number of individual cases in which the long term stability of the mine shaft was considered.

Immersion tests involving 3 liquid groups (public water supply, static acidic mine water and continuous flow of acidic mine water) designed to

- Obtain information relative to deterioration of both shaft lining and shaft fill materials.
- Obtain data related to the loss in volume of material especially those used for backfilling as a subsidence inducing mechanism.

were implemented. The range of materials (Figure 2.3.1.2.3-3) chosen for the immersion tests were:

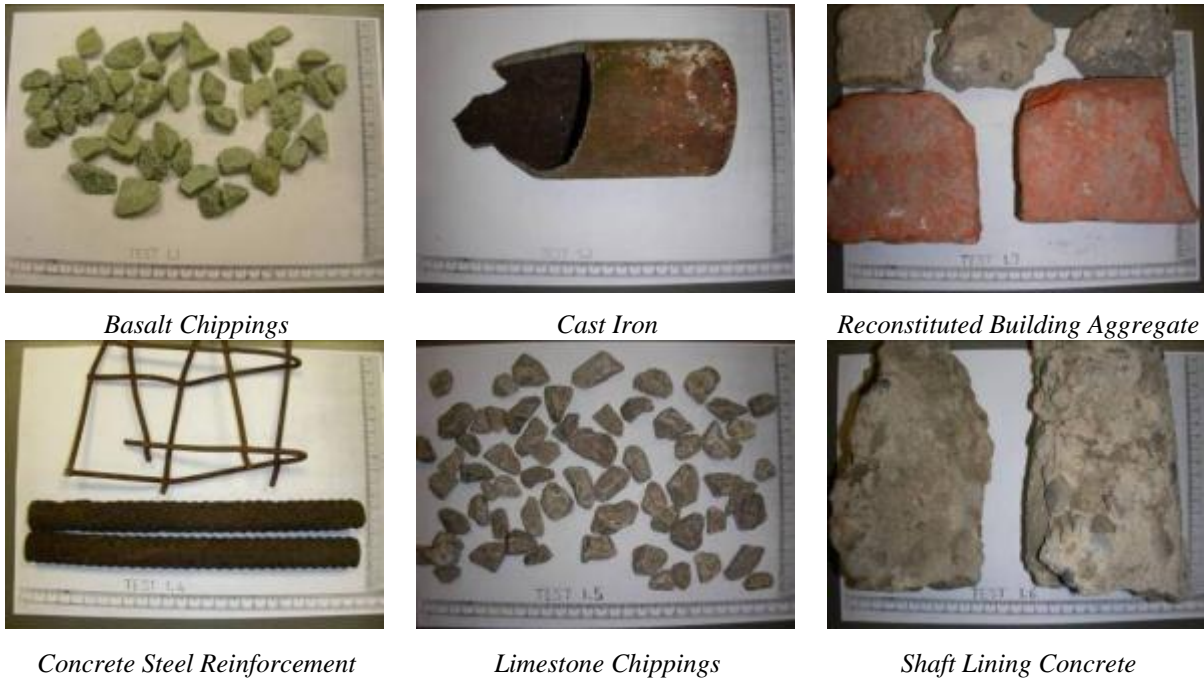


**Figure 2.3.1.2.3-3 Materials chosen for the Immersion Tests**

Material	Remarks
Basalt	Fine grained igneous rock not normally found in close proximity to coal mines. Igneous material, having no quartz content sometimes chosen as fill material to meet specific engineering requirements. Competent and potentially mine water resistant material.
Cast Iron	Used throughout as specialised shaft lining material to prevent ingress of water.
Reconstituted Aggregate (Crushed Brick / Concrete)	Readily available and cost effective fill material for disused mine shafts.
Steel Reinforcement.	Used with concrete in shaft lining. Fixtures and fittings within mine shafts.
Limestone	Either Permian or Carboniferous, normally found in close proximity to coal mines in the UK - used for infilling mine shafts.
Concrete	Used as shaft lining.

After the samples were collected and cleaned, they were all air dried at room temperature to a constant weight. Consideration was given to number of tests that can be practically established and to fit within the scope of the project and ensure ability to complete work within the other tasks and sub-tasks of each work package involvement.

Each of the chosen test materials was subjected to all three test groups giving the establishment of eighteen individual test immersion tanks. The test set up was established in a room where temperature control and ventilation was possible. The temperature was set to 20°C. The water base line and stagnant acidic mine water tests were initiated by filling the tanks with liquid to the maximum fill level. This level was maintained with water to combat evaporation loss and ensure complete and constant soaking of all the test materials. The pH was monitored from test initiation using the data logging equipment for several hours to monitor the initial reaction rates.

The immersion tests consisted of three groups:

- Immersion test in potable water and left to stagnate - to be used as a base line comparison
- Immersion test in acidic mine water and left to stagnate
- Immersion test with continuous flow of acidic mine water.

The immersion tests with the continuous flow of acidic mine water were initiated by first filling the immersion tanks with the acidic mine water up to the overflow outlet port. The flow from the header tanks was then released and maintained at the lowest possible flow rate to simulate a slow percolation or up welling flow. The tests were initiated at the earliest possible opportunity and were maintained for the longest possible period during the project lifespan. The tests were terminated at a time deemed adequate to allow final observations, recording final measurements, sample preparation and the carrying out of special tests and analysis to be made. Extracts from the logging of pH are shown graphically in (Figures 2.3.1.2.3-4) and (2.3.1.2.3-5) for potable and acid mine water. Equipment failure required termination of Test Group 3 after 46 weeks.

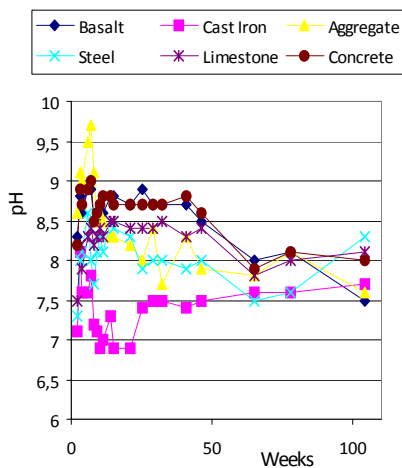


**Figure 2.3.1.2.3-4 pH Values Potable Water**

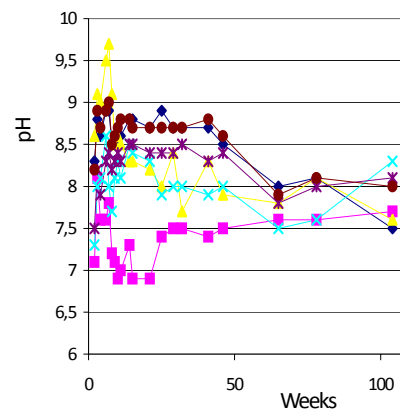


**Figure 2.3.1.2.3-5 pH Values Acidic Mine Water**

Whilst pH readings were being taken it was noticeable that degradation to the immersed samples was occurring as indicated in (Figure 2.3.1.2.3.-6).



**Figure 2.3.1.2.3-6 Degradation of Tests Samples**

The samples were recovered, dried and reweighed with the following results (Figure 2.3.1.2.3-7):

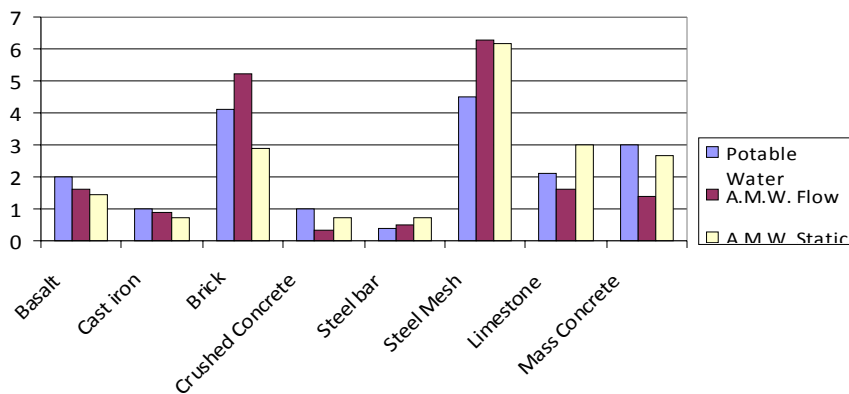


**Figure 2.3.1.2.3-7 Percentage Loss in Weight Long Term Immersion Samples**

Analysis of the test results indicates the following mechanisms for degradation of potential shaft fill and construction materials from the adverse effects of acidic mine water. (Table 2.3.1.2.3-2)

Test	Results	Observations
Basalt	1-2 % weight loss for all test solutions	White deposit likely to be calcite and other carbonate minerals which have precipitated out of the potable water solution system. Calcite is known to precipitate out at a pH of approximately 9. Calcium-containing minerals are more likely to be dissolved in AMW.
Cast Iron	<1% loss for all test solutions	Weight loss data is not necessarily equated to amount of material lost from the original samples. There can be mass increases for example, when iron is converted to iron oxide, the mass of iron oxide is greater than the mass of iron alone due to oxygen
Reconstituted Aggregate	Brick 3-5% Concrete <1% weight loss for all test solutions	Large mass losses for brick are possibly due to leaching from the clay component and/or binder of the brick material or the result may be due to the porous nature of the material. Mass loss of concrete aggregate due to chemical leaching effects on

Test	Results	Observations
		the smoother grained matrix.
Steel Reinforcement	Bar <1% Mesh +6% loss for all test solutions	Mass losses are greater in the mesh materials due to the larger surface area of iron exposed to the test solution.
Limestone	1.6-3% weight loss for all test solutions	Mass losses with all solutions tested are similar for the limestone and the weathered concrete. Limestone is predominantly calcium carbonate. Suggests that the extent of calcium carbonate in the weathered concrete surface is high considering that calcium carbonate is one of the main reaction products in carbonation
Concrete	1-3% weight loss for all test solutions	Greater mass loss from the weathered mass concrete than the concrete associated with the aggregate. Weathered concrete is likely to be more carbonated on its surface than the 'freshly' crushed concrete. Material lost in the dissolution process of the weathered concrete within the test system does not affect the pH of the solution

**Table 2.3.1.2.3-2 Mechanisms of Degradation**

**Methods to neutralise the adverse effects of mine water pollutants**

To complement the research on quantification of the adverse effects of mine water pollutants additional research on identification of means of neutralising the adverse effects of mine water pollutants upon shaft fill, shaft lining and shaft capping was completed. The work covered both practical and literature research and creation of a “flash fill” material for sealing of mine shafts utilising mine discard.

Research criteria covered the following topics:

- Mine Shaft Construction Materials
- Methods to Neutralise the Adverse Effects of Mine Water Pollutants
- Alternative Solutions
- Flash Fill Material

An examples of shaft lining brickwork was recovered from an abandoned water filled shaft for strength testing but was too friable for detailed analysis and not structurally competent therefore the study criteria revolved around mechanical and chemical properties of concrete relative to the construction of shaft caps following treatment of an abandoned shaft (Figure 2.3.1.2.3-8).



**Figure 2.3.1.2.3-8 Shaft Treatment, Concrete Reinforcement and Cast Capping**

In order to research the potential benefits of concrete treatment to prevent ingress of minewater into a shaft lining a number of concrete (competent / weathered) samples (Figure 2.3.1.2.3-9) have been subjected to additional immersion tests (simulated A.M.W.) following treatment with readily available water repellent products which could principally be applied by spraying. The samples were immersed for a period of 450 days.



**Figure 2.3.1.2.3-9 Concrete Samples as Cast and Prepared for Immersion**

The samples were subject to weighing prior and subsequent to the application of a water repellent substance. These samples were subject to frequent re-weighing throughout the immersion period. On completion of testing the samples were split and were all found to be completely saturated. A representative sample of each test was air dried and reweighed to compare the pre and post immersion position. The final results of the re-weighing at the end of the testing are shown in (Table 2.3.1.2.3-3).

Treatment	Percentage Increase in Weight Pre Immersion		Percentage Increase in Weight Post Immersion	
	Concrete	Weathered Concrete	Concrete	Weathered Concrete
None	9.0	6.9	13.4	12.4
Water Seal	8.9	6.7	13.5	12.6
Spray Wax	9.0	6.3	12.4	13.0
P.V.A.	9.0	4.4	13.4	13.5
Spray Grease	7.9	4.0	13.1	12.7
Paint	9.7	8.5	16.4	14.7
Denso Tape	10.5	6.4	16.0	14.0

**Table 2.3.1.2.3-3 Increase in Weight Pre / Post Immersion**

The surfaces of samples removed from the A.M.W. were found to be pitted with a considerable amount of fine material deposited in the containers used for immersion. (Figures 2.3.1.2.3-10, 2.3.1.2.3-11).



**Figure 2.3.1.2.3-10 Pitting to Surface of Samples**



**Figure 2.3.1.2.3-11 Microscopic Examination of Sample Surface**

Following the reopening of Hatfield Colliery in the U.K after a period of 27months the presence of concentrations of Hydrogen Sulphide (75ppm) at 331m depth in the shaft water had caused corrosion to the shaft furnishings. (Figure 2.3.1.2.3-12) No deterioration of the shaft structure (concrete) was reported but research (Jofriet et al 2006) in the agricultural industry does suggest that large concentrations of hydrogen sulphide dissolved in water can weaken the structural strength of concrete.



**Figure 2.3.1.2.3-12 Corrosion to Shaft Furnishings**

There is therefore potential for an aggressive mine water containing relatively low quantities of hydrogen sulphide to affect the concrete structure of a mine shaft, any steel support or furnishings or fill material. There are commercially available products (such as hydrogen peroxide / specialized coatings) that can be added to the water to reduce / prevent the effects of hydrogen sulphide. However these could prove to be costly and / or not viable to implement.

Stabilisation of soils, aggregates or waste materials has been achieved successfully with fly ash using a binder or stabilizer or with self-cementing, class C fly ashes. Experimental research to achieve the required strength characteristics for a “flash fill” material containing colliery discard was undertaken to investigate means of stabilising shaft fill material especially in locations with deep unconsolidated superficial deposits.

The “flash fill” material was placed into sample tubes to mould test samples. The sample tubes were made of PVC piping which was cut along its length to allow easy removal of the test sample (Figures 2.3.1.2.3-13 & 2.3.1.2.3-14), cured initially at room temperature then tested for Uniaxial compressive strength until destruction. (Figure 2.3.1.2.3-15).



**Figure 2.3.1.2.3-13 Sample Mould**



**Figure 2.3.1.2.3-14 Test Sample**



**Figure 2.3.1.2.3-15 Samples Post Testing**

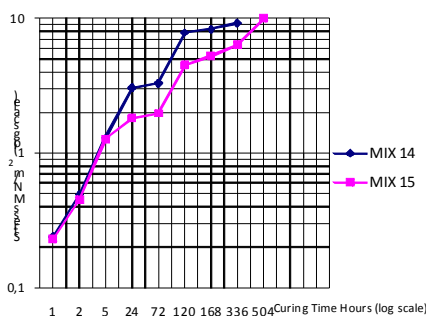


**Figure 2.3.1.2.3-16 Comparative Strength of 2 mixes**

On achieving early strengths, long term tests were carried out on Mix 14 and Mix 12. The result of these long term tests is shown graphically in (Figure 2.3.1.2.3-16).

The work concluded that minimum amount of cement which will give the required strength was 22% OPC (Mix 15) as 25% OPC (Mix 14) gave a higher strength. No shrinkage of samples occurred on curing and both slurries could be easily mixed, thus giving good potential flowable characteristics. Therefore the experimental work determined that a “flash fill” material giving required strength and flow characteristics can be developed from coal mining waste.

There is a need to further investigate the effects of temperature within an abandoned mine shaft relative to curing rate which may give improved / reduced early strength characteristics.

As a substitute for cementitious grouting of shaft fill a number of potential solutions were researched of which two options could provide an innovative technique for the treatment of mine shafts. (Table 2.3.1.2.3-4)

<b>Polymerised Grouts External to Mine Shaft</b>	Chemical grouts which gel with soil or rock following mixing to form impermeable mass to reduce conductivity and inter-connected porosity in an aquifer / areas of thick superficial deposits. Chemical reaction formed by soluble monomers, mixed with suitable catalysts to produce and control polymerization injected into the voids to be filled. The mixture generally has a viscosity near that of water and retains it for a fixed period of time, after which polymerization occurs rapidly. The monomers may be toxic until polymerization occurs after which there is no danger. The resulting product is very stable with time.
<b>Foamed Concrete</b>	Lightweight cement bonded material produced by incorporating pre-formed foam, into a base mix of cement paste or mortar. Air bubbles reduce density of base mix, strong plasticizing effect. Easily placed, requires no compaction and flows into the most restricted and irregular cavities. Provision of a resistant seal to acidic mine waters.
<b>Kaolin Amorphous Derivatives (KAD)</b>	Kaolin is commercial clay, composed principally of the hydrated aluminosilicate clay mineral Kaolinite. KAD material has different structural and chemical properties from original kaolinite clay in particular, a very high surface area (up to 10 times higher than kaolin), and a greatly increased ability to exchange cations. Contact with mine waters containing toxic metallic ions would have a twofold effect of working to seal shafts and carry out the process of toxic metal scavenging of mine waters.
<b>Neutral Barrier Technology</b>	Interaction between two of the lowest cost chemicals available, calcium hydroxide and carbon dioxide to control fluid flow in porous strata. (Permeable rock or unconsolidated sediments.) The technique involves selectively sealing microscopic inter-pore channels that permit the passage of water through soil, sand, and porous rock. Interaction between an acidic drainage and a neutral barrier some calcite dissolves, the pH rises, and new sulphate, hydroxide and carbonate minerals precipitate.

**Table 2.3.1.2.3-4 Potential Alternative Solutions to Cementitious Grouting  
Development of monitoring and telemetry instrumentation**

The aim of this sub-task was to further develop the telemetry that was initially investigated in task 1.2.1, before the field trials of task 2.3.

After discussion with UK Coal Authority staff and other industrial users it was identified that the principal requirement was to devise a means of monitoring shaft fill stability (SFS) and a means of providing off-site telemetry from the various shaft sites to a central monitoring facility. The SFS sensor was considered to be more important than the development of, for example, arrays of extensometers. Consequently, the results of Task 1.2.1 were used to develop a laboratory prototype of the various elements of a shaft-fill stability monitor and its associated telemetry.

It was recognised that there were a limited number of capped mine shafts to which access was easily possible for the installation of equipment for trials. Given the low overall probability that one such shaft would exhibit any movement of the fill within the field evaluation period, a small-scale simulated shaft cap and fill arrangement was set up, where pre-defined movement of the fill could be induced. This is further reported under Task 2.3.

## **2.3.2. Monitoring and control of subsidence effects on surface. WP2.**

### **2.3.2.1. Task 2.1. Geometrical monitoring tools**

The task 2.1 has been performed by two project participants that were involved in two different monitoring tools. Aitemin designed and developed the monitoring system on the base of photogrammetry while EMAG attempted to use InSAR images as the auxiliary tool supporting the monitoring system developed in the task 2.2 and based on GPS. The paragraphs below describe the activities and obtained results.

#### **2.3.2.1.1. Work undertaken by Aitemin on the photogrammetry**

The technique proposed by AITEMIN could be described as remote ground deformation control by automated high-resolution digital photogrammetry, and it was to be based on a computer vision system integrating modern high-resolution digital cameras and motorised theodolites.

#### **2.3.2.1.2. Analysis of the requirements of the monitoring system**

For the proposed monitoring system to be useful when compared to a total station, it should be able to measure ground surface displacements with much higher density and not too inferior accuracy. In practical terms, this means that the system would have to detect the displacement of a multitude of points on the bare ground, instead of the displacement of a small number of retroreflector targets attached to the ground, as surveys with total stations typically do. Besides, the system should ideally do this from such a distance that the effect of ground deformation at the monitoring stations becomes negligible, or at least measurable through the observation of fixed reference stations. Therefore the exact requirements for the system would depend on the particular conditions of the area to be monitored.

One of our intended test sites was the ground surface over a coal mine exploiting a very thick subvertical (~50°) seam, where the effect of the subsidence is quite intense, but basically localized along a stripe of terrain a few hundreds of metres wide. In these conditions, the minimum admissible resolution in displacement measurements would be around 10 cm, although a much more appealing objective for our system would be to attain a resolution of 2 cm, which would be truly remarkable. From these considerations, we can establish that image resolution should ideally be of at least 1 cm per pixel at a distance of about 300 m, as the basis for the design of the system.

#### **2.3.2.1.3. Study of pertinent bibliography on digital photogrammetric techniques**

AITEMIN conducted a search of the bibliography looking for technical documentation to improve knowledge on advanced digital photogrammetric techniques, especially on close-range photogrammetry, image matching techniques, digital terrain model (DTM) generation, and other related themes. After a search of documentation, we acquired some books and obtained from the Internet a large number of articles and reports on subjects relevant to the research.

#### **2.3.2.1.4. Search of suitable hardware components**

From the basic requirements established in paragraph, a search of suitable system components was conducted, in order to define the structure of the system.

Thus, it was decided to build the image-acquisition devices by combining three different components: a computer-controlled telephoto lens, a CCD camera with digital interface, and a computer-controlled pan-tilt mechanism.

It was soon realised that it would be difficult to find a standard computer-controlled telephoto lens that could be equivalent to the telescope of standard theodolites. The problem was that standard computer-controlled lenses were zoom lenses, and calibrating the camera with a zoom lens would be almost impossible. Fortunately, a specialised supplier offered a suitable alternative to these lenses: standard photographic camera lenses attached to a special computer-controlled adapter incorporating a C mount.

This adaptor would allow the computer to control the focusing motor and the iris motor of standard Canon lenses for EOS photographic cameras.

Selecting a CCD camera with digital interface for the image-acquisition device was no problem. We decided to use monochrome cameras, in order to profit from their high resolution and to prevent image artefacts due to the colour interpolation inherent to single-chip colour cameras. The interface selected was Gigabit Ethernet (Gigabit Vision) because it allows longer camera cables (up to 100m) than other possible systems, allowing a greater distance between cameras. Image size could range from 640x480 (VGA) at high frame rates up to 5 Pixels at low frame rates. In any case, chip size would range between 1/2" and 2/3" and the lens would have a C mount.

For the pan-tilt mechanism we ruled out the possibility of building one by assembling a pair of precision rotary stages, as these stages are slow and expensive, and unsuitable for outdoor use. Thus a search for commercial pan-tilt units was conducted. Most of the available options had to be rejected due to lack of precision, but finally two pan-tilt units manufactured by the company Directed Perception were selected as suitable options: models D47 and D48.

### 2.3.2.1.5. Design of the system

The following (Figure 2.3.2.1.5-1), illustrates the principle of operation of the proposed system, in which at least two monitoring stations simultaneously watch the same patch of land from different points, obtaining images that are processed by specialised software to build a 3D model of the terrain and its main features.

In order to be able to carry out accurate measurements at the expected ranges (hundreds of metres), the cameras had to be equipped with long telephoto lenses and their separation had to be of the order of the range. Each one would be mounted on a precision pan-tilt mount, and a rough DTM (Digital Terrain Model) would have to be acquired first by other means so that the correct orientation for each camera could be computed to achieve maximal image overlap for improved matching.

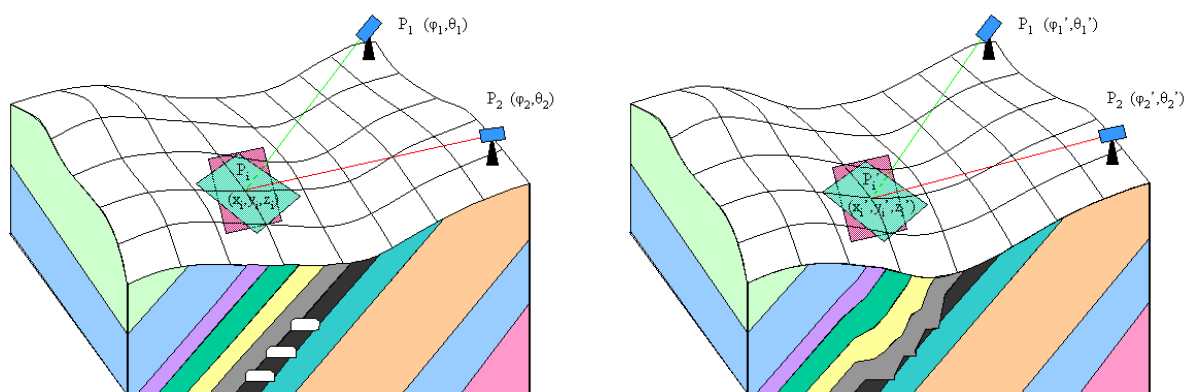


Figure 2.3.2.1.5-1 Schematic diagram of the system concept for subsidence detection

### 2.3.2.1.6. Selection, acquisition and integration of system components

After the search described in paragraph, the following main items were acquired:

- Cameras: two Basler Scout cameras (model scA1600-14gm) with Gigabit Ethernet interface. These cameras provide monochrome images of up to 1628x1236 pixels, with 8 or 12 bit/pixel, at a typical frame rate of 14 fps. Pixel size is 4.4x4.4 microns, and sensor size is 1/1.8".
- Lenses: two Canon EF 200mm f/2.8L II USM lenses, typically used with Canon EOS cameras, and two Fujinon HF50HA-1B 50mm lenses, in order to perform tests in the lab at short range.
- Lens adapters: two Birger Engineering EF232 lens controllers for Canon EOS lenses, with power supplies. These adapters incorporate a standard Canon EOS lens mount, a RS232 port for direct

connection to a controlling computer, and a C mount for direct attachment to a CCD camera. The available control features of these controllers include focus distance, aperture and zoom.

- Pan-tilt units: a Directed Perception PTU-D47, as you can see in the (Figure 2.3.2.1.6-1) pan-tilt unit was initially selected to carry out tests. It has a complete command set that allows a computer to control, either through a RS-232 port or a RS-485 port, position, speed, acceleration and other features for both pan and tilt movements. For the final system, two more rugged and precise Directed Perception PTU-D48 pan-tilt units have been acquired. Their pan amplitude is  $\pm 220^\circ$  with a resolution of  $0.006^\circ$ , and tilt amplitude ranges from  $-30^\circ$  to  $+90^\circ$  with a resolution of  $0.003^\circ$
- Software: a run-time license of Matrox MIL 8.0 image processing library was acquired, which was later upgraded to a full development license of MIL 9.0.
- Computers: a Dell Precision T3400 workstation was acquired for software development and testing, and a Dell Precision M4300 laptop computer was acquired for integration in the prototype.
- Network devices: two Advantech NPort 5230 serial port servers were acquired to connect each of the image acquisition units to the computer. Each one provides an RS-232 port and an RS-422/485 port that can be controlled from a remote computer through a 100 Mbps Ethernet link. A 5-port Gigabit Ethernet switch and suitable network cabling and connectors were also acquired to interconnect the different devices in the system: computers, port servers and cameras.
- Power supplies: As a result of the use of the serial port servers, system connections could be simplified so that they only require a 230 VAC power supply and a Gigabit Ethernet link.
- Enclosures: two outdoor enclosures have been acquired to house the camera assemblies and three cabinets have been acquired to house the different electronic devices that compose the system: power supplies, port servers, computer, etc.
- Mechanised parts: Special metallic parts were designed to attach the cameras to the pan-tilt units to carry out the acquisition of stereoscopic image pairs for software development tests.

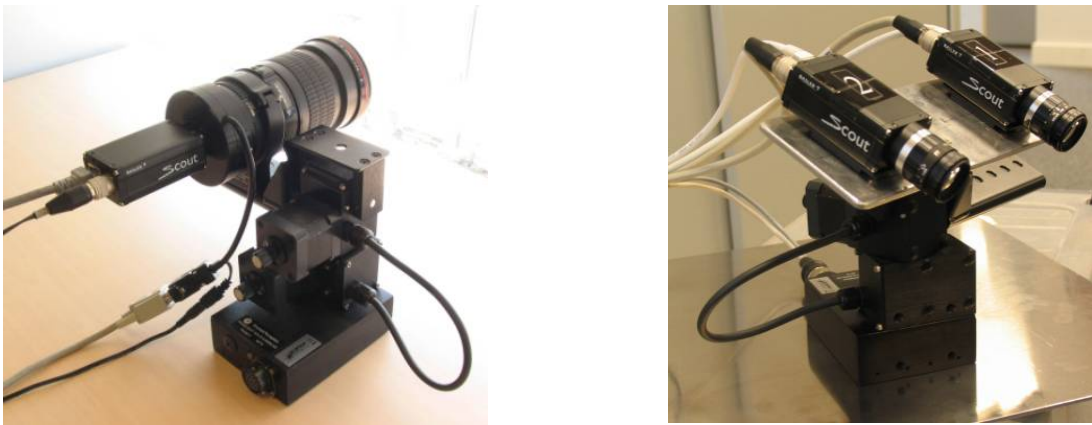


*Figure 2.3.2.1.6-1 Lens-controller-camera assembly and stereo set-up on the PTU-D47 pan-tilt unit*

### 2.3.2.1.7. Development of software for image acquisition and pan-tilt unit control

Along the project, many different programs were written to develop specific image processing functions and to perform tests of their performance under diverse conditions. These programs make use of the Matrox MIL image-processing library for image acquisition and low-level processing, but high-level processing and information extraction are done with our own algorithms, many of them based on algorithms published in the bibliography.

### 2.3.2.1.8. Development of a procedure for exterior calibration

The process of connecting real-world coordinates with image coordinates is known as exterior orientation (or extrinsic calibration). Among the different methods described in the bibliography, we decided to use the method proposed in [Tsai 1986]. This method allows to easily determine where a point of the 3D scene will appear in the figure. The reverse transformation requires additional information, because a pixel in an image is a point in a 2D space and it is not possible to transform it to a single 3D world point. We only know that the real-world point lies along the straight line running from the optical centre of the camera through the pixel.

### 2.3.2.1.9. Development of a procedure for matching points in an image pair

Once the exterior calibration parameters of each camera are computed, it is theoretically easy to calculate the real-world coordinate of a point seen in both images. But to make such a calculation we need an error-free match of a point in an image with its counterpart in the other.

Therefore a program was developed to carry out the processing of stereoscopic image pairs, from image acquisition and rectification to 3D coordinate extraction. It used the two cameras mounted on a plate with a 140 mm baseline on top of the D47 pan-tilt unit (as shown in the left side of the figure), with its position and orientation known from a previous extrinsic calibration of both cameras.

(Figure 2.3.2.1.9-1) shows an image pair after rectification along epipolar lines, and (Figure 2.3.2.1.9-2) shows the resulting disparity map. Disparity is defined as the difference between column coordinates of corresponding pixels in the left and right images of a stereo pair. Note that, in our disparity maps, lighter grey levels mean closer distance to the camera. Finally, in Figure 2.3.2.1.9-3 we can see a view of a subset of the cloud of 3D points obtained. The results are very good, providing excellent point density and accuracy. However, in the proposed system the cameras would not have such a small baseline, but would be placed in positions quite far from each other, so each one would see a totally different perspective of the scene.

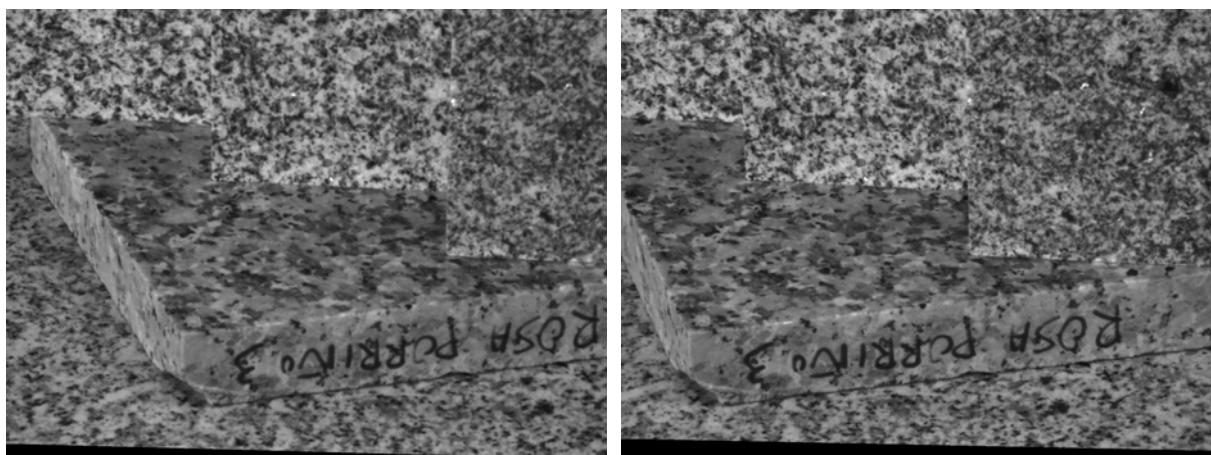


*Figure 2.3.2.1.9-1 A rectified stereoscopic pair acquired with the twin camera mount*

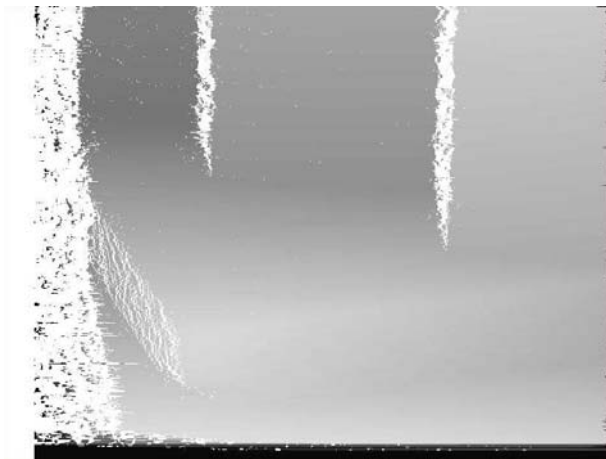


*Figure 2.3.2.1.9-2 Disparity map generated by the program*

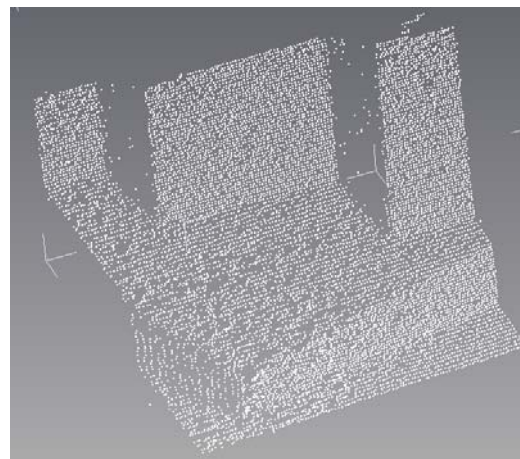


*Figure 2.3.2.1.9-3 A view of the reconstructed 3D points*

### 2.3.2.1.10. Development of a procedure for automatic calibration of monitoring stations



*Figure 2.3.2.1.10-1 Outdoor camera assembly*

As cameras will be mounted on pan-tilt units, we need a procedure to compute the exterior calibration parameters for any possible orientation of the pan-tilt units, and to estimate some additional parameters such as possible misalignments between each camera and its respective base, etc.

The software implementing the procedure can work with both simple cameras and outdoor camera assemblies (Figure 2.3.2.1.10-1), which have a computer-controlled 200 mm telephoto lens whose iris and focus settings are automatically adjusted before an image is acquired.

### 2.3.2.1.11. Development of applications to extract terrain model data

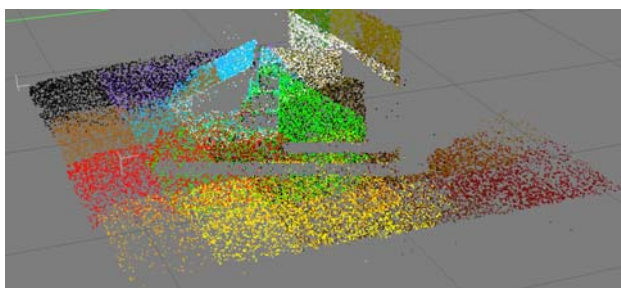


*Figure 2.3.2.1.11-1 Outdoor camera assembly*

An application was developed to extract 3D terrain model data from a scene. The program aims monitoring stations to a world point given in (X,Y,Z) coordinates, acquires a pair of images, corrects lens distortion, performs the epipolar rectification, computes a disparity map with the points that are correctly matched, and produces a file with the 3D coordinates of those points. Another application performs the same operations

on a number of 3D points according to a rectangular grid in the (X,Y) plane. The results of this latter application are shown (Figure 2.3.2.1.11-1), where the point cloud obtained for each grid point is displayed in a different colour.

The development of this application required much more effort than initially planned, because the matching of points observed from different viewpoints is far from being completely solved. Although the Census Transform applied on 15x15 windows provides good matching when the cameras are close, results become poor when large baselines are used. In order to improve the matching for horizontal or sloped surfaces, the window for the Census Transform had to be reduced to a size of 3x15 pixels, which in turn degraded the trustworthiness of a match. To reduce the amount of false matches, they were

filtered by imposing the condition that a match from the left image to the right image had to coincide with a corresponding match from the left image to the right image. Besides, points near the borders of the image were discarded, as they are prone to matching errors. This can be compensated by reducing the distance between grid points, in order to increase overlap between individual takes.

**2.3.2.1.12. Development of an application to obtain a terrain model from a cloud of points.**

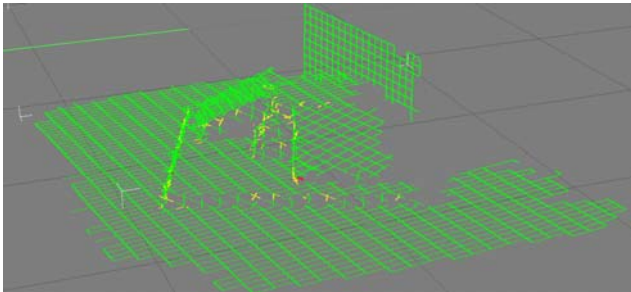


*Figure 2.3.2.1.12-1 Outdoor camera assembly*

The final aim of this work was to build a Digital Terrain Model of the surface above a mine in order to detect and measure terrain subsidence. So, it is essential to transform the point cloud provided by the previous application to some kind of model where surface height changes can be determined.

A rectangular mesh obtained from the point cloud can be seen in (Figure 2.3.2.1.12-1). Each node of the mesh was calculated as a weighted mean of the points in its proximity, after an

outliers removal process.

**2.3.2.1.13. Laboratory simulation of a subsidence.**

Originally, it was foreseen to test the control ground deformation system at a mine site, but due to the difficulties found in the development, it was only possible to test it in a laboratory simulation.

(Figure 2.3.2.1.13-1) shows the initial and final set-up of a laboratory test carried out with some granite tiles. Keeping all tiles but one in the same position, the central tile was gradually lowered in steps of 0.5 mm and the resulting 3D point cloud and terrain mesh was computed for each of the nine tile heights.



*Figure 2.3.2.1.13-1 Initial and final positions of a laboratory test set-up for subsidence monitoring*

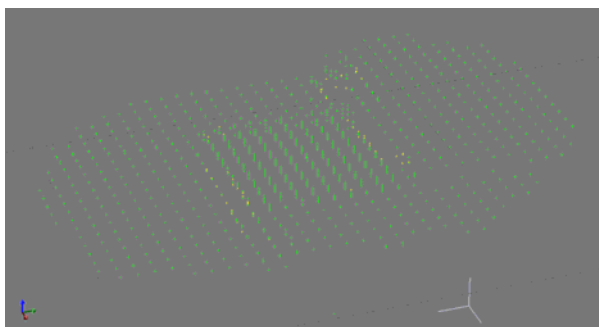


*Figure 2.3.2.1.13-2 Point grids obtained with the laboratory test set-up for central tile heights for 4, 3, 2, 1 and 0 mm*

(Figure 2.3.2.1.13-2) shows a simultaneous perspective view of five point grids, corresponding to central tile heights of 4, 3, 2, 1 and 0 mm. Only the grid points corresponding to the intersection of mesh lines are shown, in order to better appreciate the descent of the central tile surface.

#### **2.3.2.1.14. Work undertaken by EMAG on InSAR technique**

The purpose of EMAG participation in the task 2.1 was the assessment of a usefulness of SAR technique as the subsidence monitoring tool. There was assumed that the assessment would be more credible if related to the results of observation obtained under the work performed in the task 2.2. Therefore for the both tasks the same territory was assumed to be monitored.

#### **2.3.2.1.15. Requirements for applying SAR image technique**

The analysis of requirements for applying this tool to the project was carried out. As the result, the following requirements of the InSAR technique use in the project have been arranged and accepted:

- the InSAR technique will be applied for the monitoring of the same territory as in the observed by other tools in the task 2.2
- the images should include scenes of the monitored area before, during and after completion of the mining activity
- the compatibility of the acquired consecutive scenes must be provided – all the scenes should present an area of the same co-ordinates
- all adverse factors that affect the image processing result, must be taken into account if possibly.

#### **2.3.2.1.16. InSAR image type selection**

On the base of the delivered by the JasMos mine co-ordinates of the longwall no. 10 and seam 510/2 - the object of observation in task 2.2, the boundaries of the area to be observed have been determined. Among considered various available types of SAR images, ASAR types produced by ENVISAT satellites of the European Space Agency have been chosen for the analysis in the project. Within that type a kind of images ASAR Image Mode; VV was chosen. The result of searching proved that available images of chosen type, cover territories of constant co-ordinates.

As the interesting area was not divided into two or more images, the acquisition of single scenes of the above co-ordinates was sufficient for a single comparative analysis.

#### **2.3.2.1.17. Acquisition of SAR scenes**

The choice of suitable radarograms for satellite interferometry was a relatively complex task - the selection of the available archival data of a chosen research area. On the basis of the parameters of the available scenes, pairs of radarograms have been pre-selected. In the next step, among the pre-selected data, the radarograms possible to be fitted into a time base corresponding with the period of mining activity in the monitored area, have been designated for further processing.

Three distant in time acquisitions of SAR scenes were realized for the project aim:

1. Three scenes scanned on 11th March (A), 15th April (B) and 29th July 2008 (C),
2. Three scenes scanned on 11th May (D) , 20th July (E) and 24th August 2009 (F),
3. One scene scanned on 2nd November 2009 (G).

The scenes were chosen to show the monitored area before the longwall extraction (A, B, C), at the start and during the excavation (D, E, F) and after the extraction had been completed (G).

#### **2.3.2.1.18. Analyses of the selected images**

The first analyses were carried in 2008 and concerned the scenes A, B and C. The object of considered analysis were two pairs of images: A (master) & B (slave) and B (master) & C (slave). The analysed radarograms that refer to observed period, proved that deformations due to mining activity above previously excavated seam 510/1 were settled and the area was generally free of ground movements.

Comparison of scenes from 2009 to those from 2008 resulted unsuccessfully due to very low coherence. Interferograms including scenes only from 2009, despite their careful selection, produced good results

only in two cases. A pair of images E&F revealed a local subsidence trough above the observed longwall of maximum 15 [mm] – the result of its current excavation. The levelling surveys at the mentioned area showed subsidence ~ 18 – 22 [mm]. A pair of images D&G showed a local subsidence trough distant to the monitored longwall interpreted as the residual result of earlier mining activity. Maximum value of subsidence was estimated 20 [mm], while corresponding levelling subsidence was 15 [mm].

#### **2.3.2.1.19. InSAR Summary**

- Seven SAR scenes covering the period from 11th March 2008 to 2nd November 2009 have been analysed during the project. Various couples of images were subjects of analyses.
- Analyses of three 2008 scenes leads to conclusion that the area to be monitored shows stability.
- An attempt of comparison the scenes scanned in 2009 to the scenes scanned in 2008 failed due to the very low coherence
- Comparative analysis of the scenes scanned in May, July and August 2009 showed difficulties in interpretation of the interferograms due to the factors that affect incoherence like: weather conditions, clusters of trees and buildings. On the base of one pair of scenes the emerging subsidence trough has been detected at the edge of the monitored and being excavated longwall.
- As the result of acquisition of one scene scanned in November 2009 an image of another subsidence trough distant about 400 [m] from the monitored longwall was detected. The trough is probably the residual effect of the earlier mining of 510/1 seam.

The extensive description of EMAG activity in task 2.1 is included in Appendix/Deliverable D.2.1 “Analysis of satellite radar images of the mining area monitored in task 2.2”

#### **2.3.2.2. Task 2.2. Seismic and GPS monitoring tools**

##### **2.3.2.2.1. Objective and scope of the undertaken work**

Task 2.2 in WP2 was entirely realized by EMAG. Its aim was a development of a modern tool – a system for monitoring of surface at areas of mining activity. The innovation of the proposed solution consist in quasi constant monitoring of vibrations and subsidence at selected points. This makes an opportunity of more complex approach to the assessment of hazards due to subsidence and seismicity accompanying excavation of underground deposits. Monitoring of surface hazarded by mining activity is very useful, but also important is prediction of hazards that could happen. The functionality of the developed system allows to assess the envisaged surface behaviour on the base of the assumed models (prediction) and its verification on the base of the obtained precise GPS measurements (monitoring).

Two kinds of undertaken work have been performed in the project. Scientific work was focused on:

- a development of the mathematic models describing an impact of the mining activity on ground deformations and seismic events,
- research and experiments carried out on the base of the implemented system prototype.

Engineering work was focused on:

- the design of the system structure, its performance, installing and implementation
- the software development and run.

To accomplish the mentioned work, the appropriate order of actions had to be maintained. The following paragraphs describe in more details the work done.

##### **2.3.2.2.2. Mathematic models of processes**

In the task 2.2 one of the assumed goals was the possibility of using the developed monitoring system for prediction of envisaged hazards before the start of coal excavation to evaluate negative effects of

deposits exploitation. To achieve that aim, the application of proposed and accepted mathematic models was crucial and necessary. The developed models describe envisaged geodetic processes of surface deformation and probable effects of the observed seismic events on surface. The models represent approximation of certain real processes that may occur as the results of the planned coal mining within a selected research area. The following models have been developed within the work accomplished in the project.

#### *Models of deformation*

##### *Static model of deformation*

The model represents the stationary surface behaviour after the mining area excavation had been completed. The model is the Cauchy's solution of the equation describing general movement of infinitely small rock mass element. The model have been developed on the base of the following assumptions:

- around the observed mining area the zone of subsidence influence of "r" radius is formed,
- model includes the fact that within the observed territory may be more that one mining area, while each of them affect the surface (superposition of an influence),
- acceptable variants composed of partial exploitation are allowed.

##### *Kinematic model of deformation*

The kinematic model represents approximated description of the evolutionary displacement process. A displacement of the point may be described by a differential equation that determines its curve trajectory and boundary conditions of the process.

#### *Models describing an influence of seismic events on surface*

Two groups of models have been developed within the project work

##### *Models representing the relation of ground vibrations parameters to the measured data.*

The harmfulness of mining bump impact may be described by parameters of accompanying vibrations. Those parameters are: maximum amplitudes of recorded vibrations AM, duration of vibrations, resonant frequencies. Vibrations can harmfully influence on surface, if their frequency is less 10 [Hz], so the recorded waveforms are subjected to mandatory low-pass filter up to that frequency. The developed models allow to estimate the above parameters on the base of recorded signals of vibrations. Estimating of vibrations parameters must be performed individually for each waveform recorded at various measurement stations (data loggers) deployed in the observed area. In the models, signals of vibrations have been described as products of two mutually orthogonal factors: envelope  $\zeta t$  and oscillatory factor  $\eta t$ . Two types of models of that group have been considered:

- Models describing signals of vibrations in time domain
- Models describing signals of vibrations in spectral domain.

In case of simple vibrations – with single resonant frequency the parameters can be estimated both in time and spectral domain, while for vibrations with several resonant frequencies estimation in time domain is impossible.

### *Models representing distribution of vibration parameters on the surface in the mining area.*

That group of models represents the relation between parameters of a seismic event (bump energy, coordinates of bump sources, epicentral radii) and vibration parameters (maximum amplitude, amplitude attenuation, signal duration). Seismic parameters are evaluated by the analysis of recorded seismic events detected in underground measuring stations located in mine workings. The model assumption is, that in a certain neighbourhood of a bump focus called an epicentral zone, predicted values of vibration parameters: amplitude  $A_{epc}$  and duration  $t_{epc}$  can be considered constant, while outside that area an influence of attenuation must be taken into account depending on the distance to the source called a radius. The following four models of that group have been considered:

- A model representing the relationship between maximum amplitudes of vibrations and bump energies within epicentral zones
- A model representing the relationship between attenuation of maximum vibration amplitudes and epicentral radii of bumps
- A model representing the relationship between duration of vibrations and bump energies within epicentral zones
- A model representing the relationship between duration of vibrations and epicentral radii of bumps outside epicentral zones.

To identify a model its parameters must be first estimated. Estimation by the least square method requires historical data: the mentioned parameters of seismic bumps associated with, estimated on the base of previously described models, parameters of corresponding vibrations. The estimated values of model's parameters depend on the period of the historical data involved in the calculation process. On the base of the identified model it is possible to evaluate parameters of vibrations induced by bumps of requested or foreseen energy and location anywhere within the monitored mining area.

#### **2.3.2.2.3. Identification of the models' parameters**

For the models of deformations preliminary verification tests have been carried on the base of empiric subsidence measurements collected at seven points. Those points were located directly over the longwall 22a of 510/1 seam in JasMos mine. The longwall situated 640 – 710 m deeply, was 3.2 – 3.6 m thick and was extracted in the years 2006 - 2007. GPS technology was used for the model's verification. That technology allowed to determine current co-ordinates of 7 selected points in R3 space. The surveys were carried out by the static method of the period  $T > 0,5$  hour at a single point. Post-processing corrections were calculated by dedicated software with the use of data delivered from 3 reference stations Wodzisław, Żywiec i Katowice. 25 series of measurements were performed in 8 – 30 days intervals. Ellipsoidal altitudes were converted to Kronshtad system by taking into account one, average correction for undulation function, which has been determined by the "geoid"  $N=42,022m$ . The procedure was carried out for both types of models: static and kinematic.

The result of foreseen distribution of vertical and horizontal ground movements is presented in (Figure 2.3.2.2.3-1).

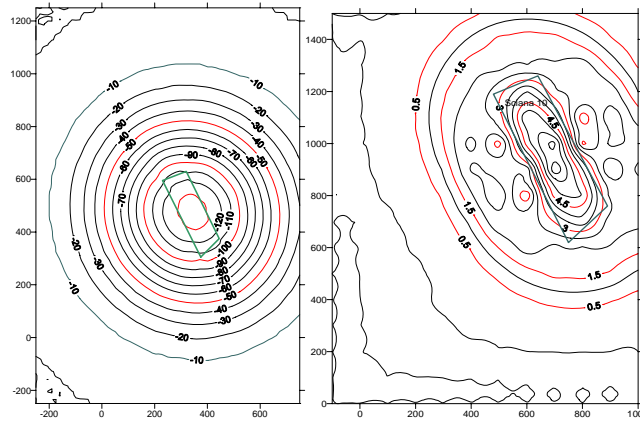


**Figure 2.3.2.2.3-1 Vertical and horizontal displacements above the longwall No. 10 of 510/2 seam calculated on the base of the static model**

The parameters of seismic models were calculated on the base of seismic data collected in previous years and made available by the JasMos mine. The identification has been carried out by the least squares method.

#### **2.3.2.2.4. Architecture of the developed system**

The developed system for monitoring and prediction of hazards induced by mining, permits for observation of changes in surface of the selected area and recording of signals of vibrations, which arise on surface as the effects of seismic bumps.

The system consists of two parts:

- measuring – fitted with hardware installed and used directly at an area to be observed
- control and monitoring - a centre of visualization, data analysis and hazard assessment.

The measuring part of the system includes only recording of seismic and geodetic parameters on surface. It does not include parameters of seismic events recorded by underground seismic systems oriented mainly to control the security of crews and equipment working underground. The system associates the control of tremors resulting from the effects of mining activities with monitoring of deformation and surface subsidence. Distributed, modular structure of the measuring part of the system facilitates the control of large areas and a successive growth of the system capabilities. That part of the system consists of: stands of constant observation, points for periodical surveys, reference stations, source of seismic parameters.

The measuring part of the system consists of the stations (concentrators) - data loggers, adapted for continuous collecting of recorded parameters of vibration and data of their position. Information on vibrations are generated by the 3D (x, y, z) sensors of vibration acceleration, which are connected to the concentrator's electronic. Information on position are generated by the GPS receivers that are also connected to the concentrator. Each concentrator is fitted with the additional GPS receiver used for time synchronization, which provides a common time axis for recorded information. Recorded data are stored in the logger's memory. The concentrator is also fitted with the hardware modules that enable a transfer of collected data to the central part of the system by GSM link, or GPRS technology. That allows to set configuration and send organizing commands from the central system's part to concentrators. Complementary part of the system are points of periodical measurements – stabilized locations designated for observation of parameters of position on surface to be surveyed by mobile GPS receivers.

The central part of the system consists of: station of seismic events qualification, station of post-processing of GPS surveys, station of analysis and visualization.

Stations may be installed on one or more computers. Regarding that two first stations are used for data preparation in off-line mode a distributed architecture of the central part of the system is logically

justified for the station of analysis and visualisation, though it does not have to be justified economically.

The main sources of data used by the central part of the system are measurements. These measurements due to their nature, are twofold origin: surveys, measurements of seismic parameters. In general three types of measurement data are collected: 3D surveys of the position, 3D components of seismic ground vibrations on surface, parameters of seismic bumps recorded underground.

The most important element in the central part of the system is its software. The software consists of the modules developed and accomplished under the project and the acquired programs indispensable in the process of data post-processing as well, (Figure 2.3.2.2.4-1).

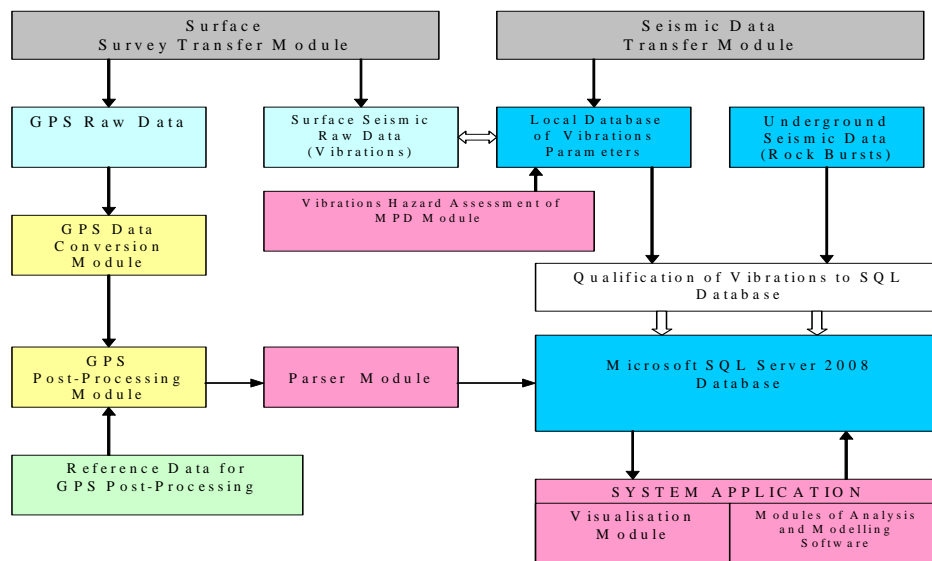


Figure 2.3.2.2.4-1 The chart of Monitoring Centre software, data and information flow

### 2.3.2.2.5. The prototype of the system

Location of the mining territory

According to earlier assumptions, considering the need of reducing the costs of upgrading the measuring part of the system, the following criteria have been taken into account:

- currently existing equipment delivered by EMAG in a mine to be chosen,
- an access to historical data being in the mine's possession,
- the mine's plans of production.

Considering locations, which fulfilled the above conditions the location of the JasMos mine situated near the border between Poland and Czech Republic has been selected. The crucial decisive factors were: the mine's intention of upgrading and modernization of the measurement base by the own resources and the mine's interest in the project results, due to the impact of mining on the situated in proximity motorway.

Structure of the measurement network

On the base of the above assumptions the measurement network was designed with measuring points located on surface above the mentioned longwall No.10 of the 510/2 seam and at its surroundings. The network consisted of four sites of constant (permanent) measurement for collecting geodetic and seismic data and about 70 points for periodical GPS surveys. Three of the sites of constant measurements (Nos. 2, 3, 4) were situated above the longwall, while the fourth site (No.1) was located approximately 1 km away from the longwall to determine the zone of the mining influence on surface. For periodical measurements of surface deformation the points for GPS positioning surveys, were

formed in two lines: one running above the longwall No. 10 in parallel direction to its extraction (line 300 with 34 points Nos. 317 – 352) and the other perpendicular to the direction of extraction (line 400 with 34 points Nos. 414 - 452). The lines intersected each other above the longwall i.e. they both crossed the longwall. The points on each line were distant from each other by about 50 m.

#### *Prototype system installation*

The elements of the system prototype have been completed and prepared to be installed in the selected sites of the research area. The modernized existing hardware elements of measuring part of the system were complemented with the acquired devices upgrading the equipment to prototype system requirements.

Finally four data loggers for collecting constant measurements have been installed were situated at sites marked on the map (Figure 2.3.2.2.5-1) and equipped with sensors of vibration acceleration and GPS receivers of two different types: GSR 2700 ISX and 3100 IS. Wiring and power supply have been provided. Concentrators were mounted inside, while GPS receivers and sensors of vibrations outside buildings. GPS receivers were placed in specially designed structures, which also provided their protection. The installed elements of the system's equipment were insured. The fifth measuring station, originally intended as a reference base station to support periodical GPS surveys by the RTK method, was installed on the stable ground away from the monitored area, and fitted with the data logger and GSR 2700 ISX GPS receiver. It was not equipped with a sensor of vibrations.

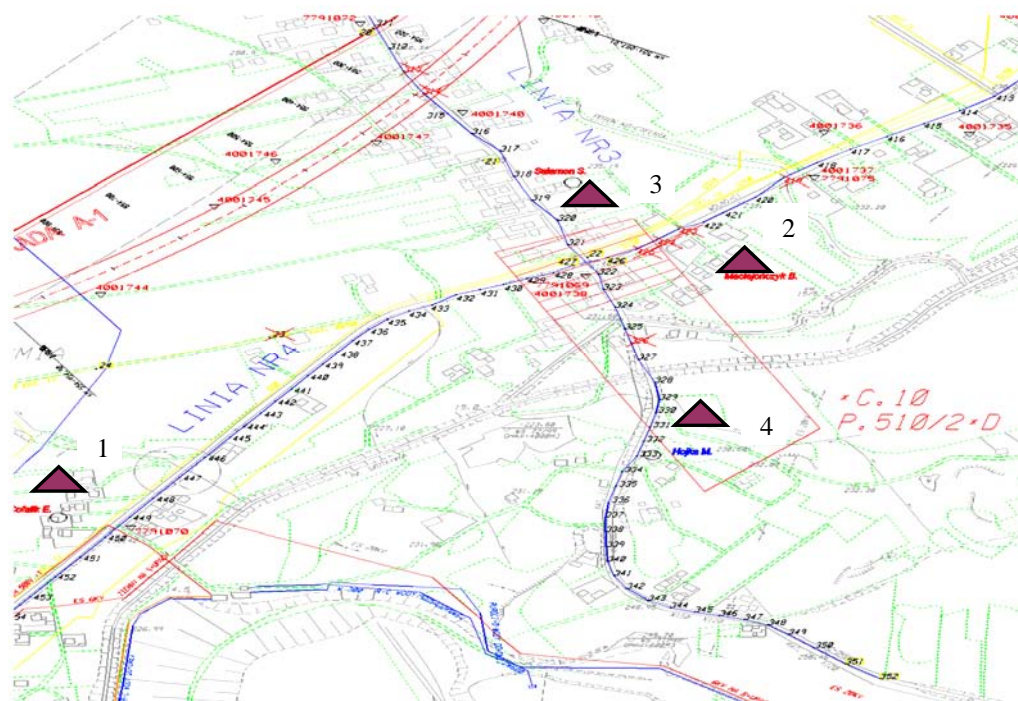


**Fig.2.3.2.2.5-1 A map of the research area with points of constant and periodical measurements**

### 2.3.2.2.6. Monitoring of subsidence process

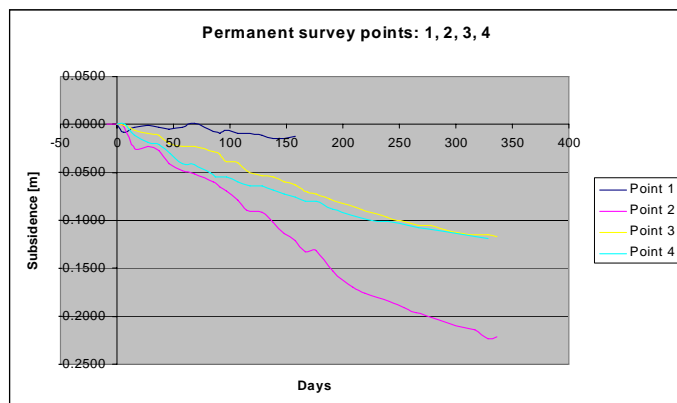


**Figure 2.3.2.2.6-1 Comparative diagram of subsidence recorded at sites of constant observation**

The postponement of the start of the longwall no. 10 at 510/2 seam extraction caused, that the observation began in July 2009. The GPS receivers have been configured for 5 seconds sampling of the recorded data. The collected measurements (Figure 2.3.2.2.6-1) were transformed to the unified Rinex2 form and then post-processed. From among three initially tested post-processing method, that using the virtual station has been chosen to be applied for all measurements due to the least dispersion of the obtained data.

The geodetic research on the base of GPS receivers at the four sites of constant observation have been carried out for almost 10 months form July 2009 to May 2010. Only at the distant to the monitored longwall point no. 1 of less subsidence, the measurements were completed at the end of 2009.

For each measuring site of constant monitoring, the data for presentation of the slow process of surface deformation have been selected in 10 days intervals. Though those sites were principally envisaged to show the GPS data recorded directly before and after the moment of a seismic event, the values of subsidence due to the longwall excavation may be shown in the digital or graphic form. To compare the values at various points the particular signals were referenced to “the zero day” - 16th July 2009.

The presented trajectories of subsidence at particular points are results of their relative position to the observed surface over the longwall no. 10. Location of the point 2 over the central longwall’s part implies greatest subsidence. Positions of the points 3 and 4 over the both longwall’s ends confirm subsidence relatively less to that at the point 2 and of similar values. Insignificant subsidence was also detected at the point 1 located beyond the impact of the longwall no. 10. It is the effect of the previous mining influence and was confirmed by the results of InSAR analysis.

As the planned for periodical surveys RTK method was substituted by the more reliable and accurate static method, which required the greater time consumption and regarding encountered weather conditions, only four sessions of periodical survey have been completed in the following time periods: 8 – 13.07.2009, 18 – 21.08.2009, 28.09 – 2.10.2009, 9 – 17.11.2009.

On the base of GPS surveys the assessment of hazard for objects located on the monitored surface have been performed. Every structure situated on the mining area is associated with the individual category of resistance  $x_k$  and  $k \in [0...4]$ . The objects located on the observed area were of the third category. The crucial for hazard assessment indices of deformation: inclination and horizontal strain have been calculated for individual points of periodical surveys. The results proved that the values did not exceed the limits allowable for the located objects. That was confirmed by the fact that no real structural damage have been noticed.

### 2.3.2.2.7. Monitoring of seismic events impact on surface

After the prototype of the system had been installed the observation of vibrations started. Two purposes of the observation were most important:

- monitoring of hazards at surface due to vibrations induced by underground bumps,
- attempt of searching for an interrelation between seismic and geodetic processes.

Unfortunately during the period of the longwall no. 10 observation in the second half of the year 2009

only few seismic events happened.

The conclusion carried out on the base of performed analysis shows that the seismic events recorded from July to December 2009 were not hazardous for the objects on surface. Only one event was of the greater amplitude 309 [mm/s<sup>2</sup>] but no structural damage on surface was the effect of its occurrence.

### 2.3.2.2.8. Research of interrelation between GPS and seismic data

According to the foreseen plan, interrelation between subsidence and surface deformation was sought.

In the search for relations of seismic to deformation processes, and attempt to find a similarity of signals recorded by sensors of vibration and GPS receivers before and after seismic event occurrence has been undertaken. Recorded vibrations are of course of the wavy nature, so the goal of the attempt was to examine whether geodetic data are of the similar character. In the (Figures 2.3.2.2.8-1) and (2.3.2.2.8-2) an example of the horizontal Y and vertical H components of displacement vector could be seen.

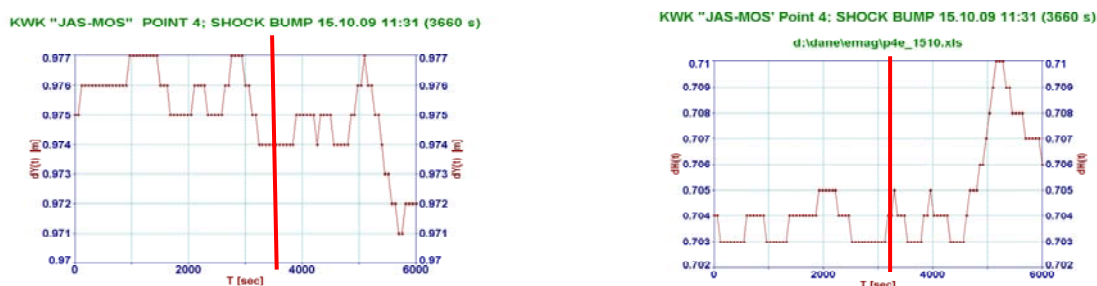


**Figure 2.3.2.2.8-1 and 2.3.2.2.8-2 Example of the horizontal Y and vertical H components of displacement vector – changes recorded by GPS at point 4 before and after the bump (3660 s) on 12.10.2009 11:31 and  $E = 9.2 \times 10^4$  [J]**

The above remarks are based on the sample of only several seismic events. More general conclusions require testing on a more representative sample of data, therefore the research should be continued in future with the use of a new generation equipment – high frequency GNSS receivers.

### 2.3.2.2.9. Verification and validation of the results

Verification and validation of subsidence has been performed by comparative analysis of GPS surveys to the levelling measurements. Concurrently with four periodical GPS survey series the levelling measurements at the same points have been conducted. Being in force allowable value of deviation of levelling surveys for mining areas should not exceed 8-10 mm. For the performed measurements the following results have been obtained: August 2009 - 1,7 mm, September 2009 - 2,1 mm, November 2009 - 4,0 mm.

As the above results fulfilled the conditions of allowable tolerance, the levelling surveys were applied for verification of the periodical GPS data by comparative and appropriate statistic analyses. The process was performed for the data recorded at line 300. The following analyses have been performed.

The graph of dispersion of levelling with reference to GPS surveys for values of subsidence between July and November 2009, with assumed confidence level 0,95 indicates, that a linear transformation of the levelling to GPS results of measurements is possible according to the determined formula. The obtained high coefficient of correlation 0,751 proves, that statistically GPS surveys are consistent with surveys done by the levelling method (even though approximated estimation of undulation).

### **2.3.2.3. Task 2.3. Surface monitoring of shafts stability**

This task continued the developments undertaken earlier in the project in tasks 1.2.1 and 1.2.3.

#### **2.3.2.3.1. Field trials with the developed monitoring and telemetry instrumentation**

##### **Shaft field sensor: summary of previous work**

In Task 1.2.1 a review of telemetry and instrumentation methods was undertaken resulting in a design for a shaft-fill stability (SFS) sensor linked to a custom-designed low-power data logger and a GPRS (i.e. 'cell phone') transmitter. The purpose of the field trials was to evaluate the shaft-fill sensor and the logging and telemetry components.

##### **Programme of field trials**

In drawing up a programme for field trials it soon became apparent that the long-term evaluation of the SFS would not be straightforward. Two obvious difficulties were foreseen, namely i) that environmental and biological damage to the sensor might only become apparent after very long-term exposure and ii) that shaft fill instability events would occur only at very infrequent intervals. It was decided that it would be necessary to concentrate on certain specific elements of the design and, initially, to run trials on those elements alone; essentially to do 'accelerated lifetime' trials with, e.g., more frequent events.

In order to undertake sufficient trials it was considered necessary to construct several SFS prototypes. However the original design was aimed at a high-performance, rugged, environmentally-protected device that would last for many years in the field and, as such, it was expensive to construct. It was therefore decided to design a cruder device that could be manufactured at very low cost for "indoor" use during initial trials, for which a test rig was constructed that would allow the SFS to be operated repeatedly to order. The low-cost SFS is described in an appendix to this report. It was also considered that, in the short term, a greater benefit would be obtained by testing the components separately and by monitoring parameters other than shaft stability.

##### **Summary of Initial trials**

The results of tests on individual elements of the system are now described. Some further detail of these elements is given in an appendix.

*Data Logger.* Initial trials concentrated on verifying the software framework for the logger.

*Telemetry transmitter.* Software development was undertaken prior to an integrated field trial and concentrated mainly on the testing of the communications protocols.

*Web server.* Operation of the web server was initially simulated using synthesised data. Programs running on one web server simulated the operation of the remote data-logger by sending daily HTTP requests containing small amounts of data to a second web server which stored these in a database. The issues of scalability are discussed below, under 'network capability'. It was originally envisaged that the data would be stored in a relational database such as MySQL. However, although such a database would be useful if the data were collected from thousands of sensors over a prolonged period of time, it was considered that during the initial system development there would be no advantage to using MySQL and so, instead, the database was managed initially as a simple text file and then as a simple key/value-pair database using the Berkeley-style Database Abstraction Layer (DBA) class in PHP.

The aspects of the trials considered in the 'risks' table above, are now considered.

*Battery Life.* The results of the field trials allowed the conclusion to be drawn that the current consumption of the logger, reporting its status once every two days, would be around 400 mAh/year, so a 'twin' set of LiFeS<sub>2</sub> cells should last for 15 years, which is their recommended lifetime. It should be noted that, because the cells are small and cheap, there is really no practical limit to the number of sets that can be used as a power source if a more frequent data transmission is required.

*Network access.* A review of cellular network coverage in the primary areas where disused shafts are located in the UK suggested that the use of standard antennas would be adequate. (It is understood that the situation is broadly similar in other EU member states).

*Corrosion and biological activity.* Careful attention was paid to the design to attempt to minimise these risks and it was considered that – within the scope of the field trials– the situation was adequately addressed.

*Stiction of mechanical parts.* Initial trials included an investigation into the effect of a very slowly moving shaft-fill of the order of 2 mm/hr. There was some ‘binding’ of the components due to stiction. However, in all cases the sensor became unstuck immediately if small vibrations or air currents were present. It is considered that a production component could be adequately designed, but it is not known how corrosion and biological activity could affect this aspect of the operation.

*Network capability.* The remaining aspect of the initial field trials was to investigate whether the system could cope with a large number of units. This was not possible to test with a small network, and a sufficient simulation was considered to be far from straightforward. To mitigate any potential problem, each unit in the field was programmed to call the server at a different time but, in general, it should be noted that data clashes ought to be dealt with by the GPRS network and the server software, and should not cause a problem – the situation being no different to conventional use of the network where web servers must accept multiple simultaneous connections.

#### *Preliminary Conclusions*

In conclusion, the initial field trials have not indicated any serious problems and it has been recommended that the prototype sensor be considered for a wider implementation.

#### **2.3.2.3.2. Development of techniques in water-filled shafts**

This sub-task aims to develop effective techniques in water filled shafts with potentially turbid media, investigating the use of high-resolution pulse-echo ultrasonic imaging.

An initial scoping exercise prepared under Task 1.2.1 (Novel Techniques for Monitoring the Condition of Disused Mine Shaft Linings in Turbid Water) into methods of inspecting the linings of disused mine shafts flooded with turbid water was carried out.



**Figure 2.3.2.3.2-1 Imagenex 881 Profiler**

Although specialist ultrasonic borehole scanners are mostly inapplicable for use in mine shafts (despite the apparent similarity of the application) and are hugely expensive, more general purpose underwater imaging scanners were considered to be of potential value (especially in highly turbid water) and were recommended for evaluation in an actual flooded mine shaft.

The ultrasonic scanner evaluated in this exercise was the Imagenex 881 Profiler. (Figure 2.3.2.3.2-1).

Tests were carried out in a flooded shaft (549.5m deep, 4.3m in diam; brick lined and flooded to within about 37 metres of the surface) at the former Collins Green Colliery near Newton-le-Willows, Cheshire, UK, – involved lowering the scanner into the shaft at a fixed rate while recording data as a series of 360° scans. Follow-up work involved processing the data to demonstrate a range of ways in which it can be visualised. A Technical Report: Evaluating Ultrasonic Imaging Equipment for Inspecting the Lining of Disused Mine Shafts in Turbid Water giving full details of this test, conclusions and recommendations was submitted as a contribution to Deliverable 2.4.

Data was displayed live from the scanner and also recorded for play back later using the Win881AL software provided with the Imagenex 881 Profiler. A screenshot of the software is shown in

(Figure 2.3.2.3.2-2). Data is continually drawn while the target is swept in an angular fashion as in a radar display.

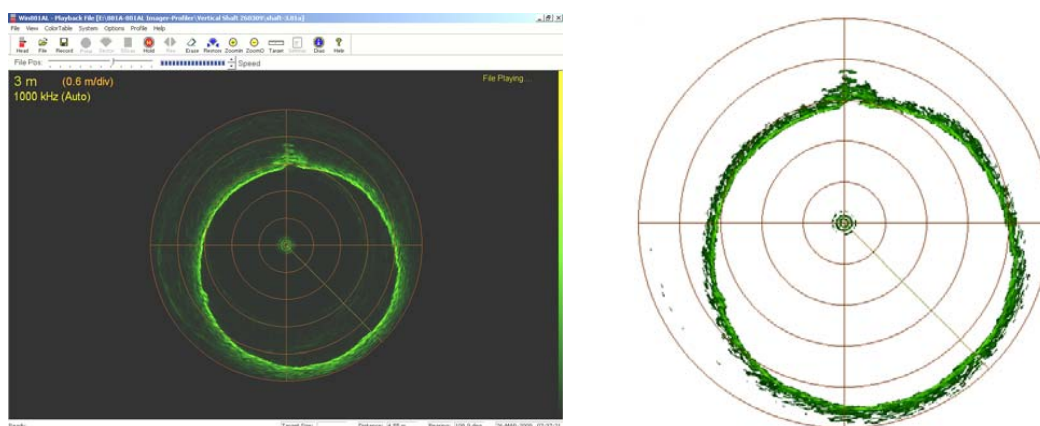


**Figure 2.3.2.3.2-2 Actual display and Clarified Image**

The evaluation proved that marine type ultrasonic scanners are capable of detecting features – some of which could represent deterioration – in the linings of flooded disused mineshafts, where optical methods are largely ineffective due to the turbidity of the water. Real time display permits the condition of the lining to be monitored while scanning is in progress, and recording of the data allows a subsequent in-depth analysis.

The improvement with respect to optical imaging is illustrated in (Figure 2.3.2.3.2-3) which compares footage from a previous optical survey of an adjacent shaft (in which the lining is barely visible) to a profile scan obtained in the evaluation exercise. The improvement in the ability to detect features (in this case an indentation in the shaft lining – circled in red) in turbid water is clearly visible.



**Figure 2.3.2.3.2-3 Comparison of Optical Imaging and Profile Scan as Obtained in the Evaluation**

The results of the trial were compared with a transcript of the 1980 video survey when the water level in the shaft was 170m from the surface with a good correlation of results achieved.

Research and on-site evaluation has indicated that Ultrasonic scanning provides a means of inspecting the linings of mine shafts, flooded with turbid water, in which optical inspection is often ineffective. A system with the following characteristics could therefore be produced. Note that these points refer to brick lined shafts since they tend to be the oldest and, hence, the more likely to suffer damage. Nevertheless, the system is inherently suitable for shafts with concrete lining and aspects such as the resolution would be identical.

Whilst the resolution of the system, as described above, is adequate to detect salient features it is often not possible to unambiguously identify a feature in a scan. So, except in the case of severe deterioration of the lining, which will often be clearly obvious, it is probably better to consider ultrasonic scanning as

a tool for detecting changes in the condition of a shaft by comparing the results with those obtained on a previous occasion.

### 2.3.2.3.3. Field trials with prototype of Laser Profiler System

#### Test site

In Task 1.2.1 a prototype of a shaft scanner system has been presented. The purpose of the field trial was to evaluate the operability of the system in an existing abandoned mine shaft. The shaft identified for the field trial is an old mine shaft of German company K+S nearby the city of Hildesheim in central Germany, named Shaft Rössing-Barnten (Figure 2.3.2.3.3-1). The Shaft provides an easy access to its approx. 1050 m depth and 5 m diameter. For trial purposes, a section of approx. 100 m (530 - 430 m depth) was selected for all test runs, thus including a former gallery to be identified at approx. 500 m depth (500m Sohle).

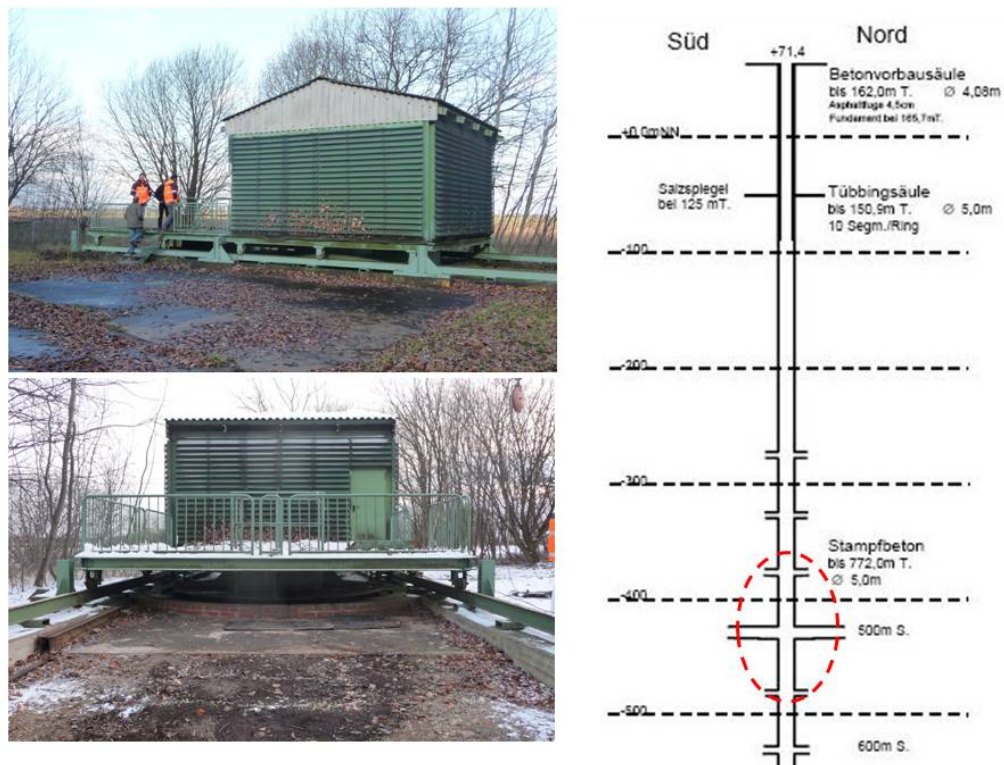


**Figure 2.3.2.3.3-1 Shaft Rössing-Barnten**

Beside the rack integrating the inertial measurement unit, scanner, power supply and additional weights, main components of the trials were composed of a truck mounted winch with 2.600 m cable and digital control unit (Figure 2.3.2.3.3-2) and an additional truck-crane to position a cable roll over the shaft.



**Figure 2.3.2.3.3-2 Winch installed on truck**

**Program of field trials**

The program for the field trial included several runs performed at different speeds and data capture rates (Table 2.3.2.3.3-1). Main objective of these variations is to determine the best combination of parameters for an optimized scan data. Previous experiences from static measurements in shafts showed, that a maximum difference of 1 cm between adjacent scan points should not be exceeded to ensure a complete and detailed shaft lining surface, thus enabling a visual interpretation of the shaft condition.

	Scan 1	Scan 2	Scan 3	Scan 4
Range	530 - 430	530 - 430	530 - 430	530 - 0
IMU-Data	X	X	-	-
Laser Power	Low	High	High	High
Mirror Rotation (rps)	25	25	12,5	25
Data Capture Rate (pps)	250.000	250.000	122.000	250.000
Pixel / 360°	10.000	10.000	10.000	10.000
Winch Speed (cm/s)	12	12	12	50
Vertical Profile Distance (cm)	0,5	0,5	1,0	2,0
Data (GB)*	2,26	1,42	0,71	2,35

\*Including data captured while descending

**Table 2.3.2.3.3-1 Table of test parameters**

As scanner control parameters were provided via WLAN, the scanner had to be switched on before descending, thus capturing data even on the way down the shaft with a speed of approx. 1m/s until reaching the start point in 530 m depth.



**Figure 2.3.2.3.3-3 Profiler prototype**

The following (Figure 2.3.2.3.3-3) shows the prototype, integrating the inertial measuring unit (IMU) in vertical position, weights for stabilization purposes and the bottom mounted laser profiler unit.

Data has been stored on a local CF-Drive, separating files of approx. 250 MB, so that data had to be downloaded via WLAN between the test runs. The inertial measurement unit has been operated separately, thus using its own power and data storage device.

## Results

To check completeness and quality of the scan data, a first evaluation could be made directly after downloading the data on a portable computer still on site. It could be asserted that the scanner operation has been successful. Data have been collected in function of the chosen parameters. Pendulum and rotational movements, temperatures below zero degree haven't caused any problem in the operation of the scanner. All mechanical and electronic components have worked satisfactorily.

Main difficulties were foreseen, namely rotation and pendulum movements of the measurement system, caused by rotation of the cable and ventilation pushing into the shaft. These effects can be recognized clearly in the scan data (Figure 2.3.2.3.3-4 and Figure 2.3.2.3.3-5). As the shaft is considered straight vertical, the point cloud shows a swinging effect. Scanner rotation leads to a drift of vertical structures in the unwrapped scan data. Despite of these movements, single shaft lining structures or known galleries can be clearly identified in the scan data.



**Figure 2.3.2.3.3-4 Scanner Pointcloud Visualisation (Leica Cyclone Software)**

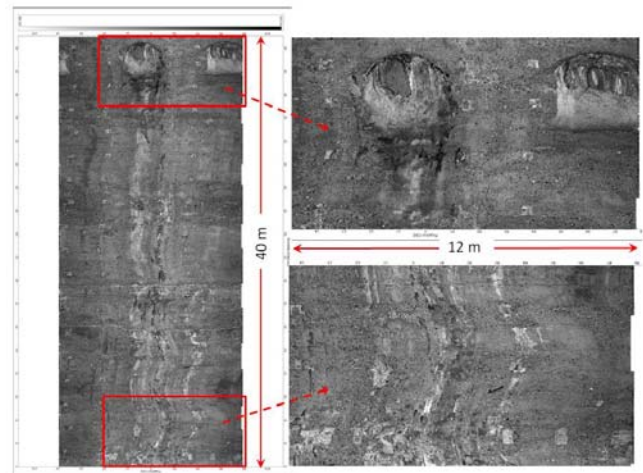


**Figure 2.3.2.3.3-5 Unwrapped scan data of shaft lining approx 500 m depth (Amberg TMS Software)**

Scan data has been imported into Leica Cyclone Software, thus enabling the visualization of the point clouds. Further data processing has been performed with Amberg TMS-Software, resulting in unwrapped shaft lining data and horizontal sections indicating deviations from a theoretical true vertical and circular shaft column (Figure 2.3.2.3.3-6). Inertial data has been collected simultaneously, but not yet processed.

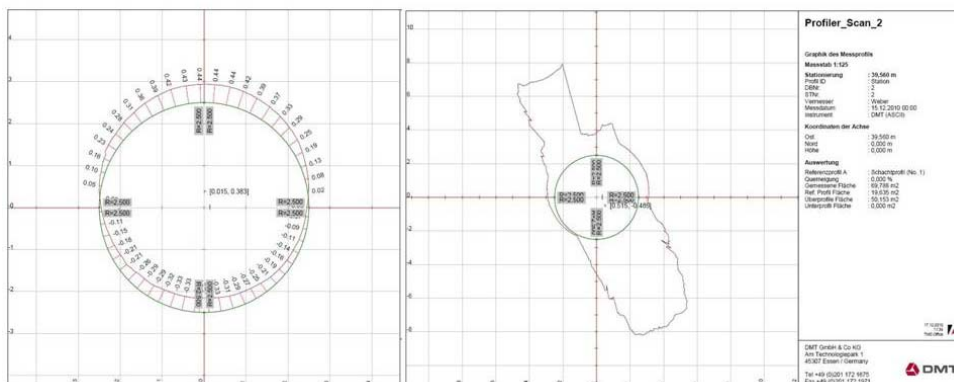


**Figure 2.3.2.3.3-6 Horizontal Sections (Amberg TMS Software)**

### 2.3.3. Risk Management of subsidence hazards on surface. WP3.

#### 2.3.3.1. Task 3.1. Integrated monitoring at surface

RAG and RAG’s subcontractor, Clausthal University of Technology, Institute for Geotechnical Engineering and Mine Surveying (TUC) worked on an integrated monitoring for an active colliery and for a neighboured abandoned mine with a controlled decrease of water mine drainage and a slowly rising mine water table. Both areas are covered by levelling lines with periodical measurements of about three months for the active and annual measurements for the old mining. All available data should be imported into a “4-D” point database, the GeoMon-DB, with possibilities to detect identical points that are affected by 3D ground movements over several years in position and height.

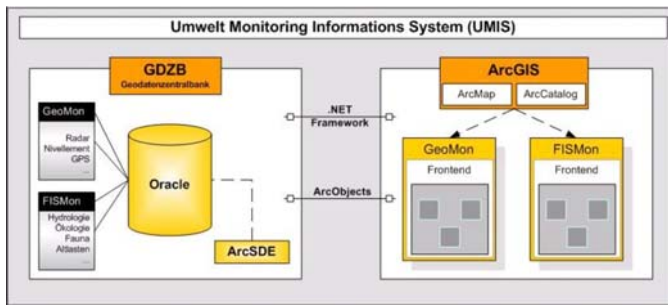


Figure 2.3.3.1-1 GeoMon database architecture.

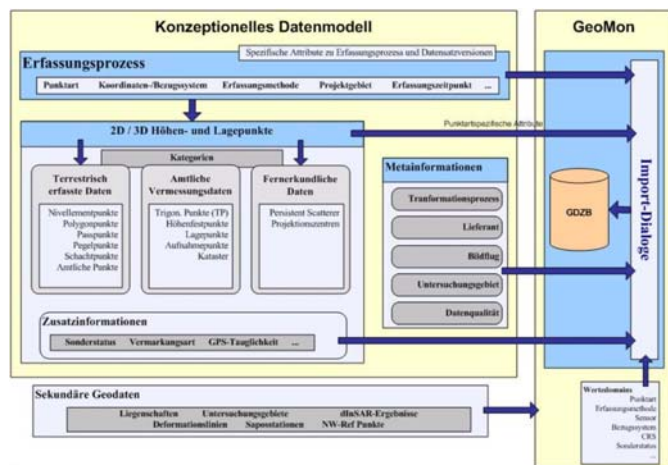


Figure 2.3.3.1-2 GeoMon database model and structure.

The requirements for the database have been determined and the database model and database structure have been stated (see Figure 2.3.3.1-2). The acquisition of specific metadata and attributes as well as import formats, import dialogues and versions have been determined for terrestrial and remote sensing data, geodetic reference systems, measurement campaigns. Tools for identification, selection, analysis and visualisation have been developed (see Figures 2.3.3.1-3 and 2.3.3.1-4).

RAG’s GeoMon-DB was used to compare the terrestrial and space borne data. The GeoMon-DB was designed for RAG’s purposes as a part of the environmental monitoring system “UMIS” as a “4D Point Information System” for the integrative and documented storage, management and access of survey results from heterogeneous sources and quality levels for a combined

consideration of terrestrial and remote sensing data for the detection and analysis of surface deformation. The Oracle database is based on ESRI ArcGIS 9.2 and ArcSDE 9.2 (see Figure 2.3.3.1-1). The GIS implementation and database functionalities are programmed with Visual Basic .NET and the ArcGIS Developer framework ArcObjects.

The requirements for the database have been determined and the database model and database structure have been stated (see Figure 2.3.3.1-2). The acquisition of specific metadata and attributes as well as import

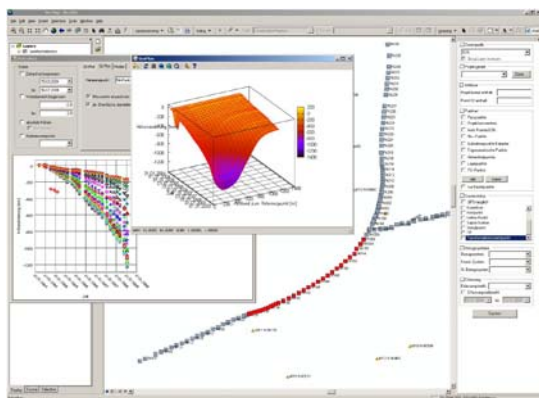


Figure 2.3.3.1-3 GeoMon-DB: visualisation of a time series for a levelling line

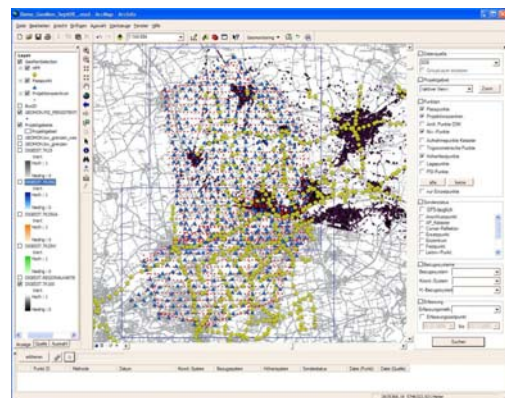


Figure 2.3.3.1-4 GeoMon-DB: visualisation of different point information: yellow - line levelling, blue - aerial ground control points, red - projection centres of aerial images. violet - persistent scatterer.

The intention was to combine and evaluate independent high accurate data like terrestrial levelling, different GPS methods (real-time, static, permanent) and space-borne data from radar satellites. So two permanent GPS stations (see Figure 2.3.3.1-5) and six points for Corner Reflectors (CR) were installed near levelling lines. The CR points are suitable for GPS measurements (see Figure 2.3.3.1-6).



**Figure 2.3.3.1-5 Permanent GPS stations “hospital” (left) and “shaft” (mid) with GPS receiver and power supply (right).**



**Figure 2.3.3.1-6 Corner Reflector no. 2 near levelling line aligned to ENVISAT orbit (left) and static GPS measurement on CR pillar (right).**

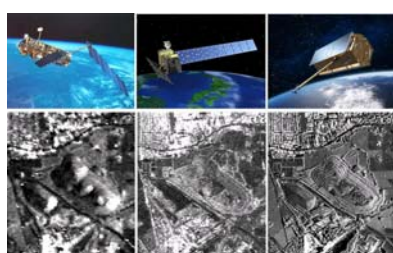


**Figure 2.3.3.1-7 Radar satellites and their averaged intensity images for ENVISAT-ASAR (left), ALOS PALSAR (mid) and TerraSAR-X (right).**

The SAR interferometric processing of the radar satellite data was performed by TUC and assisted by the Swiss company Gamma Remote Sensing (Gamma). The available satellite data was from the European ENVISAT-ASAR, C-band (49 scenes since 2003 on, 24 archived and 25 current scenes), the Japanese ALOS-PALSAR, L-band (from august 2006 on, 6 scenes track 644 and 9 scenes track 645) and the German satellite TerraSAR-X, X-band (30 scenes from 2008-02-11 on), as you can see in the (Figure 2.3.3.1-7) ENVISAT satellite data was normally purchased. ALOS data were provided through Gamma by JAXA for scientific investigations within ALOS ADEN AO 3567 and ALOS RA-094. TerraSAR-X data in stripmap mode were provided through Gamma by the German Aerospace

Centre DLR for scientific investigations within the AO GEO\_0162.

For ENVISAT all scenes are present with 35 days period, for ALOS with 46 day period but due to JAXA’s scientific program with gaps of up to 250 days for one track. For TerraSAR-X the period is 11 days but not all scenes were recorded due to satellite maintenance or overlap with other orders.

The SAR processing was performed for two different methods, “Differential SAR Interferometry” (DInSAR) for area-wide analysis and the “Interferometric Point Target Analysis” (IPTA©, Gamma) for

point-wise ground movement detection on Persistent Scatterer (PSI, Persistent Scatterer Interferometry).

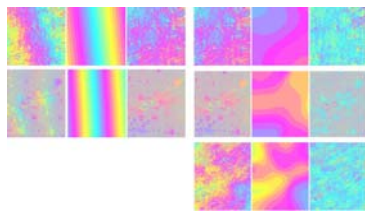


**Figure 2.3.3.1-8 Upper row: ENVISAT-ASAR, mid row: ALOS-PALSAR, lower row: TerraSAR-X. Block left: Differential interferograms (left), orbit related trend (mid) and orbit corrected differential interferogram (right). Block right: Orbit corrected interferogram (left), low frequency phase = atmospheric (mid) and orbit- and atmosphere corrected interferogram (right).**

DSAR can be performed with a minimum of three satellite scenes but the practice showed that a stack of at least ten scenes is necessary to identify and eliminate errors in the imagery caused by un-exact orbits, topographic phase and influences due to atmospheric disturbance (see Figure 2.3.3.1-8).

For IPTA©/PSI at least a minimum of 20, better 30 satellite scenes is required. For this reason IPTA©/PSI could only be performed for ENVISAT and TerraSAR-X but not for ALOS due to only 6 and 9 scenes per track.

TUC processed all satellite data with several DEM: high resolution photogrammetric DEM, DEM from the ordnance survey North Rhine-Westphalia, SRTM-X (1''), SRTM-C (3'') and Intermap Technology's NEXTMap© 5m resolution DEM (see Figure 2.3.3.1-9).

Knowing these primary basic premises and requirements the satellite data was processed by TUC regarding, detecting and eliminating these influences for the derivation of best fitting ground movement results.

EMAG's work in WP3 was focused on the following data

- information on surface subsidence on the base on SAR images,
- information on 3D displacement of points at surface, recorded by GPS receivers,
- seismic data recorded on surface and underground.

The SAR data is related to such a small number of scenes because their meaning is rather auxiliary as they will be used to confirm general changes of surface subsidence due to mining activity. Three images of ENVISAT ASAR were bought and are the subject of analysis.

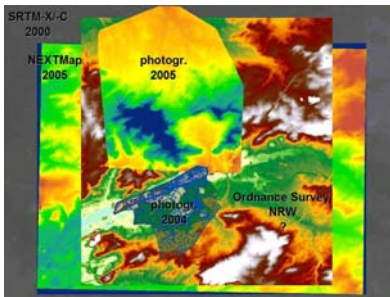


**Figure 2.3.3.1-9 Overview of Digital Elevation Models (DEM) used within the SAR interferometric process for the active and abandoned mining regions.**

GPS measurement for the Jas-Mos colliery data has been recorded GPS and post-processed. The data was collected constantly at four stations and periodically at about 70 survey points and delivered to RAG in two text files including measurements in BLH WGS84 coordinate system and arranged in the settled form and order. For the collected numerous constant surveys, the 10 days distant measurements samples with most representative for each day have been selected. The data from EMAG then had successfully been imported into RAG's GeoMon-DB:

**Figure 2.3.3.1-10 Gauss-Krueger coordinates, 6th meridian (left) delivered by EMAG, Gauss-Krueger coordinates edited for 2nd meridian's visualisation in RAG's ArcGIS (right).**

From EMAG RAG received a digital map in AutoCAD DXF and DWG format and two ASCII-files with GPS measurements of about 76 points for the Polish colliery for the year 2009. For the visualisation in RAG's ArcGIS and due to restrictions of the GeoMon-DB domains for RAG's purposes it was necessary to adapt the number of the meridian from "6" (Poland) to "2" (Germany) for the easting, see (Figure 2.3.3.1-10).

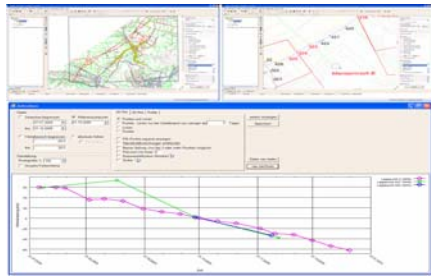


**Figure 2.3.3.1-11 Georeferenced map for the Jas Mos Colliery. Overview (left) and detail (right), measured movement behaviour of selected points 2, 421 and 422 in GeoMon-DB.**

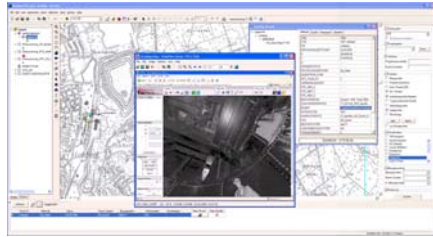


**Figure 2.3.3.1-12 GeoMon-DB: Visualisation of 3D Laserscanner data for a shaft.**

In this case this procedure is legitimate because the map of the Polish colliery, too, had been georeferenced to Gauss-Krueger, 2nd meridian by only changing the meridian from “6” (Poland) to “2” (Germany) for the easting, (see Figure 2.3.3.1-11).

An example for the possibility of connecting completely different data delivered by the third party is the visualisation of 3D-Laserscanner data within the GeoMon-DB (see Figure 2.3.3.1-12). It is possible to apply one file with standard formats, like doc, xls, pdf, wmv, avi, jpg, tif, ..., as “BLOB” (Binary Large Object) to one point of the GeoMon-DB.

Two measurements from AITEMIN’s test site data with points derived from terrestrial photogrammetry and an afterwards calculated grid could successfully imported and visualized in the GeoMon-DB, too (see Figure 2.3.3.1-13).

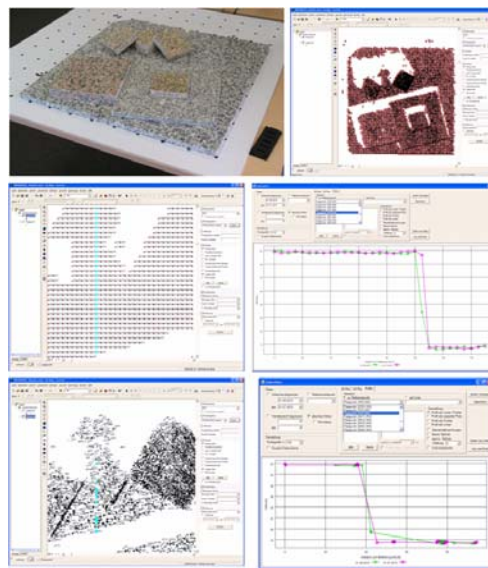


**Figure 2.3.3.1-13 GeoMon-DB: Integrated photogrammetric DEM point data from Aitemin.**

### 2.3.3.2. Task 3.2. Detection of hazardous areas at surface

To quantify the hazardous areas at surface MRSLS has focused on the evaluation of the potential risks that present the abandoned mineshaft; while ARMINES, EMAG and GEOCONTROL have worked on methods to defined and evaluate the hazardous areas at surface.

Geocontrol has developed a methodology that allows to assess the damage that may involve the excavation of a roadway, or its collapse after it was built on the buildings located in the surface.

This methodology is based on the tensile strain calculation applied to geomechanical models, representing the roadway and the ground on which it is excavated.

To relate the results of the tensile strain calculations with its possible involvement on the buildings, the most modern criteria have been applied to assess the damage produced on buildings during the construction of urban tunnels.

#### 2.3.3.2.1. Potential risks in abandoned mineshafts

There are approximately 168,000 recorded coal mine entries throughout Great Britain. Most of these are now abandoned and are not visible at the surface. Shaft collapses can result in significant surface

subsidence and catastrophic surface problems especially in populated areas. (Figure 2.3.3.2.1-1)



**Figure 2.3.3.2.1-1 Hazardous Areas at surface from collapse of shafts**



The date of entry, type of construction and techniques used may indicate points of potential weakness, excessive water flow or other abnormal conditions. Most disused shafts have at some time been wholly or partly filled and, with the exception of those which are permanently marked (for example by a cover slab or monument), are concealed at the surface. (Figure 2.3.3.2.1-2).

**Figure 2.3.3.2.1-2 Concealed Shaft No Surface Treatment**

The treatment of disused coal mine shafts has differed and developed over a time spanning the Middle-Ages to the present. Many historical shafts were simply covered with a rough timber capping and covered with soil. Trees were often planted adjacent to such capping with a view to providing a natural reinforced cap by the growth and interlocking of the roots in the soil of the cap. (Figure 2.3.3.2.1-3) Entrances were often closed and secured after abandonment by placing a platform or makeshift plug a short distance down the shaft and filling with any available material. In time the staging deteriorates or becomes overloaded and collapses. The total fill is then lost into the void below, possibly being followed by collapse of the lining and cratering of the ground at the surface. (Figure 2.3.3.2.1-4).



**Figure 2.3.3.2.1-3 Old Mine Shaft defined by Tree**



**Figure 2.3.3.2.1-4 Depression of Old Mine Shaft**

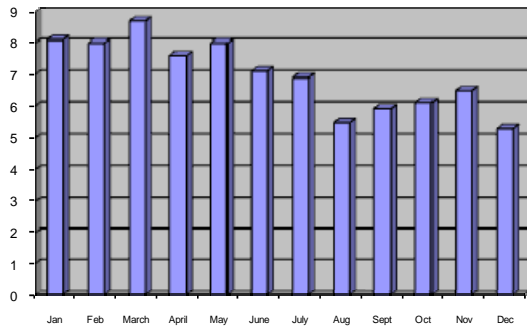


**Figure 2.3.3.2.1-5 Incidents in the U.K. involving Mine Shafts - 10 year average**

Analysis of field data indicates that the occurrences of shaft collapses in the U.K. (Figure 2.3.3.2.1-5) are more likely to occur in the early months of the year as the ground temperatures and rainfall increases followed by a second period when rainfall increase in the late autumn / early winter after a “dry” summer

### 2.3.3.2.2. Methods to identify the hazardous areas at surface

Identification of hazardous sub-areas in mining territories should be carried by analytic methods supported with specialized measuring techniques.

Measuring system based on the data collected at surface sites should provide calculations and simulations of adequate hazards and creating of maps.

Alike geodetic surveys also recording of appropriate geophysical measurements, both in underground stations and at surface sites, is necessary for the assessment of seismic hazards influence on mining areas.

Measurements on surface should be carried to obtain the evaluation of ground vibration parameters. Deployment of measuring stations must be designed to provide the assessment of vibration propagation within the whole monitored area.

The assessment of bumps on surface is performed on the base of distribution of vibration parameters induced by seismic events. The crucial are relations among maximum amplitude, and signal vibration duration to bump energy and hipocentral or epicentral radii.

An impact of harmful vibrations on surface may be also evaluated on the base of data recorded at a selected surface station by the analysis of relations between maximum resultant value of horizontal amplitude components of vibrations to the time of the event duration. The evaluation of above parameters should be performed for the frequencies less than 10 Hz, because only vibrations within that band have the harmful impact on surface.

The knowledge of a seismic bump parameters and vibration parameters relation makes possible to estimate vibration parameters values induced by that bump in any point of the monitored mining area i.e. calculation of surface vibration parameters distribution. The obtained distribution permits for location of zones hazarded by bump influence while parameter values determine the level of harmfulness on surface, buildings and infrastructure.

#### **Risk scales:**

The (Table 2.3.3.2.2-1) shows conditions of damage occurrence that have to be taken into account depending on risk value and risk probability:

<b>evaluated risk value</b>  <b>probability of risk occurrence</b>		
	<b>low risk</b>	<b>high risk</b>
	low $p < 0.4$	risk should be taken into account
high $p \geq 0.7$	sequence of adverse events should be taken into account	risk must be absolutely taken into account

**Table 2.3.3.2.2-1 Damage occurrence depending on the relation of risk value to risk probability**

Regulations applied for the assessment of hazard caused by bumps may be based on various methods. Those methods are included in the scales of hazard. An international scale MSK (Medvedev-Sponheuer-Karnik) or MSK-64 is based on maximum vibration acceleration within the band range below 10 Hz. It consists of twelve intensity levels. The scale assumes an impact of vibrations in turn on:

- people and their direct environment,
- buildings,
- nature.

On the base of observed measurements and effects of bumps, successive intensity levels are assigned to resultant amplitude values of ground vibration acceleration. Those relations are presented in the (Table 2.3.3.2.2-2).

Intensity level	Vibration acceleration* $10^3 \text{ m/s}^2$	Effect on surface
I	5—12	not noticeable
II	12—25	scarcely noticeable
III	25—50	weak, only partial observation
IV	50—120	Widespread observation
V	120—250	Awakening
VI	250—500	Frightening
VII	500—1000	damage to buildings
VIII	<b>Earthquakes !!!</b>	Destruction of buildings
IX		general damage to buildings
X		general destruction of buildings
XI		catastrophe
XII		landscape changes

**Table 2.3.3.2.2-2 Relation of vibrations intensity to values of accelerations and effect on surface by MSK- 64 scale.**

Except MSK-64, developed local GZI-GZW and GZI-GZW-A are other scales used in Poland. The scales determine risk values on the base of maximum horizontal amplitude components of vibration velocity (GZI-GZW) or acceleration (GZI-GZW-A) in relation to the recorded event duration within the band frequency below 10 Hz. The relations for both scales are presented on the (Figures 2.3.3.2-1 and 2.3.3.2-2).

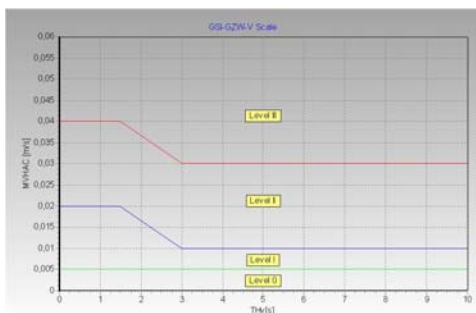


**Figure 2.3.3.2.2-1 Mining and scale**

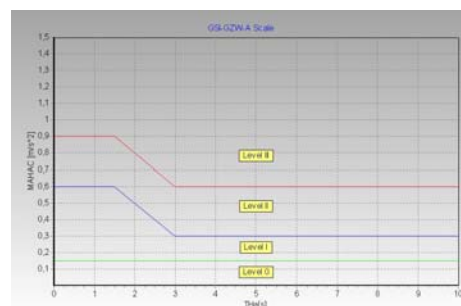


**Figure 2.3.3.2.2-2 A Mining Intensity of Vibration Scale**

### 2.3.3.2.3. Quantification of hazardous areas at surface

This task has performed works to study two type of phenomenon which can produce hazardous areas at surface; the first one is the evolution in time of abandoned mines that are susceptible of flooding. The second one is geared towards the provision of subsidence that may result from mining galleries and their impact on existing building to the surface.

In both cases a similar calculation methodology has been carried out, since the works have been performed using geomechanical models resolved through the FLAC software.

The analyses of flooded European colliery basins and especially the French Lorraine basin which is currently under flooding and which has been particularly studied in this project had shown, as illustrated by (Figure 2.3.3.2.3-1), that the surface behaviour of a longwall coal mine is marked by the following episodes: subsidence induced by mining, residual subsidence, reactivation of subsidence induced by flooding, uplift induced by water table rise and uplift induced by swelling of argillaceous rocks under special depth conditions.

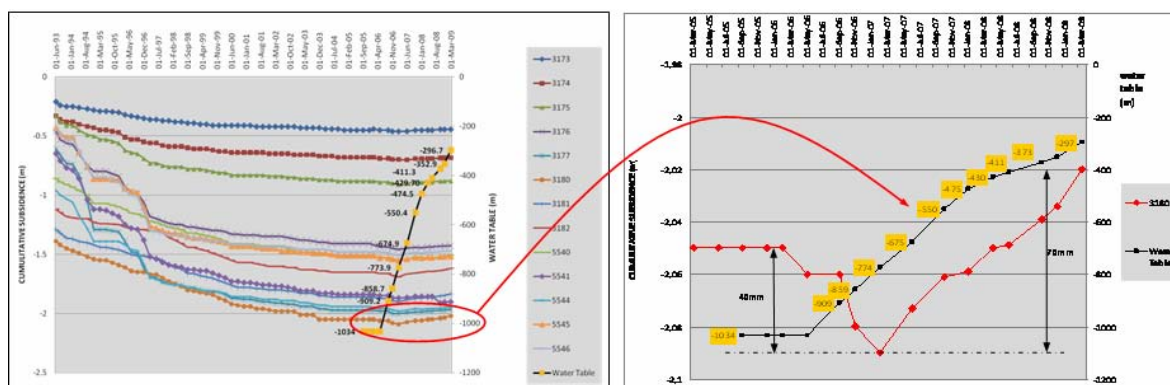


**Figure 2.3.3.2.3-1 Illustration of the surface behaviour during the different episodes of longwall coal mine (Lorraine colliery basin).**

Thanks to these two main acquired results, a parametric study was conducted in this task to highlight the capability of the proposed modelling to describe accurately the surface behaviour of a caved longwall mine and to emphasise the governing parameters which may induce hazards on the surface.

The main conclusions which can be drawn up from all the analyses conducted on the surface behaviour of a longwall coal mine during the different episodes of its life can be summarized as follows:

- The modelling approach developed allows to account for all the observed phenomena of the surface behaviour: mining subsidence, residual subsidence, reactivated subsidence due to water effect, uplift induced by swelling and uplift induced by pore pressure
- This modelling approach could be used to assess the hazards and the risks when flooding caved coal mines. The major difficulty in such a modelling lies in describing properly the behaviour of each material, especially the selection of the reliable law and parameters.
- Caved rocks and overburden are governing the mechanics of subsidence when flooding coal mines: effect of water, swelling, creep behaviour of overburden
- Swelling is governed by the swelling pressure and is therefore linked to the mining depth.
- Swelling is a rapid process and continuous swelling is due mainly to the presence of argillaceous materials in overburden.
- Pore pressures are not totally active and a Biot's coefficient has to be introduced to weight their effect.
- Uplift is governed by the dilation of a reservoir constituted by the caved rocks under the effect of

pore pressures, the contribution of swelling on this phenomenon is very limited.

- The formula proposed by Pöttgens could be wisely used to assess the amount of uplift (see deliverable D1.1.2).

Regarding to the quantification of the damage produced by the subsidence on buildings located on hazardous areas, a work of synthesis has been performed on the criteria that would be applied to these cases. This work has been supplemented with a practical example of application, which has led to a part of the Deliverable 3.2.

The damage levels to building were classified by Burland et al (1977), as shown in (Table 2.3.3.2.3-1).

CATEGORY OF DAMAGE	DEGREE OF SEVERITY	DESCRIPTION OF TYPICAL DAMAGE	WIDTH OF CRACKS (mm)
0	Negligible	Cracks almost imperceptible	< 0,1
1	Very slight	Fine cracks easily treated during normal decoration. Damage generally restricted to internal wall finishes. Close inspection may reveal some cracks in external brickwork or masonry.	< 1,0
2	Slight	Cracks easily filled. Re-decoration probably required. Recurrent cracks can be masked by suitable linings. Cracks may be visible externally and some repointing may be required to ensure weathertightness. Doors and windows may stick slightly.	< 5
3	Moderate	Cracks require some opening up and can be patched by a mason. Repointing of external brickwork and possibly a small amount of brickwork to be replaced. Doors and windows sticking. Service pipes may fracture. The use of the building must be stopped until repairation.	5 to 15 (many cracks > 3 mm)
4	Severe	Extensive repair work involving breaking-out and replacing sections of walls, specially over doors and windows. Door frames and windows distorted and floor considerably sloping. The building must be evacuated.	15 to 25
5	Very severe	The repairation can imply the partial reconstruction of the building. Cracks affects the structure and there is danger of instability.	> 25

**Table 2.3.3.2.3-1 Classification of visible building damages (Burland et al, 1977)**

Usually, categories 0, 1 and 2 are referred to visual damages (level 1), categories 3 and 4 to functional damages (level 2) and category 5 to structural damages (level 3). As the foundation movements increase, the damages to the building progress from level 1 to 3.

The cracks produced at building non structural elements (walls and others non structural elements) are generally due to tensile strains. Therefore, Burland and Wroth (1974) developed the idea that tensile strain is a fundamental parameter in determining the origin of cracking.

After several studies of large scale tests carried out at the U.K. Building Research Establishment, it was concluded that, for a given material, the beginning of visible cracking is associated with an average value of tensile strain which is independent from the mode of deformation. This value was defined as critical tensile strain  $\epsilon_{crit}$ .

CATEGORY OF DAMAGE	NORMAL DEGREE OF DAMAGE	LIMITING TENSILE STRAIN $\epsilon_{lim}$ (%)
0	Negligible	0 - 0,050
1	Very slight	0,050 - 0,075
2	Slight	0,075 - 0,150
3	Moderate	0,150 - 0,300
4 to 5	Severe to very severe	> 0,300

**Table 2.3.3.2.3-2 Relation between damage and maximum tensile strain (Boscarding and Cording, 1989).**

In 1977, Burland et Al replaced the concept of “critical tensile strain” with “limiting tensile strain”,  $\epsilon_{lim}$ . The importance of such consideration is the fact that the  $\epsilon_{lim}$  can be used as a serviceability parameter, being able to vary to take into account different materials and serviceability limit states. Boscarding and Cording (1989) developed this concept to associate ranges of  $\epsilon_{lim}$  to the six categories of damages previously defined. These ranges are shown in (Table 2.3.3.2.3-2).

To determine damages at present study, the building front is assimilated to a beam whose deflected shape assumes the resulting from the subsidence vertical displacements in “greenfield” conditions (without building modelling in the calculus of the subsidence curve).

Following the methodology proposed by Burland, maximum horizontal tensile strain is calculated taking account of the combination of modes of shear deformation and bending, to which horizontal

tensile strain is directly added. The resultant value is compared to the previously established limits to determine the level of damage in the building.

As an example of the Boscarding and Cording criterion, the case of a building located above the Tunnel of Elche (Alicante, Spain) is exposed.

The tunnel is excavated in tertiary materials of medium geomechanical quality. It corresponds to a formation composed of sandstone, limestone and marlstone inter bedded horizontally. T

To calculate the potential damage to the building, tensile strain calculations were performed, with the geomechanical model that is exposed in (Figure 2.3.3.2.3-2).

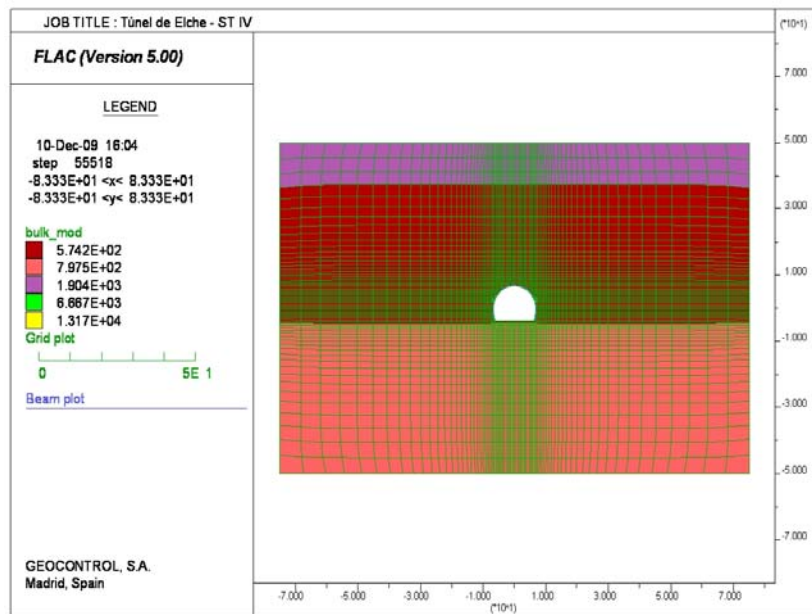


**Figure 2.3.3.2.3-2 Geomechanical model for the Elche's Tunnel**

The natural stresses adopted are:

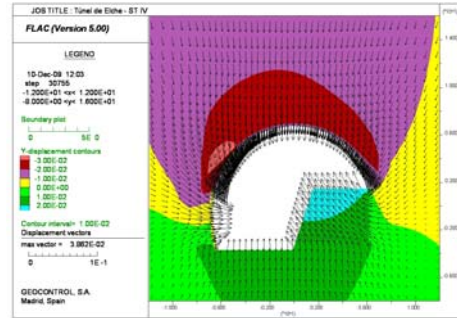
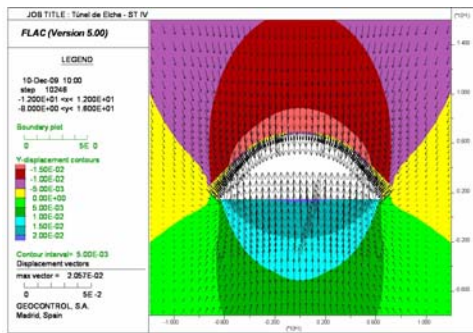
- Vertical stress: 1.25 Mpa
- Maximum horizontal stress: 1.65 MPa
- Minimum horizontal stress: 0.95 MPa
- And the support consists of the following elements:
  - i) 20 cm of reinforced shotcrete HM-30.
  - ii) Steel arches THN-29, spaced each 1 m.

The excavation is done with a top and benching sequence. The span for the top excavation is 1m and an elephant foot is used, while for the benching a span of 2 m has been adopted.

The geomechanical model was solved, in the three excavation phases, with the FLAC V:2.00 software. In the (Figure 2.3.3.2.3-3), the displacements calculated after stabilizing the excavation, for each of the three construction phases are shown. FLAC V:2.00.

**A.- After top heading completed**

**B.- After first half benching completed**



**C.- After fully section completed**

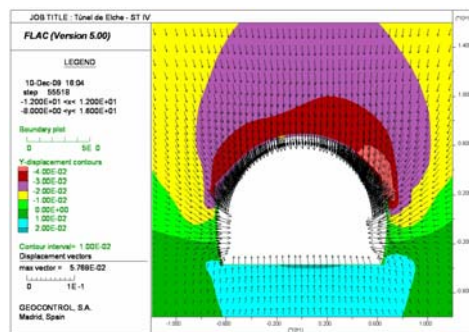


Figure 2.3.3.2.3-3 Vertical displacement after the calculations.

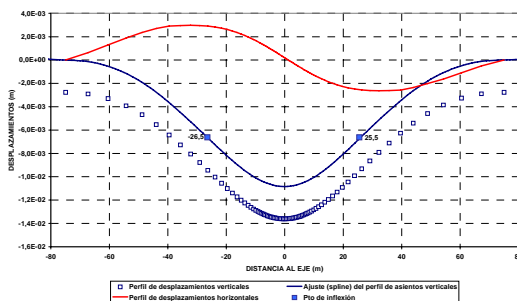


Figure 2.3.3.2.3-4 Subsidence profile and horizontal displacements distribution calculated and a cross section that includes the building over Elche's Tunnel.

From the results of the performed calculations with the FLAC software, the subsidence profile and the distribution of the horizontal displacements were determined, and are shown in the (Figure 2.3.3.2.3-4).

According to the performed calculations calculations the tensile strain was determined for the building area, as shown in the (Table 2.3.3.2.3-3).

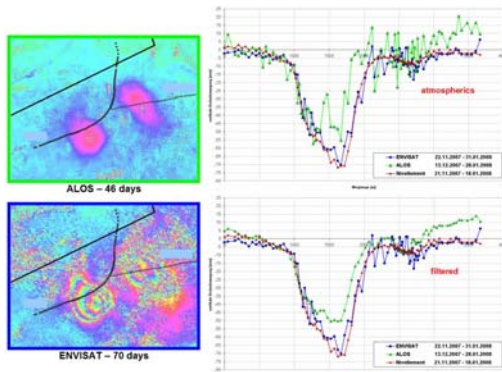
BUILDING DATA			
Building height: H (m)	6,00		
Initial distance from building to tunnel axis: X1 (m)	43,00		
Final distance from building to tunnel axis: X2 (m)	60,00		
Distance X1 <sub>CALCULO</sub> (m)	43,00		
Distance X2 <sub>CALCULO</sub> (m)	60,00		
Distance from inflection point to tunnel axis: l (m)	25,50		
Poisson coefficient:	0,30		
Relation E/G:	2,60		
	Left zone (Hogging)	Central zone (Sagging)	Right zone (Hogging)
Maximum relative vertical displacement: Δh (m):			2,35E-04
Reference length: L (m):	0,00	0,00	17,00
Maximum deflection ratio: Δh/L:			1,38E-05
Moment of inertia: I (m <sup>4</sup> ):	72	18	72
Position of neutral fiber: t (m):	6,0	3,0	6,0
Horizontal deformation (ground): ε <sub>g</sub> :			7,5E-05
Bending unit deformation: ε <sub>b</sub> :			2,0E-05
Shear unit deformation: ε <sub>s</sub> :			9,1E-06
Total bending unit deformation: ε <sub>b</sub> <sup>T</sup> :			9,5E-05
Total shear unit deformation: ε <sub>s</sub> <sup>T</sup> :			7,5E-05
Maximum deformation: ε <sub>max</sub> (%):			0,009
Damage evaluation:			NEGLIGIBLE

Table 2.3.3.2.3-3 Maximus tensile deformation.

The calculated value for  $\epsilon_{max}$  (%) was 0,05; ; which indicates, according to the (Table 2.3.3.2.3-1), that the expected damage to the building fall into the category of NEGLIGIBLE.

### 2.3.3.3. Task 3.3. Validation and verification of results

In following three examples for the applicability of a combined analysis of terrestrial and remote sensing data for the area-wide detection of hazardous areas due to mining induced subsidence and flooding induced uplifts will be presented:



**Figure 2.3.3.3-1 DInSAR analysis and comparison of ENVISAT-ASAR (blue) and ALOS-PALSAR (green) to levelling line measurements (red).**

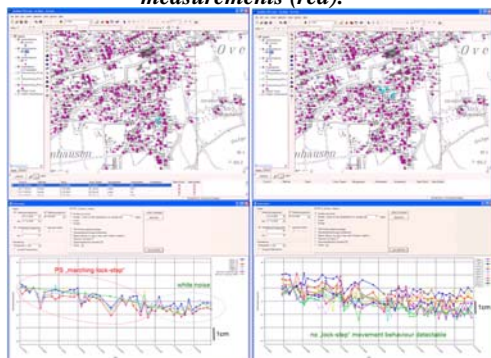


**Figure 2.3.3.3-2 GeoMon-DB: Movement behaviour of selected PS over known discontinuity (left) and for prolongation of the discontinuity (right).**

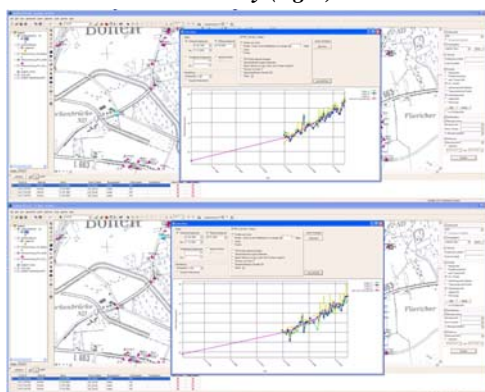


**Figure 2.3.3.3-3 GeoMon-DB: PSI verification for uplift movements at two different locations (magenta levelling of the ordnance survey North Rhine-Westphalia 1996 - 2006, others: selected Persistent Scatterer from ENVISAT ASAR, Dec. 2003 - Dec. 2008).**

First example: Within the GeoMon-DB the validation of DInSAR and IPTA© results was performed for all three satellites with ground reference measurements on levelling lines, GPS points and for the ground movements of the CR. (Figure 2.3.3.3-1) presents a comparison of ALOS-PALSAR (46 days) and ENVISAT-ASAR (70 days) DInSAR results to the measurements of a levelling line (30 days). For ALOS data an influence of atmospheric could be reduced by filtering. The analysis showed for all sensors and scenes the influence of the short time and seasonal coherence and the atmosphere that only could be reduced by a stack of more than 10 satellite scenes.

Second example: A Mine Survey Department received notifications of claim for the prolongation of an area with known discontinuities. Some house owners claimed mining induced damages against the colliery. For a reappraisal the GeoMon-DB was consulted. The influence of the active mining to the discontinuity could be proved for the known area by a bunch of PS marching in “lock-step” from 2004 until beginning 2007. In mid 2006 the exploitation ended for this working panel and, as expected by the Mine Survey Dept., from 2007 on no significant movement behaviour over the discontinuity could be detected. The movement behaviour of the ground surface was similar to white noise (see Figure 2.3.3.3.-2).

From the technically point of view these notification of claim could be rejected by the colliery.

Third example: RAG was confronted with a complaint from the mining authorities concerning inappropriate height measurements (uplift) on an official levelling line that crosses the area of a colliery out of RAG’ responsibility. This mine was abandoned in the 1970s and since then was flooded. The most northern parts of this line were fortunately covered by the most southern ENVISAT PSI points. With the aid of the GeoMon-DB the measured uplift of about 4cm from 2004 to 2009 on special levelling points could be compared and verified with the radar-interferometric PSI results (that are available from December 2003 on) for neighbored Persistent Scatterer (PS), (see Figure 2.3.3.3-3). In this way an unknown area with uplifts due to the flooding of a mine could be detected!



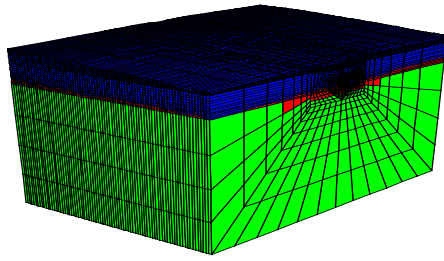


Figure 2.3.3.3-6 3D model

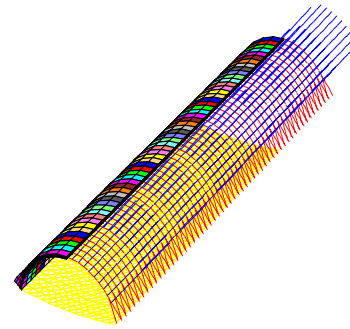


Figure 2.3.3.3-7 Modelling of the support elements.

GROUND	GROUND PROPERTIES						K <sub>0</sub>
	Bulk density ρ <sub>ap</sub> (t/m <sup>3</sup> )	Elastic parameters		Long term shear strength parameters		Dilantacy (°)	
		E (MPa)	ν	c' (kPa)	φ' (°)		
Soil alteration. Level 1.	1,65	45	0,35	25	21	5	1,0
Soil alteration. Level 2.	1,95	200	0,3	60	25	5	
Marl	2,36	300	0,28	100	30	5	

Table 2.3.3.3-1 Ground properties in the stage prior to the rupture .

As indicated the behaviour of the post-rupture of these materials was simulated with the strain softening constitutive model that varies the cohesion and friction of the ground according to the strain.

In this case, it was also considered essential to make variations depending on the terrain deformation and therefore a specific routine was established, integrated into the FLAC 3D software.

In (Figure 2.3.3.3-8) the properties that were taken for this ground in the post-break are shown.

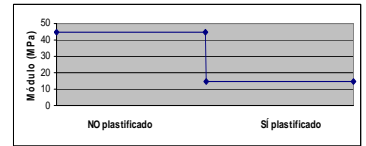
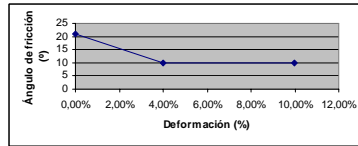
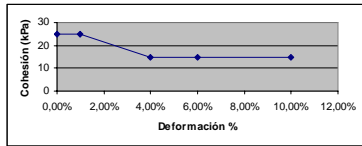
After performing the 3D model with the FLAC software, the distribution of the ground movements was obtained, which are shown in (Figure 2.3.3.3-9), while in (Figure 2.3.3.3-10) the distribution of the plasticized elements are shown.

As shown in (Figure 2.3.3.3-11) in surface, coinciding with the axis of the tunnel, five milestones were placed for the topographic control of the ground movements.

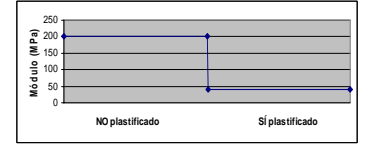
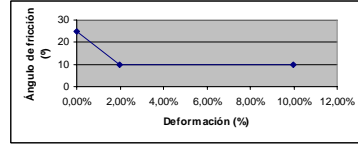
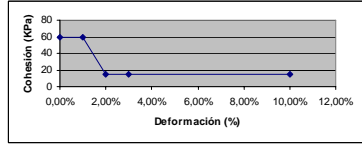
(Figures 2.3.3.3-12 and 2.3.3.-13), show, respectively, the evolution of the movements of the milestones PC-23 and PC-24 which are obtained from the calculations and those measured in field.

From the data in (Figures 2.3.3.3-14 and 2.3.3.3-15), (Table 2.3.3.3-2) was performed, which shows the actual subsidence measured.

**Weathered argilites Qv/C1 Level 1**



**Un-weathered argilites Qv/C1 Level 2**



**Marls C1**

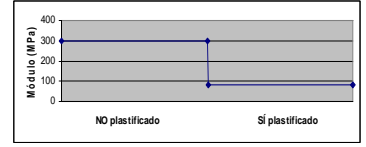
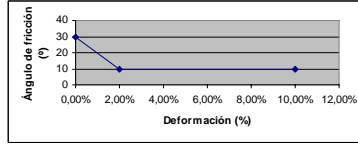
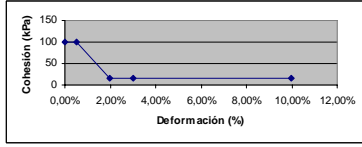


Figure 2.3.3.3-8 Ground properties in the stage after the rupture.

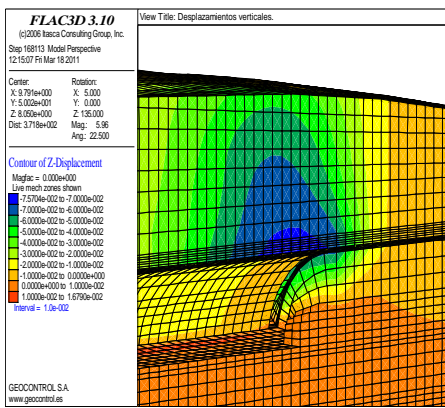


Figure 2.3.3.3-9 Distribution of the vertical displacements on the calculated

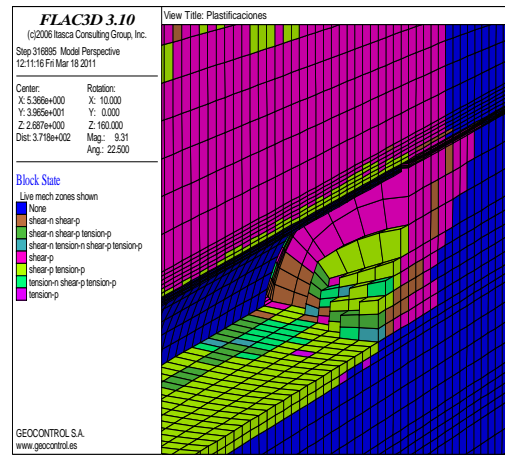


Figure 2.3.3.3-10 Distribution of the yielded elements after the excavation.

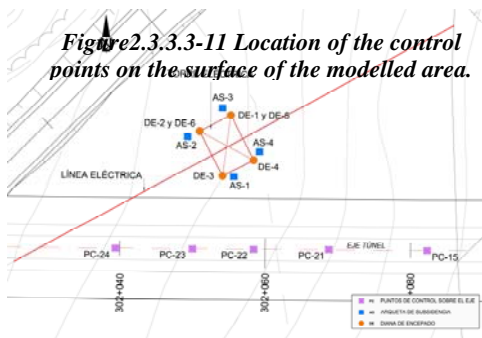
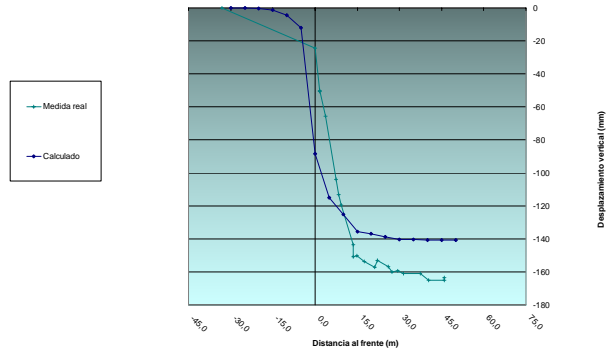
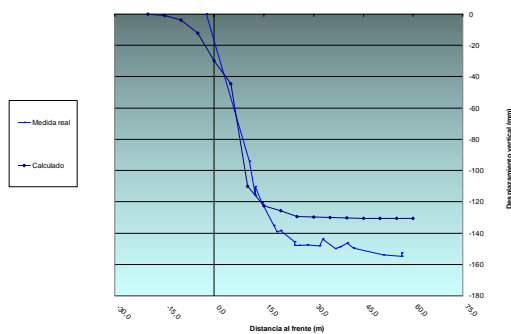


Figure 2.3.3.3-11 Location of the control points on the surface of the modelled area.





*Figure 2.3.3.3-13 Evolution of the measured and calculated subsidence in the PC-24 milestone*

MILESTONE	PC-23	PC-24
Max. Subsidence calculated	140 mm	132 mm
Max. Subsidence measured	163 mm	156 mm
Percentage deviation	+16,4 %	+18,2

*Table 2.3.3.3-2 Comparison between the calculated subsidence and the topographical measure.*

It exceeds the calculated in 16,4%, for the PC-23 milestone, and 18,2% for the PC-24 milestone.

These results confirm that the methodology of calculation of the subsidence that has been performed, gives reasonable results.

### 2.3.4. Project assessment and conclusions WP4.

#### 2.3.4.1. Review of all techniques in the light of mining experience

##### 2.3.4.1.1. Prediction of surface and subsurface subsidence (WP.1)

The prediction of the subsidence produced at surface has been studied under two major aspects; the first one **generated by the coal underground mines**, and the second one, the ones produced by **the roadways and shafts**.

##### 2.3.4.1.1.1 Prediction of subsidence caused by coal exploitations

The prediction of the subsidence caused by the coal underground mines has been extensively studied since in 1949, Oskar Niemczyk published his treatise “Bergschadenkunde” and later Knothe (1957) which assimilated the subsidence basin in a Gaussian distribution, which boosted the analytical study of the subsidence. Later on, Everling (1973), developed a program, based on the theory of elasticity, to calculate the subsidence produced by several layers and, nearly simultaneously the National Coal Board (1975) published the second edition of his acclaimed Subsidence Engineers Handbook.

With the widespread obtained by these tensile strain calculation programs, it became clear that this calculation tool was much more precise than the empirical-analytic methods that were developed at the end of the last century.

In this research project tasks 1.1.1, 1.1.2 and 1.1.3 have been directed to study the implementation of the FLAC code, which performs geomechanical models through finite difference algorithms, the **calculation of subsidence produced by coal mines (RMT/UK Coal)**, the **determination of the residual subsidence produced by the flooding of abandoned mines (ARMINES/RMT)** and the **prediction of the subsurface deformation (RMT/UK Coal)**.

In order to verify the adequacy of the FLAC code to calculate the subsidence, there have been performed two simulations, one working on the Barnsley Seam at Naborn in North Yorkshire and the other one on the A63 Leeds Road.

In both cases, similar conclusions have been reached, which conclude that the value of the maximum subsidence can be reasonably calculated, but not the shape of the subsidence basin.

#### **2.3.4.1.1.2 Prediction of surface deformation and to water rebound**

The performed application to calculate the influence of the flooding of old mines has allowed to obtain the following conclusions.

- The modelling approach developed, allows to be taken into account all the observed phenomena of surface behaviour; mining subsidence, residual subsidence, reactivated subsidence due to water effect, uplift induced by swelling and uplift induced by pore pressure.
- This modelling approach could be used to assess the hazards and the risks when flooding caved coal mines. The major difficulty in such a modelling lies in describing properly the behaviour of each material, especially selection of reliable law and parameters.
- Caved rocks and overburden govern the mechanics of subsidence when flooding coal mines; effect of water, swelling, creep behaviour of overburden.
- Swelling is governed by the swelling pressure and is therefore linked to the mining depth.
- Swelling is a rapid process and continuous swelling is due mainly to the presence of argillaceous materials in the overburden.
- Pore pressures are not totally active and a Biot's coefficient is required to weight their effect.
- Uplift is governed by the dilation of a reservoir comprising the caved rocks under the effect of pore pressure; the contribution of swelling on this phenomenon being very limited.

#### **2.3.4.1.1.3 Prediction of subsurface deformation**

To calculate the ground deformation, between the surface and the exploitation, several modelling works have been performed; being the most evolved the one performed to simulate the Welbeck Deep Soft panels exploitation using the FLAC 3D code to perform the three-dimensional geomechanical model.

The obtained results, which are close to reality, indicate that above unworked Parkgate, a GSI of 80 showed minimal roof movement with some rib and floor movement for a stress range of 20-35MPa. This matches the experience in 244 LG well. Above Parkgate waste, the vertical stress was expected to be in the range 5-15MPa and the GSI to be lower than above unworked Parkgate. At locations away from the influence of any waste edges the gates experienced minimal roof movement and the rib and floor movement was less than above unworked Parkgate. Assuming a GSI of 60 provided the best match although the roof movements predicted by the model were larger than those actually experienced. Above Parkgate waste, where influenced by waste edges, the stress may be higher if full stress relief is not obtained and the GSI lower if on the edge of the subsidence trough. Using a GSI of 50 gave increased roof movement, matching the 50mm on A tell-tales with minimal B movement experienced in sections of 242 and 240 L/G.

This back analysis from Welbeck can now be applied to modelling the gate roadways being developed in similar interaction circumstances at the neighbouring Thoresby colliery. FLAC3D models for Harworth and Kellingley collieries were also completed and are now available for application to mine roadway support design using the principles outlined above for overworking previous longwall panels.

#### **2.3.4.1.1.4 Prediction of subsidence caused by underground structures**

In the research on the methods to evaluate the subsidence caused by roadways and shafts the works have been directed in three lines; the two first are focused in the use of innovative techniques to recognize roadways and shafts and the third one is focused on the effect of water on concrete and

mortar used to fill abandoned excavations.

#### **2.3.4.1.1.5      *Shafts survey using innovative geophysical tools***

As regarding the shafts survey the work has been focused in the obtainment of direct optical imaging and laser scanner.

A programme of experimental work was carried out to determine the level of improvement that can be obtained by using various incremental improvements to the current generation of optical imaging equipment. Several methods for improving the performance of optical imaging equipment were proposed so the number of permutations was quite large. Furthermore, it was felt desirable to test at more than one range (i.e. multiple shaft diameters). The implication of this is that the experimental process would take several days. Because of access restrictions this precluded the use of an actual flooded mine shaft so a surface test facility was built for this purpose. This approach also permitted much greater control over the experimental conditions than would have been possible in an actual flooded shaft.

The following techniques were used in various combinations for the two ranges (i.e. from the camera to the optical imaging target) of 1.1m and 3.1m:

- use of green and blue monochrome light, with white light for comparison,
- separation of the lights from the camera, with zero separation for comparison,
- the use of cross-polarised filters over the lights and camera, with no filters for comparison.

The research, designed to establish incremental improvements to optical imaging, an evaluation of which is described in the Technical Report: “Appraising Methods of Improving the Performance of Optical Imaging in Turbid Water for Inspecting the Linings of Disused Mine Shafts”, was not able to demonstrate any appreciable benefits over the current generation of CCTV equipment. Even the best combinations of techniques are generally not capable of providing an acceptable optical image over a range of much more than a metre even in only slightly turbid water.

In order to inspect the conditions of the shafts, the scanner was fixed at a bracket in a headover-position beneath the hoist cage, while all scanner control was done from within the cage.

As the situation for future logging shaft campaigns will be totally different, a new suitable shaft survey system, consisting of the following components is going to be developed:

#### **2D-Laserscanner (‘Profiler’)**

Initially, the use of the 3D-Laserscanner ‘Imager5006ex’ was planned, which actually is being developed in cooperation with Zoller+Fröhlich. Due to new and higher requirements, instead of the 3D-Scanner a 2D-Scanner (‘Profiler’) will be considered.

The development of the 2D-Scanner will be based on components of existing laserscanners from Zoller+Fröhlich, which are able to fulfil the main technical requirements for the kinematic use (speed, range, precision). Additional advantages are known details of scanner elements which have been used in the former 3D-Scanner project.

## ISSM

An inertial measurement system is essentially made up of three acceleration sensors and three rotational sensors (gyroscope), whose measurement axes are orthogonal to each other. An inertial surveying system for shaft applications has been developed, the ISSM (Inertial Shaft Surveying Mining).

The most important key point in the design of the scanner is the strong coupling between the demands of the safety enclosure and the proper function of the rotating mirror.

The protection type of the scanner is a combination of pressurized and flameproof enclosure (as other combinations or intrinsic safety are not realizable). However the rotating mirror has to be placed outside the enclosure, resulting in the demand for a force transfer through the enclosure.

### 2.3.4.1.1.6 Roadways survey using innovative geophysical tools

In order to perform the survey of the state of the roadways, three techniques have been tested: Ground Penetrating Radar 3D; Tunnel Scanner and Capacitive Resistive Imaging.

Using Ground Penetrating Radar (GPR) to detect voids in the ground has been known for decades. Although in many cases excellent results were obtained in other cases it was not effective due to the high frequency signals, which are the ones that give higher resolution, then were attenuated.

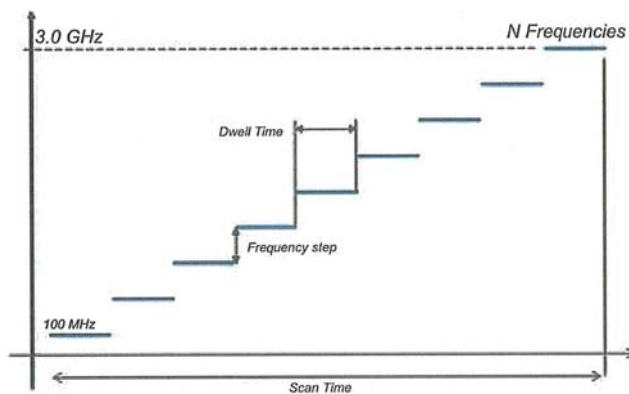


Figure 2.3.4.1.1.6-1 Frequency variations in a three-dimensional antenna



Figure 2.3.4.1.1.6-2 View of a three-dimensional antenna, Step-frequency type and towed by a Vehicle during the works

In (Figure 2.3.4.1.1.6-3) the planes levels at depths of 0,25 m, 1,8, 3,2 m and 3,8 m corresponding to a stretch of 120 m of the Tunnel of Archidona are shown.

To improve the performance of the GPR, in the last years, innovative antennas have appeared, so-called 3D, which, in fact are several antennas mounted on a single device. With this as shown in (Figure 2.3.4.1.1.6-1), the range from 100 MHz to 36 HZ is covered using 29 antennas simultaneously.

To carry out the inspection, the equipment must include a sender and a receiver device, and it should be displaced at a relative constant speed, as shown in (Figure 2.3.4.1.1.6-2).

To check the effectiveness of the GPR with a 3D antenna, a data collection campaign was performed in the Tunnel of Archidona (Malaga, Spain).

The GPR data was recorded with a multichannel 16 bits equipment, using a frequency range between 100 and 800 MHz, with measurement intervals of 2,5 MHz. GPR readings were made every 7,5 cm, which were measured with a specific GPR odometry wheel.

Once the information of the GPR is processed a three-dimensional image of the surveyed ground is performed, which, for a better understanding is cut in several horizontal

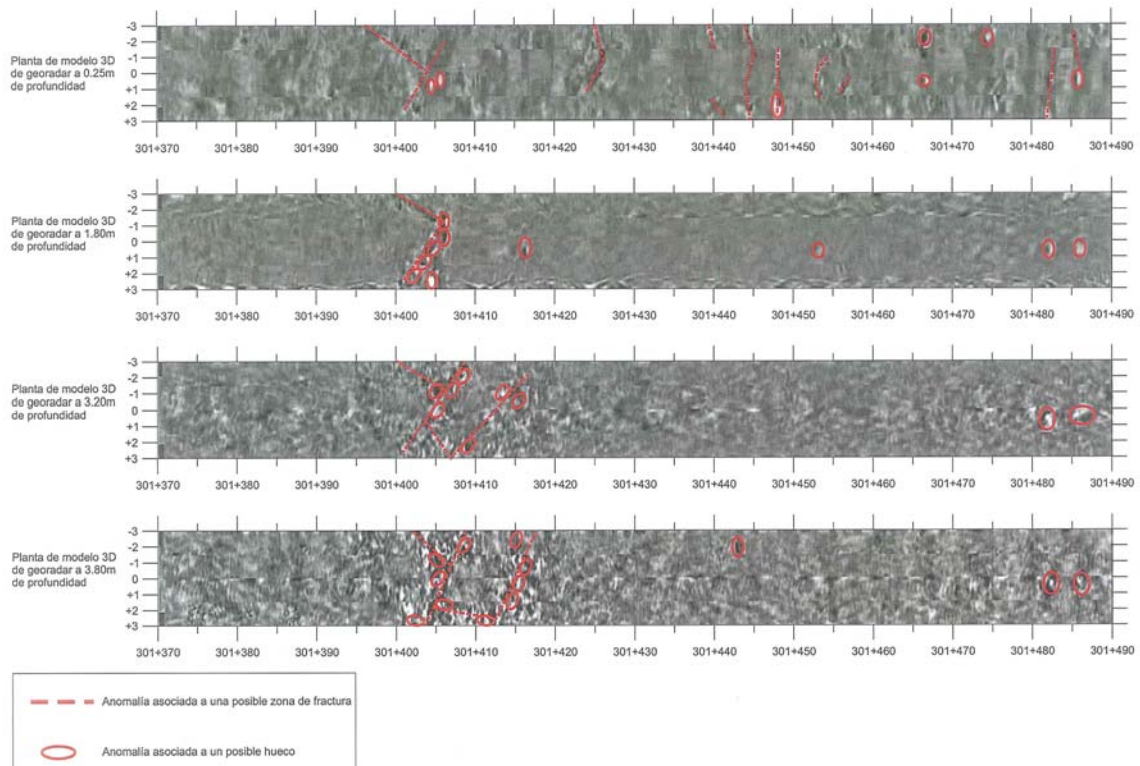


**Figure 2.3.4.1.1.6-3 Survey results with the GPR-3D.**

The results obtained with the GPR-3D in the Tunnel of Archidona show that this innovative technique offers results much more accurate than the traditional GPR and allow to detect, with reliability, the existing voids in the ground to a depth of about 10m.

The “Tunnel Scanner 360” system, developed by the German company Spacetec, allows to recognize the state of roadways and tunnels and it’s geometry, in a fast and accurate manner.

This system has the three following channels:



- VISUAL: Records real time image inside the tunnel.
- PROFILE: Provides a continuous profile of the tunnel.
- THERMOGRAPHY: By measuring the temperature variation on the outer surface of the tunnel lining, it is able of determining its state and the areas where there are anomalies in the backfill.

The two first channels, VISUAL and PROFILE use the laser technique, while the so-called THERMOGRAPHY employs the technique of temperature measurement by infrared rays.

The equipment to perform inspections for the TS-360 is composed of a trunk that is mounted in a Vehicle, as shown in (Figure 2.3.4.1.1.6-4).

In the Tunnel of Abdalajís (Malaga, Spain) a state inspection of the surface using the computer perimeter TS-360 was performed.

**Figure 2.3.4.1.1.6-4 Tunnel Scanner**

The inspection performed with the TS.360 has allowed to inventory all the points of upwelling water in the tunnel and also to locate the damage to the segments and to locate the existing cracks on the surface of the tunnel perimeter.

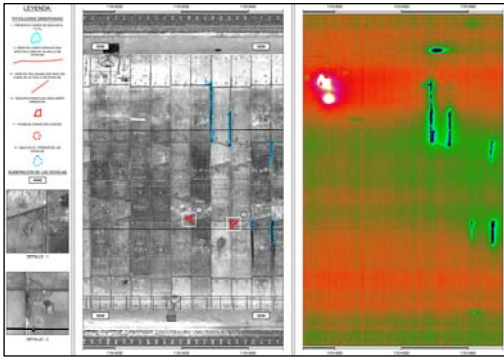


**Figure 2.3.4.1.1.6-5** The result of applying the TS-360 to the Tunnel of Abdalajís

In (Figure 2.3.4.1.1.6-5) one of the outputs of the TS-360 in the Tunnel of Abdalajís is shown.

This method has proved very effective to obtain accurately the losses of galleries section, which is directly related to the convergence, as well as to detect areas with water, susceptible to evolve in long-term into a collapse and cracked areas that represent areas of weakness susceptible to collapse.

Capacitive Resistivity Imaging (CRI) is a technology that allows to obtain in a fast manner a three-dimensional image from the subsurface with a resolution in the order of centimetres, through sensors with electrical resistivity

capacity arranged in multiple dipole that do not require pre-ground anchor.

The physical basis of this technique is very similar to conventional electrical tomography, which principal is to deliver electric currents to the subsoil and to measure through electrodes the potential difference between them. Increasing the distance between the electrodes increases the depth of investigation.

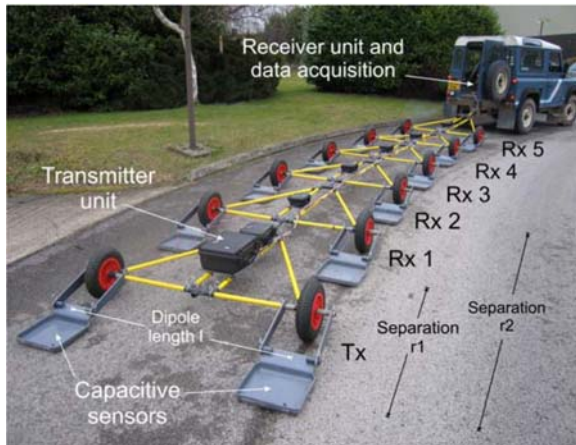


**Figure 2.3.4.1.1.6-6** Functional diagram and devices that make up the CRI towed by a vehicle.

As shown in (Figure 2.3.4.1.1.6-6) the device can be attached to a mechanic vehicle, which allows to investigate large areas, in order of 150x25 m in one day of work.

The CRI allows to recognize grounds with an electrical resistivity contrast, to a depth of 3-4 meters from the surface, especially suited to detect voids, areas of weakness, fracture zones, or stretches of water input, in the backfill of underground works.

As shown in (Figure 2.3.4.1.1.6-7) it is possible to generate images at different depths, which allows to obtain a three-dimensional view of the underground resistivity's, showing in this case the geometry of the void.

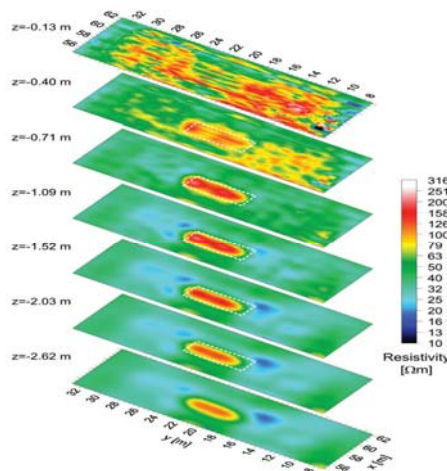


**Figure 2.3.4.1.1.6-7** Underground resistivity's sections at different depths obtained with the CRI. Geometry of a mineshaft detected.

### 2.3.4.1.1.7 *Effect of mine water on concrete, reinforced concrete and fill materials*

This task investigated the aggression of mine water on concrete elements that constitute a barrier to the movement of water in abandoned mines and also on the materials employed as fillers on shafts.

As a result of the performed tests, (Table 2.3.4.1.1.7-1) presents the weight losses due to water aggression on the materials considered as the most significant.

<b>Test</b>	<b>Results</b>	<b>Observations</b>
Basalt	1-2 % weight loss for all test solutions	White deposit likely to be calcite and other carbonate minerals which have precipitated out of the potable water solution system. Calcite is known to precipitate out at a pH of approximately 9. Calcium-containing minerals are more likely to be dissolved in AMW.
Cast Iron	<1% loss for all test solutions	Weight loss data is not necessarily equated to amount of material lost from the original samples. There can be mass increases for example, when iron is converted to iron oxide, the mass of iron oxide is greater than the mass of iron alone due to oxygen
Reconstituted Aggregate	Brick 3-5% Concrete <1% weight loss for all test solutions	Large mass losses for brick are possibly due to leaching from the clay component and/or binder of the brick material or the result may be due to the porous nature of the material. Mass loss of concrete aggregate due to chemical leaching effects on the smoother grained matrix.
Steel Reinforcement	Bar <1% Mesh +6% loss for all test solutions	Mass losses are greater in the mesh materials due to the larger surface area of iron exposed to the test solution.
Limestone	1.6-3% weight loss for all test solutions	Mass losses with all solutions tested are similar for the limestone and the weathered concrete. Limestone is predominantly calcium carbonate. Suggests that the extent of calcium carbonate in the weathered concrete surface is high considering that calcium carbonate is one of the main reaction products in carbonation
Concrete	1-3% weight loss for all test solutions	Greater mass loss from the weathered mass concrete than the concrete associated with the aggregate. Weathered concrete is likely to be more carbonated on its surface than the 'freshly' crushed concrete. Material lost in the dissolution process of the weathered concrete within the test system does not affect the pH of the solution

*Table 2.3.4.1.1.7-1 Test results of the aggression due to mine water.*

Alternative materials for filling have also been investigated, and as a result of the tests, four types of materials are recommended as can be seen in (Table 2.3.4.1.1.7-2).

<b>Polymerised Grouts External to Mine Shaft</b>	Chemical grouts which gel with soil or rock following mixing to form impermeable mass to reduce conductivity and inter-connected porosity in an aquifer / areas of thick superficial deposits. Chemical reaction formed by soluble monomers, mixed with suitable catalysts to produce and control polymerization injected into the voids to be filled. The mixture generally has a viscosity near that of water and retains it for a fixed period of time, after which polymerization occurs rapidly. The monomers may be toxic until polymerization occurs after which there is no danger. The resulting product is very stable with time.
<b>Foamed Concrete</b>	Lightweight cement bonded material produced by incorporating pre-formed foam, into a base mix of cement paste or mortar. Air bubbles reduce density of base mix, strong plasticizing effect. Easily placed, requires no compaction and flows into the most restricted and irregular cavities. Provision of a resistant seal to acidic mine waters.
<b>Kaolin Amorphous Derivatives (KAD)</b>	Kaolin is commercial clay, composed principally of the hydrated aluminosilicate clay mineral Kaolinite. KAD material has different structural and chemical properties from original kaolinite clay in particular, a very high surface area (up to 10 times higher

	than kaolin), and a greatly increased ability to exchange cations. Contact with mine waters containing toxic metallic ions would have a twofold effect of working to seal shafts and carry out the process of toxic metal scavenging of mine waters.
<b>Neutral Barrier Technology</b>	Interaction between two of the lowest cost chemicals available, calcium hydroxide and carbon dioxide to control fluid flow in porous strata. (Permeable rock or unconsolidated sediments.) The technique involves selectively sealing microscopic inter-pore channels that permit the passage of water through soil, sand, and porous rock. Interaction between an acidic drainage and a neutral barrier some calcite dissolves, the pH rises, and new sulphate, hydroxide and carbonate minerals precipitate.

*Table 2.3.4.1.1.7-2 Potential Alternative Solutions to Cementitious Grouting*

### 2.3.4.1.2. Monitoring and control of subsidence effects on surface

This set of tasks has approached the problem of selecting the control systems of the subsidence, depending if they are focused on the geometric or seismic control of the surface, and a special attention was dedicated to the shafts monitoring.

#### 2.3.4.1.2.1 Geometrical monitoring tools



*Figure 2.3.4.1.2.1-1  
Photogrammetric cameras in the  
lab*

In this task two different lines have been worked; on one hand to develop a new station based on two digital cameras motorized computer-controlled and on the other hand to exploit the potential of satellite telematics.

(Figure 2.3.4.1.2.1-1 shows a view of the two motorized cameras, employed in this research.

The proposed system, although initially based in existing photogrammetric and stereo matching technologies, is highly innovative and challenging in its final implementation and application.

The system was conceived to overcome the main disadvantages of traditional surveying techniques when applied to the monitoring of subsidence, namely the low temporal and spatial density of the measurements, and their high cost, without losing too much measurement accuracy, which is their main advantage. In practical terms, this means that the system has been designed to detect the

displacement along time of a multitude of points on the ground or on structures built on the ground, instead of the displacements of a small number of retro-reflecting targets attached to the ground, as surveys with total stations typically do.

When compared to current laser 3D scanners that can capture large clouds of point data, our system has the advantage of a lower cost, longer range and continuous unattended operation.

The performed works to exploit the possibilities offered by the SAR technique as the subsidence monitoring tool were performed in the following stages:

- analysis of requirements for the InSAR technique
- selection of the tools for SAR image analysis
- criteria of SAR images selection
- acquisition and analyses of the selected images
- summary and conclusions

From the performed work the following conclusions are deducted:

- Seven SAR scenes covering the period from 11th March 2008 to 2nd November 2009 have been analysed during the project. Various couples of images were subjects of analyses.
- Analyses of three 2008 scenes leads to conclusion that the area to be monitored shows stability.
- An attempt of comparison the scenes scanned in 2009 to the scenes scanned in 2008 failed due to the very low coherence
- Comparative analysis of the scenes scanned in May, July and August 2009 showed difficulties in interpretation of the interferograms due to the factors that affect incoherence like: weather conditions, clusters of trees and buildings. On the base of one pair of scenes the emerging subsidence trough has been detected at the edge of the monitored and being excavated longwall.
- As the result of acquisition of one scene scanned in November 2009 an image of another subsidence trough distant about 400 m from the monitored longwall was detected. The trough is probably the residual effect of the earlier mining of 510/1 seam.

#### **2.3.4.1.2.2      *Seismic and GPS monitoring tools***

The aim of this task was a development of a modern tool – a system for the monitoring of surface at areas of mining activity. That tool employs stationary and mobile GPS receivers for great precision measurements which may be used for various analyses and for the assessment of hazards of objects located on surface. The innovation of the proposed solution consist in quasi constant monitoring of vibrations and subsidence at selected points. This makes an opportunity of more complex approach to the assessment of hazards due to subsidence and seismicity accompanying excavation of underground deposits.

Those both phenomena are of different kind. Seismic events in relation to their location and the time of the occurrence are of the random character, while ground movements that cause surface deformation are effects of determined process. Monitoring of surface hazarded by mining activity is very useful, but also important is prediction of hazards that could happen. The functionality of the developed system allows to assess the envisaged surface behaviour on the base of the assumed models (prediction) and its verification on the base of the obtained precise GPS measurements (monitoring). The system prototype was implemented in the selected research area and used to carry out research activities.

The proposed system, although based on existing technologies, GPS and vibration monitoring, is highly innovative and ambitious instrument in its final version of the implementation and applicability. Innovation of the solution consist in the fact, that it is the first attempt to combine the monitoring of the risks caused by two processes of a different nature: a deterministic relatively slow process of surface deformation and a random process of vibrations induced by underground mining tremors. On the other hand, application of the developed models allows to use the system not only for monitoring but also, what is sometimes more desirable, for the prediction of surface behaviour and phenomena that may likely occur. The applied software contains newly developed algorithms of a sophisticated process of calculation the parameters affecting hazards, that may arise due to mining activity.

A key product of the project is also a station for the continuous measuring of seismic data and information on a position, collected in a data logger located in the common point of observation. The station can be used either as only a measuring equipment, a reference station for other survey points and regarding the continuous character of measurements, the device warning in case of detection an unexpected behaviour of surface or seismic events occurrence.

Another advantage of the system is its modular structure that allows to apply only certain elements of measurement - seismic or deformation - these, which are required in a given circumstances. Developed software of a layer structure based on the GIS element and digital map of the monitored area facilitates comprehensive visualisation of the recorded events and objects in a single center of monitoring. On the other hand the applied solution allows the use of the resulting data by other, not included in the system software modules for visual or another purpose selected by a user.

### 2.3.4.1.2.3 Surface monitoring of shafts stability

In Task 1.2.1 a review of telemetry and instrumentation methods was undertaken resulting in a design for a shaft-fill stability (SFS) sensor linked to a custom-designed low-power data logger and a GPRS (i.e. ‘cell phone’) transmitter. Data can thereby be uploaded to a web server on the Internet, from where any manner of data processing and distribution of data can be achieved. The purpose of the field trials was to evaluate the shaft-fill sensor and the logging and telemetry components, first separately and then combined, in an extended trial at several sites.

In drawing up a programme for field trials it soon became apparent that the long-term evaluation of the SFS would not be straightforward. Two difficulties were foreseen, namely i) that environmental and biological damage to the sensor might only become apparent after very long-term exposure and ii) that shaft fill instability events would occur only at very infrequent intervals. It was decided that it would be necessary to concentrate on certain specific elements of the design and, initially, to run trials on those elements alone; essentially to do ‘accelerated lifetime’ trials with, e.g., more frequent events. This changes the nature a ‘field trial’ considerably, and so it was considered helpful to draw up an assessment, as shown in the (Table 2.3.4.1.2.3-1).

Investigation	‘Risk’ to be Investigated	Mitigation	Field Assessment	Merit of Field Trial
Battery Life	High degree of activity will reduce battery life.	The SFS sensor is not expected to result in much activity. Any high degree of activity would be a cause for investigation.	No field assessment necessary.	<b>Low.</b> Laboratory measurements of power consumption will be sufficient to characterise this parameter
Battery Life	Poor cell-phone coverage at remote site will require increased transmitter power.	A mast and high-gain antenna may provide better performance.	Power consumption should be monitored at field site over a period to assess cell-phone network performance.	<b>Medium.</b> Although data on real-time communication to cell-phone base station is an important result it can be obtained without the need to field-trial a prototype. <b>High</b> only if units are deployed at multiple sites where conditions vary.
Corrosion and biological activity	Corrosion of moving parts or biological attack will cause draw wire to seize.	Construction uses plastic components. However, prototype has no biological protection.	Field assessment unlikely to be of benefit over the short/medium term, especially since prototype may differ from production models.	<b>Low</b> in short-term. <b>Medium</b> in medium term, but only if units are deployed at multiple sites where conditions vary. <b>High</b> in long term, but only if fully-protected environmental units are used.
Stiction of mechanical parts	Very-slowly moving fill may not trigger sensor	Problem unlikely to persist for long in presence of vibration, air currents, etc		<b>High</b> for lab. test rig
Network capability	System may not cope with a large number of units	Software can be developed to counter any potential risks	Not possible with small network. Simulation is possible, although a sufficient simulation would not be a simple task.	<b>None.</b> A trial would require a large number of field units. <b>Medium</b> if a simulation using third-party web-servers can be implemented.

*Table 2.3.4.1.2.3-1 Shaft-fill sensor, logging and telemetry; a ‘risk’ assessment of the field trials.*

Investigations made for the feasibility study for a shaft laser scanner system showed, that the quality of the results depends on the carrier system that transports the scanning unit. A logging unit that is mounted at a rope is a system of spring and mass, which will oscillate in a number of modes. The precise knowledge of this oscillating behaviour is the basis for the development of a system, which shall provide satisfactory results

Camera systems are capable of generating a signal (image), which can be interpreted by human beings easily. The rotation is visible instantaneous – also the missing of the spring pendulum movement. The processing and conversion into numerical values is possible, but has some disadvantages. The correlation procedures, which were employed here are strongly dependent on illumination and the kind of surface of the shaft wall. The illumination has to be very equally distributed over the complete

image, otherwise it behaves like a DC-offset that leads to calculation errors. The surface must contain sufficient structures to maintain a secure correlation result. As the structures are unknown, and as the surface can be totally structure less (e.g. on smooth tubes), this method can't guarantee sufficient accuracy in all future shafts that will be logged. At these examinations the correlation method gave good results and was suitable to verify the data of the inertial system. But finally the data was not error free, what makes it at least unsuitable as a stand alone system.

The laser distance logging is unsuitable in the used manner. To get a usable result at least three sensors are needed, and finally the laser scanner itself will provide this data.

The gyros and accelerometers delivered the most reliable results. Looking at small regions of time, highly resolved data can be achieved, which allow to calculate the actual oscillation behavior. The problem is the integrating behavior of these sensors respectively the integrative processing. This leads to drift over time, which distort the absolute values. Thus a lot of effort has to be made on processing, and the sensors have to be of highest quality. Another way is to reduce the rotation with a friction force free bedding.

#### **2.3.4.1.3. Risk management of subsidence hazards on surface**

This part of the research has worked on the following specific lines:

- I.- Integrated monitoring at surface.
- II.- Detection of hazardous areas at surface.
- III.- Validation and verification of results.

In the following sections a review of all employed techniques in the light of mining experience is presented.

##### **2.3.4.1.3.1 *Integrated monitoring at surface***

This task has worked on an integrated monitoring for an active colliery and for a neighbored abandoned mine with a controlled decrease of water mine drainage and a slowly rising mine water table. Both areas are covered by levelling lines with periodical measurements of about three months for the active and annual measurements for the old mining. All available data should be imported into a "4-D" point database, the GeoMon-DB, with possibilities to detect identical points that are affected by 3D ground movements over several years in position and height.

RAG's GeoMon-DB was used to compare the terrestrial and space borne data. The GeoMon-DB was designed for RAG's purposes as a part of the environmental monitoring system "UMIS" as a "4D Point Information System" for the integrative and documented storage, management and access of survey results from heterogeneous sources and quality levels for a combined consideration of terrestrial and remote sensing data for the detection and analysis of surface deformation.

The intention was to combine and evaluate independent high accurate data like terrestrial levelling, different GPS methods (real-time, static, permanent) and space-borne data from radar satellites. So two permanent GPS stations, (see Figure 2.3.4.1.3.1-2) and six points for Corner Reflectors (CR) were installed near levelling lines. The CR points are suitable for GPS measurements (see Figure 2.3.4.1.3.1-3).



*Figure 2.3.4.1.3.1-2 Permanent GPS stations “hospital” (left) and “shaft” (mid) with GPS receiver and power supply (right).*



*Figure 2.3.4.1.3.1-3 Corner Reflector no. 2 near levelling line aligned to ENVISAT orbit (left) and static GPS measurement on CR pillar (right).*

GPS measurement for the Jas-Mos colliery data has been recorded GPS and post-processed. The data was collected constantly at four stations and periodically at about 70 survey points and delivered to RAG in two text files including measurements in BLH WGS84 coordinate system and arranged in the settled form and order. For the collected numerous constant surveys, the 10 days distant measurements samples with most representative for each day have been selected. The data from EMAG then had successfully been imported into RAG’s GeoMon-DB:

From EMAG RAG received a digital map in AutoCAD DXF and DWG format and two ASCII-files with GPS measurements of about 76 points for the Polish colliery for the year 2009.

### 2.3.4.1.3.2 Detection of hazardous areas at surface

These tasks have been aimed to establish procedures to identify hazardous areas at surface in relation with the subsidence that may produce the abandoned shafts, deferred phenomena over time that affect the exploitations, galleries next to the surface and to the development of a method for identifying these areas.

Analysis of field data indicates that the occurrences of shaft collapses in the U.K. (Figure 2.3.4.1.3.2-1) are more likely to occur in the early months of the year as the ground temperatures and rainfall increases followed by a second period when rainfall increase in the late autumn / early winter after a “dry” summer.

There are approximately 168,000 recorded coal mine entries throughout Great Britain. Most of these are now abandoned and are not visible at the surface. Some have been backfilled and treated although, in the majority of cases, the treatment carried out at the time of abandonment is unknown. The mechanisms involving the collapse of a shaft are numerous and complex. Such shaft collapses can result in significant surface subsidence and catastrophic surface problems especially in populated areas (Figure 2.3.4.1.3.2-2).

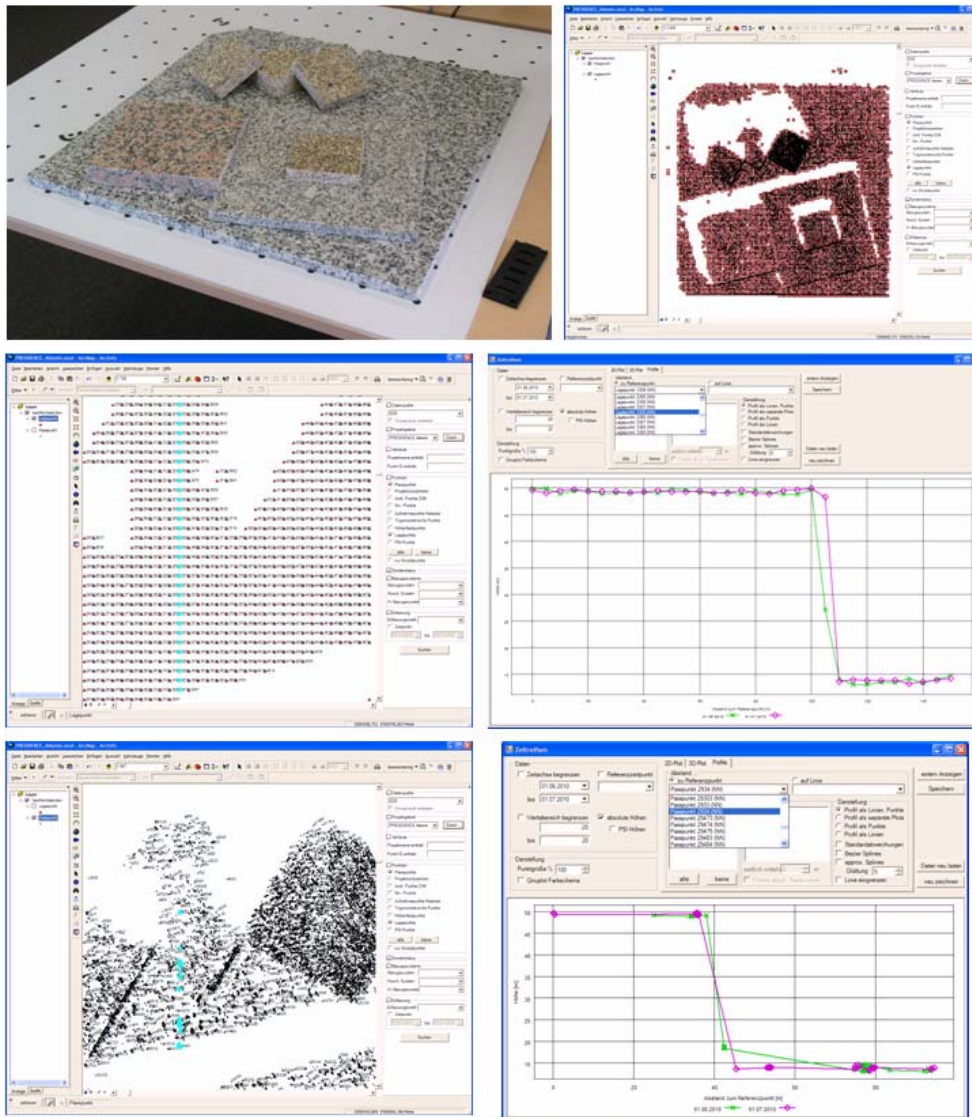
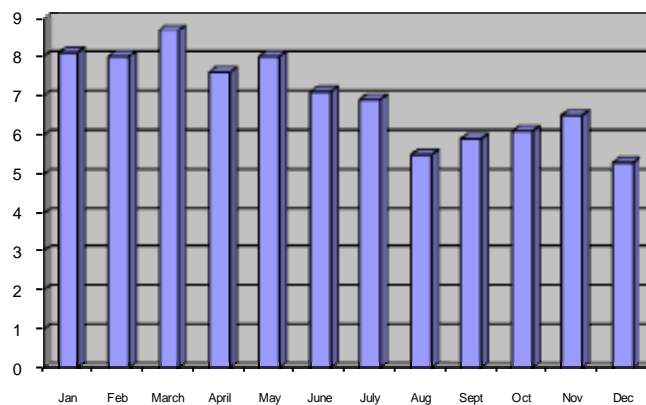


Figure 2.3.4.1.3.2-1 GeoMon-DB: Integrated photogrammetric DEM point data from Aitemin.



**Figure 2.3.4.1.3.2-2 Hazardous Areas at surface from collapse of shafts**



**Figure 2.3.4.1.3.2-3 Incidents in the U.K. involving Mine Shafts - 10 year average**

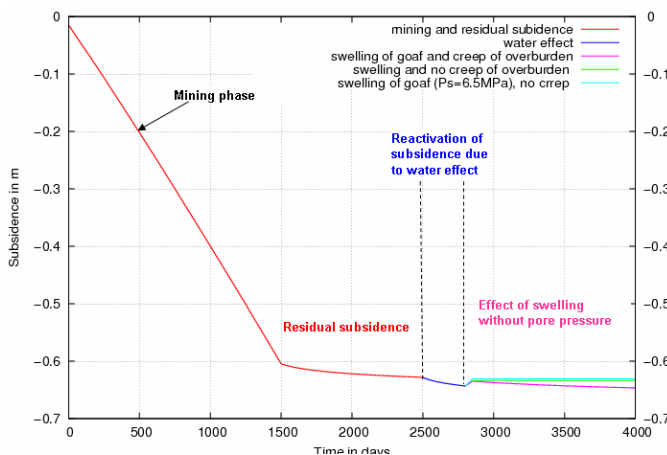


**Figure 2.3.4.1.3.2-4 Surface behaviour at different episodes of the shallow deep coal mine with a particular attention on the effect of goaf swelling.**

To evaluate the effect of the phenomena deferred over time of the mines exploitation, mainly due to the effect of water from the mines, several simulations have been performed with the FLAC code that have established the evolution of the subsidence over time, as shown in (Figure 2.3.4.1.3.2-4).

The main conclusions which can be drawn up from all the analyses conducted on the surface behaviour of a longwall coal mine during the different episodes of its life can be summarised as follows:

- The modelling approach developed allows to account for all the observed phenomena of the surface behaviour: mining subsidence, residual subsidence, reactivated subsidence due to water effect, uplift induced by swelling and uplift induced by pore pressure.
- This modelling approach could be used to assess the hazards and the risks when flooding caved coal mines. The major difficulty in such a modelling lies in describing properly the behaviour of each material, especially the selection of the reliable law and parameters.
- Caved rocks and overburden are governing the mechanics of subsidence when flooding coal mines: effect of water, swelling, creep behaviour of overburden.

- Swelling is governed by the swelling pressure and is therefore linked to the mining depth.
- Swelling is a rapid process and continuous swelling is due mainly to the presence of argillaceous materials in overburden.
- Pore pressures are not totally active and a Biot's coefficient has to be introduced to weight their effect.
- Uplift is governed by the dilation of a reservoir constituted by the caved rocks under the effect of pore pressures, the contribution of swelling on this phenomenon is very limited.
- The formula proposed by Pöttgens could be wisely used to assess the amount of uplift.

Regarding to the quantification of the damage produced by the subsidence on buildings located on hazardous areas, a work of synthesis has been performed on the criteria that would be applied to these cases. This work has been supplemented with a practical example of application, which has led to a part of the Deliverable 3.2.

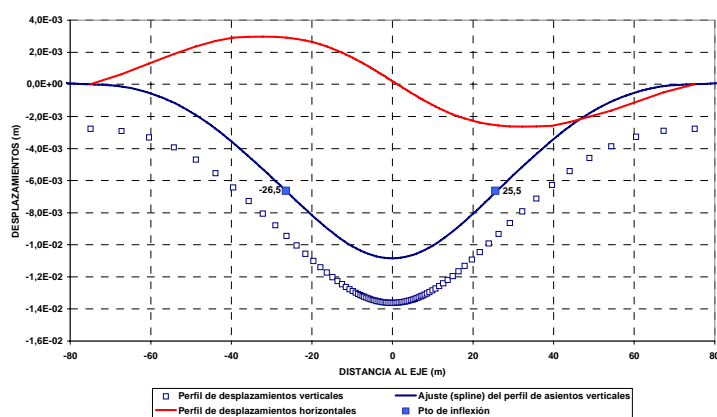


**Figure 2.3.4.1.3.2-5 Subsidence profile and horizontal displacements distribution calculated and a cross section that includes the building over Elche's Tunnel.**

To evaluate the subsidence produced by the roadways on the buildings at surface, a simulation was performed with the FLAC code which has allowed to calculate the vertical and horizontal displacements profiles, as shown in (Figure 2.3.4.1.3.2-5).

According to the performed tensile strain calculations were determined for the building area, in order to use the criterion of Boscardin and Cording on damage to buildings.

In order to establish a procedure to detect hazardous areas at surface the

following tasks have been performed:

- carrying of the research relating to mining area safety management,
- influence of mining activity,
- areas hazarded by continuous deformations (subsidence), water invasions,
- areas hazarded by discontinuous deformations,
- maps of degraded and hazarded by mining activity territories,
- preparing of monothematic raster or vector maps in databases,
- mathematic modelling of hazards induced by mining influence,
- studies on risk analysis.

(Table 2.3.4.1.3.2-1) shows conditions of damage occurrence that have to be taken into account depending on risk value and risk probability:

evaluated risk value probability of risk occurrence	low risk	high risk
	low $p < 0.4$	risk not necessary to be taken into account
high $p \geq 0.7$	sequence of adverse events should be taken into account	risk must be absolutely taken into account

**Table 2.3.4.1.3.2-1 Damage occurrence depending on the relation of risk value to risk probability**

Regulations applied for the assessment of hazard caused by bumps may be based on various methods. Those methods are included in the scales of hazard. An international scale MSK (Medvedev-Sponheuer-Karnik) or MSK-64 is based on maximum vibration acceleration within the band range below 10 Hz. It consists of twelve intensity levels. The scale assumes an impact of vibrations in turn on:

- people and their direct environment,
- buildings,
- nature.

On the base of observed measurements and effects of bumps, successive intensity levels are assigned to resultant amplitude values of ground vibration acceleration. Those relations area presented in (Table 2.3.4.1.3.2-2).

Intensity level	Vibration acceleration* $10^3 \text{ m/s}^2$	Effect on surface
I	5—12	not noticeable
II	12—25	scarcely noticeable
III	25—50	weak, only partial observation
IV	50—120	widespread observation
V	120—250	awakening
VI	250—500	frightening
VII	500—1000	damage to buildings
VIII	<b>Earthquakes !!!</b>	destruction of buildings
IX		general damage to buildings
X		general destruction of buildings
XI		catastrophe
XII		landscape changes

**Table 2.3.4.1.3.2-2Relation of vibrations intensity to values of accelerations and effect on surface by MSK- 64 scale.**

MSK-64 scale was developed on the base of correlation between data recorded on surface and results of underground seismometer measurements for every intensity of vibration level and resultant amplitude of ground vibrations.

#### **2.3.4.1.3.3 Validation and verification of results**

This part of the investigation has been directed to the applicability or a combined analysis of terrestrial and remote sensing data for the area-wide detection of hazardous areas due to mining and to the verification, through surveying procedures, the goodness of the tensile strain calculations performed to predict the subsidence caused by the galleries.

To carry out the combined control of terrestrial and remote sensing the GeoMon-DB program was employed, which was developed as a “4D” point information and management system for the integration into RAG’s environmental monitoring system (UMIS) with the aim to collect, provide and archive as much meta-information to terrestrial, photogrammetric and space-borne point coordinates. Meta-information is for instance: contractors for the surveying campaigns, diverse historic and actual geodetic reference coordinate systems, state of the art of measurements, accuracies, to attach maps or sketches and many more. The most powerful aspect is that remote sensing data from radar satellite

Persistent Scatterer Interferometry (PSI) can be imported and used for area-wide evaluation and analysis of ground movements.

RAG's GIS environment is based on ESRI's ArcGIS and ArcSDE Oracle database. The coordinate system for the visualisation of all data is performed in the Gauß-Krüger, 2nd meridian strip. For other coordinate systems and data structures the database model and database structure has to be reprogrammed anew. The data of third party project partners could be successfully imported, visualised and evaluated in the GeoMon-DB by converting the delivered coordinates to Gauß-Krüger coordinates.

The GeoMon-DB is operational at RAG since 2008 and by filled and maintained in day-to-day business since. Several analyses concerning the duration or re-activation of ground movements or the separation of mining and non-mining induced areas have been conducted meanwhile.

Working with the GeoMon-DB gave additional information concerning the accuracy and the assessment of terrestrial measurements. So measurement intervals have been optimized in that way that the date and repetition of the surveying campaigns will lead to better comparable results. High precision measurements will no longer be performed with standard GPS equipment but rather with high precision chocking antenna equipment because the comparison within GeoMon showed that the measurement accuracy of the standard GPS equipment was larger than the ground movement behaviour.

When the potential and the limitations of the remote sensing data for DInSAR and PSI will be seriously regarded and the process chain would by and by be updated with reference measurements, professional experts will be able to produce reliable results for ground movements.

Within GeoMon the comparison of these remote sensing results to terrestrial measurements reveals the high potential of PSI data so that an optimisation of the usable systems and methods will be possible for the minimum effort to reach the requirements. At RAG GeoMon has evolved to the footing for a combined measurement concept with high precision terrestrial and remote sensing data.

To verify the effectiveness of the tensile strain modelling with the FLAC code, an exercise test has been performed in the Tunnel of Archidona (Malaga, Spain).

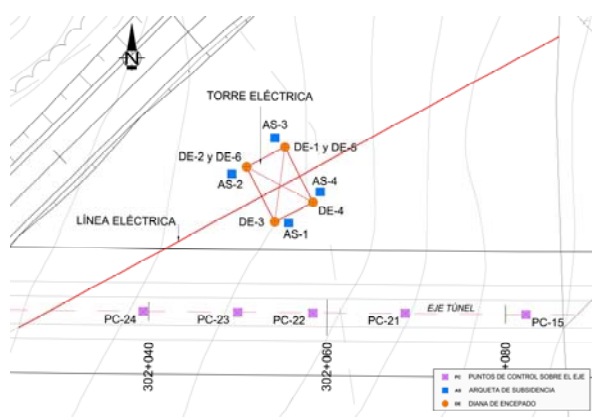


**Figure 2.3.4.1.3.3-1 Location of the control points on the surface of the modelled area.**

(Figure 2.3.4.1.3.3-1) shows the plan view of the modelled section which is characterized for being excavated near the surface and near a high voltage power tower that has to undergo a maximum subsidence of 26 mm.

(Figure 2.3.4.1.3.3-2) shows the comparison between the results of the calculations and the topographic control measures. It can be seen that the maximum subsidence calculated is 140 mm, while the topographical measure after the excavation is 164 mm, which is a deviation of 17,1 % which is considered satisfactory.

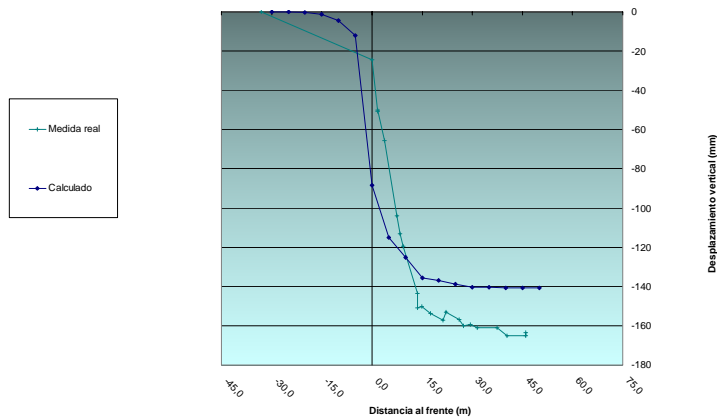


**Figure 2.3.4.1.3.3-2 Evolution of the measured and calculated subsidence in the PC-23 milestone.**

### 2.3.4.2. Evaluation and application of techniques to other areas

To have a global vision of the possibilities which offer the techniques employed in this investigation, (Table 2.3.4.2-1) shows a summary of the techniques employed in every task of this research, as well as the appropriate remarks to each task.

The techniques that have been employed can be grouped in five independent lines.

Task	Techniques employed	Promotors	Posibilities of application
1.1.1	Subsidence prediction by FLAC modellization	RMT/UK COAL	Needs to improve the constitutive model and probably employ a code for discontinuous mass (UDEC).
1.1.2	Residual subsidence by FLAC modellization	ARMINES/RMT	It is considered applicable to other flat coal fields.
1.1.3	Prediction of subsurface deformations and modellization	RMT/UK COAL	Same remarks than 1.1.1
1.2.1	Shafts survey using optical and laser techniques	DMT/MRSL	Techniques based on optical measurements have difficulty to provide precise measures in the shafts. Laser technology is completely effective
1.2.2	Roadways surveying by GPR3D, Tunnel Scanner and CRI techniques	GEOCONTROL	These three techniques are on the market, but they are limited in their scope. GPR3D and CRI have applications to detect voids next to the surface and the Tunnel Scanner
1.2.3	New materials for grouting in grounds which need to be waterproofed	MRSL	Four materials have been propose, which are commercially available to improve the grouting
2.1	InSAR images + GPS and photogrammetry	EMAG/AITEMIN	InSAR + GPS are suitable to control vertical movements in areas; specially in dynamic processes. The photogrammetry technique is appropriated to monitor areas of limited extension; of hundreds of meters in with and length
2.2	GPS + Monitoring of seismic events	EMAG	The systems is able to monitoring areas not exceeding a few Km in width and length with problems related to subsidence and vibrations. Tiandi Coal Camp is interested in the implementation of the system in China.
2.3	Ultrasonic Image Equipment in water filled shafts	MRSL/DMT	The marine ultrasonics scanners are capable of detecting features in the linings of flooded disused mineshafts
3.1	Geometric Monitoring	DSK/EMAG/	Comparison of the remote sensing results to

Task	Techniques employed	Promotors	Posibilities of application
	Database (GeoMon – DB) + remote sensing data from radar satellite Persistent Scatterer Interferometry (PSI)	AITEMIN	terrestrial measurements reveals the high potential PSI
3.2	-Inventory of abandoned mineshafts, probabilistic systems to manage the vibrations at surface. -FLAC applications to detect damages on the buildings	MRSL, ARMINES, EMAG and GEOCONTROL	At least in the UK the abandoned mineshafts are an important problem which can be framed from the obtained information. The probabilistic exploitation of vibrations recorded at surface can help to control the effects of the dynamic phenomena. FLAC code can be applied to calculate the residual subsidence and the stability of the roadways.
3.3	-GeoMon – DB + Monitoring sensors. -FLAC applications to roadways stability	DSK/ GEOCONTROL	There have been several exercises performed for the verification of the operability of these techniques, which are considered to have a great future.

*Table 2.3.4.2-1 Summary of the techniques employed in this research*

### **I. - Surveys to collect and classify information**

It is considered that this is an essential tool to frame successfully the issues that might raise in abandoned mines; this is the first step to resolve the generated problems.

It should be mentioned that in the UK there are about 168.000 entries to old mines and that every month there are between 5 and 9 incidents recorded related to subsidence in abandoned mineshafts.

### **II. – Surveying of abandoned shafts**

The survey of abandoned shafts is a difficult operation; in first place due to the access to shafts and in second place because there are full of water or filled.

In this research specific examples have been carried out to obtain images of the state of the shafts, based on laser scanners y to detect the position of the fillings.

Both techniques have worked correctly and have a promising future.

### **III. – Calculations of the subsidence through tensile strain models.**

Several tasks, performed by various partners have been dedicated to the calculations of the subsidence through tensile strain programs (basically FLAC) to calculate the subsidence produced by the coal exploitations.

Although the use of these programs to perform geomechanical models is a very promising manner to calculate the subsidence, especially in complicated cases, the fact is that the results have not been entirely satisfactory and can be improved. Probably the reason of it has to be found on one hand in the longwall, were **300 to 600 m<sup>3</sup> per meter of advance are excavated and on the other hand necessarily the excavation has to collapse after advancing the support which creates a block dynamics.**

The FLAC code performs with continuous mass, which makes it difficult to resolve accurately problems of discontinuous mass.

This manner of calculation should be subjected to new ways of research; because besides the appropriate computer program, constitutives models for the post-fracture should be developed, which are not available now.

### **IV. – Surface monitoring through satellite images combined with terrestrial sensors.**

This technique is already a fact of great future that will have a very positive evolution in the coming years.

Operating mines and those which are abandoned are those who will be benefited of the enormous potential of this technique.

## **V. – Calculation of the effects on the surface of the surface mine galleries**

Unlike the longwall the construction of galleries requires to excavate between 25 and 40 cm<sup>3</sup> of the ground per lineal meter and what is more important, these excavations should not collapse.

This explains that the application of calculation programs, like FLAC, is in these cases a very effective tool.

As a general conclusion, according to the preceding, it should be mentioned that most of the techniques developed and applied in this research have shown positive results and certainly they will be employed in the mining industry.

As it happens at the end of all the research works, the performed tasks show the desirability of continuing working to improve some tools; such as the application of the tensile strain calculations programs applied to discontinuous mass, which could be a significant step to accurately calculate the subsidence due to the coal mines.

### **2.4. CONCLUSIONS**

The achievements made in this project are included in this section. Also in this Project there is a specific Work Package (WP4), called “Project Assessment and conclusions” that completes the content of this section.

#### **2.4.1. Prediction of surface and subsurface subsidence WP1.**

##### **2.4.1.1. Prediction of subsidence caused by coal exploitations WP1.1**

###### **2.4.1.1.1. Prediction of surface deformation Task 1.1.1.**

The prediction of the subsidence caused by the coal underground mines has been extensively studied along the recent history.

With the widespread obtained by these tensile strain calculation programs, it became clear that this calculation tool was much more precise than the empirical- analytic methods that were developed at the end of the last century.

The geomechanical subsidence models (using FLAC 2D) successfully predicted maximum subsidence taking account of inter-burden geology but were not able accurately to reproduce the measured subsidence profile using the constitutive models available without predefinition of subsided and non subsided strata.. Work have showed that anisotropic models are required if the subsidence profiles are to be reproduced.

###### **2.4.1.1.2. Prediction of surface deformation due to water rebound Task 1.1.2.**

The analysis of the geomechanical-hydrological model was performed with a simplified, non-coupled approach which is adequate for most cases.

Statistical analysis of recent and historic UK case studies of water inflows to working longwalls produced a good prediction function based upon the maximum aggregate tensile strain at the base of the potential water source according to the 1966 Subsidence Engineer’s Handbook (Disturbance index) and the panel width to height ratio.

The performed application to calculate the influence of the flooding of old mines has allowed to obtain the following conclusions.

- The modelling approach developed, allows to be taken into account all the observed phenomena of surface behaviour; mining subsidence, residual subsidence, reactivated subsidence due to water effect, uplift induced by swelling and uplift induced by pore pressure.

- This modelling approach could be used to assess the hazards and the risks when flooding caved coal mines. The major difficulty in such a modelling lies in describing properly the behaviour of each material, especially selection of reliable law and parameters.
- Caved rocks and overburden govern the mechanics of subsidence when flooding coal mines; effect of water, swelling, creep behaviour of overburden.
- Swelling is governed by the swelling pressure and is therefore linked to the mining depth.
- Swelling is a rapid process and continuous swelling is due mainly to the presence of argillaceous materials in the overburden.
- Pore pressures are not totally active and a Biot's coefficient is required to weight their effect.
- Uplift is governed by the dilation of a reservoir comprising the caved rocks under the effect of pore pressure; the contribution of swelling on this phenomenon being very limited.

#### **2.4.1.1.3. Prediction of subsurface deformation Task 1.1.3.**

A combination of three dimensional boundary element (MAP3D) for stress analysis and detailed three dimensional finite difference (FLAC3D) roadway models for reinforcement design, employing the Hoek Brown GSI to account for rock condition depending upon roadway location within the subsidence trough, can be used for analysing of rockbolted gate roadways and face lines. Hybrid models for representing the longwall caving process were shown to be promising for future application but are currently constrained to two dimensional simulations.

#### **2.4.1.2. Prediction of subsidence caused by underground infrastructures WP1.2.**

##### **2.4.1.2.1. Shafts Surrey using innovative geophysical tools Task 1.2.1.**

MRSL has tested several techniques to obtain direct images of the perimeter of the flooded shafts; while DMT has concentrated his efforts on tuning laser scanner 3D whose prototype is effective to obtain indirect images.

The axis position of the shafts has been controlled by inertial surveying system, equipped with three accelerometers and three gyroscopes.

##### **2.4.1.2.2. Roadways Surrey using innovative geophysical tools Task 1.2.2.**

Geocontrol has used three innovative techniques applicable to roadways surveying:

- Laser scanner with three channels: VISUAL (real time image), PROFILE (continuous profile of the perimeter) and THERMOGRAPHY (cracks and anomalies in the back fill.)
- Georadar 3D: with several antennas (3,6 to 100 MHZ) mounted on a single device.
- Capacity Resistivity Imaging (CRI): that shows three dimensional images based on conventional electrical tomography.

##### **2.4.1.2.3. Effect of mine water on concrete, reinforce concrete and fill materials Task 1.2.3.**

MRSL has carried out an intensive campaign of laboratory test to assess the aggressiveness of the water, present in the flooded shafts, versus conventional construction materials and also on other newest chemical products.

#### **2.4.2. Monitoring and control of subsidence effects on surface WP2.**

##### **2.4.2.1. Geometrical monitoring tools Task 2.1.**

In this task two different lines have been worked:

AITEMIN has worked with photogrammetric equipment, that overcomes the main disadvantages of the traditional surveying techniques: the low temporal and spatial density of the measurements and their

high cost. The proposed system, although initially based in existing photogrammetric and stereo matching technologies, is highly innovative and challenging in its final implementation and application.

EMAG has focused his work with images obtained with IN SAR technology, where the following conclusions are deduced:

- Seven SAR scenes covering the period from 11th March 2008 to 2nd November 2009 have been analysed during the project. Various couples of images were subjects of analyses.
- Analyses of three 2008 scenes leads to conclusion that the area to be monitored shows stability.
- An attempt of comparison the scenes scanned in 2009 to the scenes scanned in 2008 failed due to the very low coherence
- Comparative analysis of the scenes scanned in May, July and August 2009 showed difficulties in interpretation of the interferograms due to the factors that affect incoherence like: weather conditions, clusters of trees and buildings. On the base of one pair of scenes the emerging subsidence trough has been detected at the edge of the monitored and being excavated longwall.
- As the result of acquisition of one scene scanned in November 2009 an image of another subsidence trough distant about 400 m from the monitored longwall was detected. The trough is probably the residual effect of the earlier mining of 510/1 seam.

#### **2.4.2.2. Seismicity monitoring tools Task 2.2.**

In this task an innovative system that consists in the combination of GPS Technology has been developed. The system allows to measure deterministic and slow process of surface deformation, with the measurement of the vibrations induced by underground mining tremors. These are the following results of the work accomplished in the task:

- developed mathematic models of deformation and seismic processes on surface for predictions of hazards due to mining activity
- the monitoring system structure – the prototype tested under real conditions.
- software dedicated for the system of seismic events and surface deformation monitoring,
- the results of the research carried out on the base of the implemented prototype.

The results confirmed usefulness of the designed and used monitoring system. The results of some experiments are encouraging but to be confirmed require continuation regarding encountered problems caused by the objective factors (too little samples).

#### **2.4.2.3. Surface monitoring of shafts stability Task 2.3.**

The review of telemetry and instrumentation methods developed in task 1.2.1, was undertaken resulting in a design for a shaft-fill stability (SFS). DMT and MRSL have focused his attention in the long life stability. Field trials with the prototype have been performed in an abandoned mine shaft. The scanner operation has been successful. Data have been collected in function of the chosen parameters. Pendulum and rotational movements, temperatures bellow zero degree have not caused any problem in the operation of the scanner. All mechanical and electronic components have worked satisfactorily.

#### **2.4.3. Risk management of subsidence hazards on surface WP 3.**

##### **2.4.3.1. Integrated monitoring at surface Task 3.1.**

RAG has used a 4D Data Base, called GeoMon-DB and designed for RAG's purposes, working with data from Germany, Poland and Spain.

It has been possible to combine and evaluate independent high precision data (terrestrial levelling), different GPS methods and space data from radar satellites.

#### 2.4.3.2. Detection of risk areas at surface Task 3.2.

MRSL has worked with the 168.000 coal mine entries located in Great Britain, analyzing the accidents occurred in the last 10 years.

ARMINES has completed a numerical simulation to evaluate the residual subsidence above flooding exploitations.

GEOCONTROL has checked the validity of Boscardin and Cording criteria to prevent the damages produced by subsidence on buildings.

EMAG has worked in the detection of occasional risks for the sudden collapses in exploited areas.

#### 2.4.3.3. Validation and verification of results Task 3.3.

RAG has focused his work in the validation of combined systems, terrestrial and remote sensing, to detect of hazardous areas due to mining; for which the GeoMon-DB program has been used. The most powerful aspect is that remote sensing data from radar satellite Persistent Scatterer Interferometry (PSI) can be imported and used for the evaluation and analysis of ground movements in wide areas. High precision measurements will be done with high precision chokering antennas; because the accuracy of the standard GPS equipment was larger than the ground movement.

GEOCONTROL has checked in the Archidona Tunnel the consistency of the FLAC 3D code to evaluate the subsidence and the tensile strain on the surface. For that a campaign of surface levelling has been performed, which has shown a good correlation between FLAC's prediction and the real measures.

#### 2.4.4. Project Assessment and conclusions WP 4.

The techniques employed in this research represent a significant advance on the current situation in forecasting and control of the subsidence.

Therefore, although some of the investigated techniques must still be refined, it can be said that the results of this research project will have a **positive effect in the monitoring of the subsidence in the coal basins of the UE** and some, as the technique of monitoring the movements of the ground with a GPS and vibrating sensors, which has been developed by EMAG, could be exported outside the UE.

### 2.5. EXPLOITATION AND IMPACT OF THE RESEARCH RESULTS

Included in the WP4, there is a special task called "Evaluation and application of techniques to other areas". To avoid duplicity of documents, the exploitation and impact of the research results are described in such Task. (Chapter 2.3.4.2 of this Final Report)

### 3. LIST OF FIGURES AND LIST OF TABLES

#### List of Figures:

<i>Figure 2.3.1.1.1-1 w/h ratio against S/m ratio, all UK data .....</i>	<i>15</i>
<i>Figure 2.3.1.1.1-2 Schematic of Nabura Model.....</i>	<i>16</i>
<i>Figure 2.3.1.1.1-3 Pressure/Volumetric Strain Goaf Properties Schematic of Nabura Model.....</i>	<i>16</i>
<i>Figure 2.3.1.1.1-4 Surface Settlement Half-Profile.....</i>	<i>16</i>
<i>Figure 2.3.1.1.1-5 The Effect of Strain Softening on the Subsidence Profile.....</i>	<i>16</i>
<i>Figure 2.3.1.1.1-6 Normal Subsidence Profiles .....</i>	<i>17</i>
<i>Figure 2.3.1.1.1-7 Comparison of model subsidence with monitoring .....</i>	<i>17</i>
<i>Figure 2.3.1.1.2-1 General behaviour of surface after floodind; resettlement followed by uplift (panel 12, Vernenjoul field, sector West.....</i>	<i>20</i>
<i>Figure 2.3.1.1.2-2 Upfit may hide the reactivated subsidence in case of low measurement frequency (panel Cocheren Sud 1, Cocheren field, sector Centre).....</i>	<i>20</i>
<i>Figure 2.3.1.1.2-3 Separate simulation separately of the different phenomena that could affect the surface of a caved longwall during the mining and the flooding .....</i>	<i>21</i>

Figure 2.3.1.1.2-4 New model of caved longwall.....	22
Figure 2.3.1.1.2-5 Showing the effect of time on subsidence and water table rise on uplift.....	23
Figure 2.3.1.1.2-6 Features of the new numerical model developed to couple the hydraulic and the mechanical behaviour).....	23
Figure 2.3.1.1.2-7 Wiston panels – Aggregate tensile strain against width to height ratio.....	27
Figure 2.3.1.1.2-8 FLAC 2D modelling of Wistow case history panels, plastic and numeric strains.....	30
Figure 2.3.1.1.3-1 Bay strain contours across goaf-ribside section, Ellington/ Lynemouth collieries.....	31
Figure 2.3.1.1.3-2 Settlement profiles measured in Main seam above Brass Thill longwall.....	31
Figure 2.3.1.1.3-3 Compaction properties used to model bulked waste material.....	32
Figure 2.3.1.1.3-4 Influence of underlying panels. Principal stress contours around sequence of panels, Ricall Colliery.....	32
Figure 2.3.1.1.3-5 Stress and displacement across waste edge at 70m above.....	32
Figure 2.3.1.1.3-6 Plan illustrating interaction for Deep Soft seam, Welbeck colliery.....	33
Figure 2.3.1.1.3-7 FLAC model showing shear strains surrounding single panel in the Parkgate seam at Welbeck colliery.....	33
Figure 2.3.1.1.3-8 Roof extensometer data at 100 days from Welbeck DS244, 242 and 240 gate roadways.....	33
Figure 2.3.1.1.3-9 Vertical stress contours during DS5 retreat.....	33
Figure 2.3.1.1.3-10 Vertical stresses 20m ahead of retreat Telltale data above ring face a) DS4, b)DS5.....	34
Figure 2.3.1.1.3-11 Vertical stress 30MPa, low lateral stress, support A – a) GSI 80, b) GSI 60.....	34
Figure 2.3.1.1.3-12 Simulated roof extensometer data for low lateral stress.....	35
Figure 2.3.1.1.3-13 Summary of model results using properties H3.....	39
Figure 2.3.1.2.1-1 Optical Imaging Tes.....	39
Figure 2.3.1.2.1-2 Scan image of reinforced shaft area.....	40
Figure 2.3.1.2.1-3 Tool frame with sensor equipment.....	41
Figure 2.3.1.2.1-4 Tool frame with sensor equipment.....	41
Figure 2.3.1.2.1-5 Components of the Laser Scanner.....	43
Figure 2.3.1.2.1-6 SwissRanger SR4000 for collision detection.....	44
Figure 2.3.1.2.2-1 GPR Fundamentals.....	45
Figure 2.3.1.2.2-2 Attenuation of GPR signals.....	45
Figure 2.3.1.2.2-3 Frequency variations in a three-dimensional antenna.....	45
Figure 2.3.1.2.2-4 View of a three-dimensional antenna, Step-frequency type and towed by a Vehicle during the works.....	46
Figure 2.3.1.2.2-5 Survey results with the GPR-3D.....	46
Figure 2.3.1.2.2-6 Tunnel Scanner mounted on a wagon.....	47
Figure 2.3.1.2.2-7 Operating principle of the “Tunnel Scanner”.....	47
Figure 2.3.1.2.2-8 Comparison between the visual channel and the thermographical channel where thermal anomalies in the backfill are seen in the backfill associated with the presence of voids.....	48
Figure 2.3.1.2.2-9 The result of applying the TS-360 to the Tunnel of Abdalajís.....	49
Figure 2.3.1.2.2-10 Functional diagram and devices that make up the CRI towed by a vehicle.....	49
Figure 2.3.1.2.2-11 Underground resistivity image obtained through CRI, which shows the position of a mineshaft.....	50
Figure 2.3.1.2.2-12 Underground resistivity’s sections at different depths obtained with the CRI. Geometry of a mineshaft detected.....	50
Figure 2.3.1.2.2-13 Aspect of the mineshaft detected with the CRI.....	50
Figure 2.3.1.2.3-1 Age of last working.....	51
Figure 2.3.1.2.3-2 Superficial Conditions.....	51
Figure 2.3.1.2.3-3 Materials chosen for the Immersion Tests.....	52
Figure 2.3.1.2.3-4 pH Values Potable Water.....	53
Figure 2.3.1.2.3-5 pH Values Acidic Mine Water.....	53
Figure 2.3.1.2.3-6 Degradation of Tests Samples.....	54
Figure 2.3.1.2.3-7 Percentage Loss in Weight Long Term Immersion Samples.....	54
Figure 2.3.1.2.3-8 Shaft Treatment, Concrete Reinforcement and Cast Capping.....	55
Figure 2.3.1.2.3-9 Concrete Samples as Cast and Prepared for Immersion.....	56
Figure 2.3.1.2.3-10 Pitting to Surface of Samples.....	56
Figure 2.3.1.2.3-11 Microscopic Examination of Sample Surface.....	56
Figure 2.3.1.2.3-12 Corrosion to Shaft Furnishings.....	57
Figure 2.3.1.2.3-13 Sample Mould.....	57
Figure 2.3.1.2.3-14 Test Sample.....	57
Figure 2.3.1.2.3-15 Samples Post Testing.....	57
Figure 2.3.1.2.3-16 Comparative Strength of 2 mixes.....	57
Figure 2.3.2.1.5-1 Schematic diagram of the system concept for subsidence detection.....	60
Figure 2.3.2.1.6-1 Lens-controller-camera assembly and stereo set-up on the PTU-D47 pan-tilt unit.....	61
Figure 2.3.2.1.9-1 A rectified stereoscopic pair acquired with the twin camera mount.....	62

Figure 2.3.2.1.9-2 Disparity map generated by the program .....	63
Figure 2.3.2.1.9-3 A view of the reconstructed 3D points.....	63
Figure 2.3.2.1.10-1 Outdoor camera assembly.....	63
Figure 2.3.2.1.11-1 Outdoor camera assembly.....	63
Figure 2.3.2.1.12-1 Outdoor camera assembly.....	64
Figure 2.3.2.1.13-1 Initial and final positions of a laboratory test set-up for subsidence monitoring.....	64
Figure 2.3.2.1.13-2 Point grids obtained with the laboratory test set-up for central tile heights for 4, 3, 2, 1 and 0 mm.....	64
Figure 2.3.2.2.3-1 Vertical and horizontal displacements above the longwall No. 10 of 510/2 seam calculated on the base of the static model .....	69
Figure 2.3.2.2.4-1 The chart of Monitoring Centre software, data and information flor .....	70
Figure 2.3.2.2.5-1 A map of the research area with points of constant and periodical measurements .....	71
Figure 2.3.2.2.6-1 Comparative diagram of subsidence recorded at sites of constant observation .....	72
Figure 2.3.2.2.8-1 and 2.3.2.2.8-2 Example of the horizontal Y and vertical H components of displacement vector – changes recorded by GPS at point 4 before and after the bump (3660 s ) on 12.10.2009 11:31 and $E = 9.2 \times 10^4$ [J].....	73
Figure 2.3.2.3.2-1 Imagenex 881 Profiler.....	75
Figure 2.3.2.3.2-2 Actual display and Clarified Image.....	76
Figure 2.3.2.3.2-3 Comparison of Optical Imaging and Profile Scan as Obtained in the Evaluation.....	76
Figure 2.3.2.3.3-1 Shaft Rössing-Barnten.....	77
Figure 2.3.2.3.3-2 Winch installed on truck.....	78
Figure 2.3.2.3.3-3 Profiler prototype.....	78
Figure 2.3.2.3.3-4 Scanner Pointcloud Visualisation (Leica Cyclone Software).....	79
Figure 2.3.2.3.3-5 Unwrapped scan data of shaft lining approx 500 m depth (Amberg TMS Software).....	79
Figure 2.3.2.3.3-6 Horizontal Sections (Amberg TMS Software).....	79
Figure 2.3.3.1-1 GeoMon database architecture. ....	80
Figure 2.3.3.1-2 GeoMon database model and structure. ....	80
Figure 2.3.3.1-3 GeoMon-DB: visualisation of a time series for a levelling line .....	80
Figure 2.3.3.1-4 GeoMon-DB: visualisation of different point information: yellow - line levelling, blue - aerial ground control points, red - projection centres of aerial images, violet - persistent scatterer.....	80
Figure 2.3.3.1-5 Permanent GPS stations “hospital” (left) and “shaft” (mid) with GPS receiver and power supply (right).....	81
Figure 2.3.3.1-6 Corner Reflector no. 2 near levelling line aligned to ENVISAT orbit (left) and static GPS measurement on CR pillar (right). ....	81
Figure 2.3.3.1-7 Radar satellites and their averaged intensity images for ENVISAT-ASAR (left), ALOS PALSAR (mid) and TerraSAR-X (right). ....	81
Figure 2.3.3.1-8 Upper row: ENVISAT-ASAR, mid row: ALOS-PALSAR, lower row: TerraSAR-X. Block left: Differential interferograms (left), orbit related trend (mid) and orbit corrected differential interferogram (right). Block right: Orbit corrected interferogram (left), low frequency phase = atmospherics (mid) and orbit- and atmosphere corrected interferogram (right). ....	82
Figure 2.3.3.1-9 Overview of Digital Elevation Models (DEM) used within the SAR interferometric process for the active and abandoned mining regions. ....	82
Figure 2.3.3.1-10 Gauss-Krueger coordinates, 6th meridian (left) delivered by EMAG, Gauss-Krueger coordinates edited for 2nd meridian’s visualisation in RAG’s ArcGIS (right). ....	82
Figure 2.3.3.1-11 Georeferenced map for the Jas Mos Colliery. Overview (left) and detail (right), measured movement behaviour of selected points 2, 421 and 422 in GeoMon-DB.....	83
Figure 2.3.3.1-12 GeoMon-DB: Visualisation of 3D Laserscanner data for a shaft. ....	83
Figure 2.3.3.1-13 GeoMon-DB: Integrated photogrammetric DEM point data from Aitemin. ....	83
Figure 2.3.3.2.1-1 Hazardous Areas at surface from collapse of shafts .....	84
Figure 2.3.3.2.1-2 Concealed Shaft No Surface Treatment. ....	84
Figure 2.3.3.2.1-3 Old Mine Shaft defined by Tree.....	84
Figure 2.3.3.2.1-4 Depression of Old Mine Shaft .....	84
Figure 2.3.3.2.1-5 Incidents in the U.K. involving Mine Shafts - 10 year average .....	85
Figure 2.3.3.2.2-1 Mining and scale .....	86
Figure 2.3.3.2.2-2 A Mining Intensity of Vibration Scale .....	86
Figure 2.3.3.2.3-1 Illustration of the surface behaviour during the different episodes of longwall coal mine (Lorraine colliery basin). ....	87
Figure 2.3.3.2.3-2 Geomechanical model for the Elche’s Tunnel .....	89
Figure 2.3.3.2.3-3 Vertical displacement after the calculations. ....	90
Figure 2.3.3.2.3-4 Subsidence profile and horizontal displacements distribution calculated and a cross section that includes the building over Elche’s Tunnel. ....	90
Figure 2.3.3.3-1 DInSAR analysis and comparison of ENVISAT-ASAR (blue) and ALOS-PALSAR (green) to levelling line measurements (red). ....	91

Figure 2.3.3.3-2 GeoMon-DB: Movement behaviour of selected PS over known discontinuity (left) and for prolongation of the discontinuity (right).....	91
Figure 2.3.3.3-3 GeoMon-DB: PSI verification for uplift movements at two different locations (magenta levelling of the ordnance survey North Rhine-Westphalia 1996 - 2006, others: selected Persistent Scatterer from ENVISAT ASAR, Dec. 2003 - Dec. 2008).....	91
Figure 2.3.3.3-4 Longitudinal profile of the studied section in the Tunnel of Archidona.....	92
Figure 2.3.3.3-5 Servo-controlled compressive test.....	92
Figure 2.3.3.3-6 3D model.....	93
Figure 2.3.3.3-7 Modelling of the support elements.....	93
Figure 2.3.3.3-8 Ground properties in the stage after the rupture.....	94
Figure 2.3.3.3-9 Distribution of the displacements on the calculated models.....	94
Figure 2.3.3.3-10 Distribution of the plasticized elements after the excavation.....	94
Figure 2.3.3.3-11 Location of the control points on the surface of the modelled area.....	94
Figure 2.3.3.3-12 Evolution of the measured and calculated subsidence in the PC-23 milestone.....	94
Figure 2.3.3.3-13 Evolution of the measured and calculated subsidence in the PC-24 milestone.....	95
Figure 2.3.4.1.1.6-1 Frequency variations in a three-dimensional antenna.....	98
Figure 2.3.4.1.1.6-2 View of a three-dimensional antenna, Step-frequency type and towed by a Vehicle during the works.....	98
Figure 2.3.4.1.1.6-3 Survey results with the GPR-3D.....	99
Figure 2.3.4.1.1.6-4 Tunnel Scanner.....	99
Figure 2.3.4.1.1.6-5 The result of applying the TS-360 to the Tunnel of Abdalajís.....	100
Figure 2.3.4.1.1.6-6 Functional diagram and devices that make up the CRI towed by a vehicle.....	100
Figure 2.3.4.1.1.6-7 Underground resistivity's sections at different depths obtained with the CRI. Geometry of a mineshaft detected.....	100
Figure 2.3.4.1.2.1-1 Photogrammetric cameras in the lab.....	102
Figure 2.3.4.1.3.1-1 Permanent GPS stations "hospital" (left) and "shaft" (mid) with GPS receiver and power supply (right).....	106
Figure 2.3.4.1.3.1-2 Corner Reflector no. 2 near levelling line aligned to ENVISAT orbit (left) and static GPS measurement on CR pillar (right).....	106
Figure 2.3.4.1.3.2-1 GeoMon-DB: Integrated photogrammetric DEM point data from Aitemin.....	107
Figure 2.3.4.1.3.2-2 Hazardous Areas at surface from collapse of shafts.....	108
Figure 2.3.4.1.3.2-3 Incidents in the U.K. involving Mine Shafts - 10 year average.....	108
Figure 2.3.4.1.3.2-4 Surface behaviour at different episodes of the shallow deep coal mine with a particular attention on the effect of goaf swelling.....	108
Figure 2.3.4.1.3.2-5 Subsidence profile and horizontal displacements distribution calculated and a cross section that includes the building over Elche's Tunnel.....	109
Figure 2.3.4.1.3.3-1 Location of the control points on the surface of the modelled area.....	111
Figure 2.3.4.1.3.3-2 Evolution of the measured and calculated subsidence in the PC-23 milestone.....	112
Figure 6.1.3.1-1 Mark II shaft fill sensor showing separate parts and assembled unit.....	128
Figure 6.1.3.1-2 Assembly for investigating very slowly-moving shaft fill.....	129

## List of Tables:

Table 2.3.1.1.2-1 International criteria for working beneath sea and bodies of water (after Allonby, Bicer and Tomlin – 1985 with additions).....	25
Table 2.3.1.1.2-2 Sample of Wistow colliery longwalls (wet and dry).....	25
Table 2.3.1.1.2-3. Disturbance indices for Ellington Brass Thill panels (1980-2004).....	26
Table 2.3.1.1.2-4. Wistow data analysis results –Wilcoxon Mann Witney U tes.....	27
Table 2.3.1.1.2-5 Asfordby water inflow data.....	28
Table 2.3.1.1.2-6 All Data Analysis Results –Wilcoxon Mann Witney U Test.....	29
Table 2.3.1.2.1-1 Summary of Survey Techniques Reviewed.....	38
Table 2.3.1.2.2-1 Resolution of the TS-360.....	47
Table 2.3.1.2.3-1 Example Calculations showing changes in stress due to flooding.....	51
Table 2.3.1.2.3-2 Mechanisms of Degradation.....	55
Table 2.3.1.2.3-3 Increase in Weight Pre / Post Immersion.....	56
Table 2.3.1.2.3-4 Potential Alternative Solutions to Cementitious Grouting.....	58
Table 2.3.2.3.3-1 Table of test parameters.....	78
Table 2.3.3.2.2-1 Damage occurrence depending on the relation of risk value to risk probability.....	86
Table 2.3.3.2.2-2 Relation of vibrations intensity to values of accelerations and effect on surface by MSK- 64 scale.....	86
Table 2.3.3.2.3-1 Classification of visible building damages (Burland et al, 1977).....	88
Table 2.3.3.2.3-2 Relation between damage and maximum tensile strain (Boscarding and Cording, 1989).....	88
Table 2.3.3.2.3-3 Maximus tensile deformation.....	90
Table 2.3.3.3-1 Ground properties in the stage prior to the rupture.....	93

<i>Table 2.3.3.3-2 Comparison between the calculated subsidence and the topographical measure. ....</i>	<i>95</i>
<i>Table 2.3.4.1.1.7-1 Test results of the aggression due to mine water.....</i>	<i>101</i>
<i>Table 2.3.4.1.1.7-2 Potential Alternative Solutions to Cementitious Grouting.....</i>	<i>102</i>
<i>Table 2.3.4.1.2.3-1 Shaft-fill sensor, logging and telemetry; a 'risk' assessment of the field trials. ....</i>	<i>104</i>
<i>Table 2.3.4.1.3.2-1 Damage occurrence depending on the relation of risk value to risk probability.....</i>	<i>110</i>
<i>Table 2.3.4.1.3.2-2Relation of vibrations intensity to values of accelerations and effect on surface by MSK-64 scale. ....</i>	<i>110</i>
<i>Table 2.3.4.2-1 Summary of the techniques employed in this research.....</i>	<i>113</i>

#### 4. **LIST OF REFERENCES**

- Álvarez L., Deriche R., Sánchez J., Weickert J.: “Dense Disparity Map Estimation Respecting Image Discontinuities: A PDE and Scale-Space Based Approach”. Institut National de Recherche en Informatique et en Automatique, Rapport de Recherche n° 3874, Sophia Antipolis, France, 2000.
- Allonby, Bicer and Tomlin: Water Problems Associated with Undersea Mining. Proc. Of 9th Mining Congress of Turkey, Ankara (1985)
- AutoSignal™ Users Guide. USA 2002.
- Bamler, R., Hartl, P.: Synthetic aperture radar interferometry. Inverse Problems 1998
- Bigby DN and Oram JS, “Longwall Working Beneath Water”. Coal International, April 1988, pp26-28.
- Bosy J., Figurski M. and Wielgosz P.: A strategy for GPS data processing in a precise local network during high solar activity. GPS Solutions 2003.
- Boucher C., and Altamimi Z.: Specifications for reference frame fixing in the analysis of EUREF GPS campaign. URL: [large.ensg.ign.fr/EUREF/memo.pdf](http://large.ensg.ign.fr/EUREF/memo.pdf)
- British Coal : Working under the Sea. PI/1969/8. Revised 1971.
- British Coal Internal Report, “Teaching an Old Pit New Tricks”. Undated
- Bromhead, E. N., (1992) The Stability of Slopes, Blackie Academic & Professional, 2 ed., London, UK.
- Bruyelle J.-L., Postaire J.-G.: “Conception et réalisation d'un dispositif de prise de vue stéréoscopique linéaire - Application à la détection d'obstacles à l'avant des véhicules routiers”. Doctoral thesis. Université des Sciences et technologies de Lille, Villeneuve-d'Ascq, France.
- Burie J.C., Bruyelle J.L., Postaire J.G.: “Detecting and localising obstacles in front of a moving vehicle using linear stereo vision”. Mathematical and computer modelling, Volume 22, n° 4-7, pp 235-246, Oxford, United Kingdom, 1992.
- Cattabeni, M., Monti-Guarnieri, A. and Rocca, F., 1994: Estimation and Improvement of Coherence in SAR Interferograms. Proceedings of IGARSS '94, Pasadena, California, 720-722.
- Chekan GJ and Listak JM, “Design Practices for Multiple-Seam Room-and-Pillar Mines”. United States Department of the Interior, Bureau of Mines Information Circular IC9403, 1994.
- Cheney M.: Introduction to Synthetic Aperture Radar. Department of Mathematical Sciences, Rensselaer Polytechnic Institute Troy, NY 12180 USA.
- Cleaver D N, Reddish D J, Shadbolt C H and Dunham R K, Statistical regional calibration of subsidence prediction models, 14th Int. Conf. on Ground Control in Mining,
- Cox I.J., Hingorani S.L., Rao S.B., Maggs B.M.: “A Maximum Likelihood Stereo Algorithm”. Computer Vision and Image Understanding, Volume 63, Issue 3, pp 542-567, New York, United States, 1996.
- Craig R.F., 'Craig's Soil Mechanics', Seventh Edition, Spon Press, ISBN 13: 978-0-415-32703-9, 2008.
- Criminisi A., Blake A., Rother C., Shotton J., Torr P.H.S.: “Efficient Dense Stereo with Occlusion for New View-Synthesis by Four-State Dynamic Programming”. International Journal of Computer Vision, Volume 71, Issue 1, pp 89-110, Hingham, United States, 2007
- Di Stefano L., Marchionni M., Mattoccia S.: “A Fast Area-Based Stereo Matching Algorithm”. Image and Vision Computing (IVC), 22(12), pp 983-1005, 2004.
- Doris InSAR Processor: Delft object-oriented radar interferometric software, developed by the Delft Institute for Earth-Oriented Space Research (DEOS), Delft University of Technology [Online], 2010, Available:(<http://www.geo.tudelft.nl/doris.html>).
- Dowd K.: Beyond Value at Risk. The new science of risk management. Wiley, Chichester

- (1998).
- ECSC Coal RTD Programme – Contract 7220-AC/806: Face and Roadway Stability: Geological Criteria (1981)
  - ECSC Coal RTD Programme – Contract N° 7220-PR-136 : Development of tools for managing the impacts on surface due to changing hydrological regimes surrounding closed underground coal mines.
  - European Coal and Steel Community, “Final Report on Project 7220/PR055, Stress Distribution Analysis By Numerical Models For The Optimisation Of Underground Coal Mine Designs”. 2003.
  - European Commission, “Final Report of Project No RFC-CR03011-GEOMOD”, Research Fund for Coal and Steel. 2007
  - European Space Agency: InSAR Principles: Guidelines for SAR Interferometry Processing and Interpretation. TM-19 February 2007.
  - Ferretti, A., Prati, C., Rocca, F.: Permanent Scatterers in SAR Interferometry. IEEE, Transactions on Geoscience and Remote Sensing, Vol. 39(1) 2001.
  - Föhr R., Ameling W.: “Photogrammetric Registration of Spatial Informations Using Standard CCD Video Cameras”. Proceedings SIFIR '89, International Workshop on Sensorial Integration for Industrial Robots: Architecture and Applications, Zaragoza, Spain, pp 194-199, 1989.
  - Förstner W., Gülch E.: “A Fast Operator for Detection and Precise Location of Distinct Points, Corners and Centres of Circular Features”. Proceedings of Intercommission Conference on Fast Processing of Photogrammetric Data, pp 281-305, Interlaken, Switzerland, 1987.
  - Franceschetti, G., Lanari, R., (1999) Synthetic Aperture Radar Processing, CRS Press, New York, USA, pp.1-284.
  - Freeman T.: What is Imaging Radar. Radar Data Center Jet Propulsion Laboratory Pasadena.
  - Garritty P Effects of Mining on surface and sub surface water bodies PhD thesis University of Newcastle on Tyne Oct 1980.
  - Geiger D., Ladendorf B., Yuille A.: “Occlusions and binocular stereo”. International Journal of Computer Vision, Volume 14, Number 3, pp 211-226, 1992.
  - Global Positioning System, Standard Positioning Service Performance Standard, Department of Defence USA, October 2001.
  - Harris C., Stephens M.: “A Combined Corner and Edge Detector”. Proceedings of The Fourth Alvey Vision Conference, Manchester, United Kingdom, pp 147-151, 1988.
  - Haycocks C, Zhou Y, “Multiple-Seam Mining State-o-the-Art”. 9th International Conference on Ground Control in Mining”. Morgantown 1990. pp1-11.
  - Hefty J.: Estimate of site velocities from GRGRN GPS campaigns referred to GERGOP Reference Frame. Reports on Geodesy 2, 2001.
  - Henkel R.D.: “Fast Stereovision by Coherence Detection”. Lecture Notes In Computer Science, Volume 1296, London, United Kingdom, 1997.
  - Hirschmüller H., Scharstein D.: “Evaluation of Cost Functions for Stereo Matching“. IEEE Conference on Computer Vision and Pattern Recognition, 2007. Minneapolis, United States, 2007
  - Hoek and Brown. “Practical Estimates of Rock Mass Strength”. Int. J. Rock Mech. Min. Sci, 1997.
  - Horn B.K.P.: “Tsai’s Camera Calibration Method Revisited”. Technical Report, Department of Electrical Engineering and Computer Science Massachusetts Institute of Technology, Cambridge, United States, 2000.
  - Hurt, KG and Nightingale K, “Rockbolt Support in Roadways Subject to Interaction from Underlying Workings: G40s District, Easington Colliery”. Presented to Inst. of Min. Eng., 1991
  - Käck P.J. “Robust stereo correspondence using graph cuts”. Master’s Thesis in Computer Science, Numeriks analys och datalogi KHT, Stockholm, Sweden, 2004.
  - Kamphans, K.; Walter, D.; Hannemann, W.; Nickel, S.; Busch, W.; Spreckels, V.; Vosen, P.: Integration klassischer und radarinterferometrischer Daten im GIS-basierten Monitoring bergbaulicher Bodenbewegungen. Lecture from Kay Kamphans on ESRI Conference 2008, Munic, Germany, April 16, 2008.
  - Kamphans, K.; Walter, D.; Hannemann, W.; Busch, W.; Spreckels, V.; Vosen, P.: GIS-Einsatz im Monitoring bergbaubedingter Oberflaechenbewegungen. In: Angewandte Geoinformatik

2008. Beitrage zum 20. AGIT-Symposium Salzburg, Austria, June 02-04, 2008 . Hrsg.: J. Strobl, Th. Blaschke, G. Griesebner. H. Wichmann Verlag, Heidelberg. pp. 572 – 577.
- Kanade T., Okutomi M.: “A Stereo Matching Algorithm with Adaptive Window: Theory and Experiment”. Proceedings of the IEEE International Conference on Robotics and Automation, Sacramento, United States, 1991.
  - Kangni F., Laganière R.: “Rectification and Pose Recovery for Spherical Images”, Chapter 2, “Epipolar Geometry and Projective Image Rectification”. Thesis in Electrical and Computer Engineering, School of Information Technology and Engineering, Ottawa, Canada, 2007.
  - Kolmogorov, V. Zabih, R. “Computing visual correspondence with occlusions using graph cuts”. Computer Science Department, Cornell University, Ithaca, United States, 2001.
  - Kraus K.: “Photogrammetry. Geometry from Images and Laser Scans”. Second edition, Walter de Gruyter GmbH & Co, Berlin, Germany, 2004.
  - Kurczynski Z.: Obrazowanie mikrofalowe i interferometria radarowa – InSAR. Warszawa 2006.
  - Lamparski J. : GPS w geodezji. Katowice 2003
  - Lee, K. M. & Rowe, R. K. (1989). Deformations caused by surface loading and tunnelling: the role of elastic anisotropy. *Geotechnique*, 39, No. 1, 125-140
  - Lee K.-M., Street W.N.: “Model-based detection, segmentation, and classification for image analysis using on-line shape learning”. *Machine Vision and Applications*, Volume 13, Issue 4, pp 222-233, 2003.
  - Lim S.-N., Mittal A., Davis L.S., Paragios N.: “Uncalibrated Stereo Rectification for Automatic 3d Surveillance”. *International Conference on Image Processing*, BVOLUME 2, pp 1357-1360, 2004
  - Linder W.: “Digital Photogrammetry. A Practical Course”. Second edition, Springer Verlag, Berlin, Germany, 2003.
  - Lloyd, P.W., Mohammed, N. & Reddish, D. J. (1997). Surface subsidence prediction techniques for UK coalfields – an innovative numerical modelling approach. 15th Mining Congress of Turkey, Guyuguler, Ersayin, Bilgen(eds), 111-124
  - Luhmann T., Robson S., Kyle S., Harley I.: “Close Range Photogrammetry: Principles, Methods and Applications”. Whittles Publishing, Dunbeath, United Kingdom, 2006.
  - Mair, R. J., Gun, M. J. & O’Reilly, M. P. (1981). Ground movements around shallow tunnels in soft clay. *Proc. 10th Conf. Soil Mech.*, Stockholm, 323-328
  - Marchand É, Chaumette F.: “A New Formulation for Non-Linear Camera Calibration Using Virtual Visual Servoing”. *Institut National de Recherche en Informatique et en Automatique, Rapport de recherche n° 4096*, Rennes, France, 2001.
  - Massonnet D.: *Satellite Radar Interferometry*. Scientific American No 2, 199
  - Mikhail E.M., Bethel J.S., McGlone J.C.: “Introduction to Modern Photogrammetry”, John Wiley & Sons, Inc, New York, United States, 2001
  - National Coal Board: *Subsidence Engineers’ Handbook*. NCB Mining Department, 1966.
  - National Coal Board: *Subsidence Engineers’ Handbook*. NCB Mining Department, Revised 1972.
  - National Coal Board Mining Department Working Party, “Design of Mine Layouts (with reference to geological and geometrical factors)”. 1972.
  - National Coal Board, “Procedures in Coal Mining Geology”. NCB Mining Department, 1984.
  - National Coal Board. “Face and Roadway Stability in Underground Coal Mines: Geotechnical Criteria”. Final Report under European Coal and Steel Community Research Contact 7220-AC806. 1981.
  - Niemczyk, O: “Bergchadenkunde”. Glückauf. Essen 1949
  - Papoulis A.: *Prawdopodobieństwo, zmienne losowe i procesy stochastyczne*. Wydawnictwa Naukowo-Techniczne, Warszawa 1972 r.
  - Parkinson B. and Spilker j. j.: *Global Positioning System: Theory and Applications*. American Institute of Aeronautics and Astronautics, Washington 1996.
  - Penati A, Pennacchi G.: *Extending Diffusion Processes to Allow for Jumps* (2001).
  - Peduzzi P, Concato J, Kemper E, Holford TR, Feinstein AR (1996) A simulation study of the number of events per variable in logistic regression analysis. *Journal of Clinical Epidemiology* 49:1373-1379.
  - Perski, Z., Chybiorz, R., Nita, J., 2001. Monitoring osiadań terenu pod wpływem eksploatacji

- gorniczej metodą satelitarnej interferometrii radarowej. *Archiwum Fotogrametrii i Teledetekcji*, 2001, Vol. 11, s. 35-40.
- Pilu M., Lorusso A.: “Uncalibrated Stereo Correspondence by Singular Value Decomposition”. Hewlett-Packard Research Laboratories, Bristol, United Kingdom, 1997.
  - Piwowarski W.: Model prognozy niestacjonarnego procesu odniesiony do opisu przemieszczeń pogórnicznych identyfikowany pomiarami geodezyjnymi. PIGiK Warszawa , 1999
  - Piwowarski W.: O ryzyku wystąpienia szkody górnicznej. VII Dni Miernictwa Górniczego i Ochrony Terenów Górniczych, Główny Instytut Górnictwa 2005 r .
  - Pratti C., Rocca F., Monti Guarnieri A. Pasquali P., 1994: Report on ERS-1 SAR interferometric techniques and applications. ESA report 10179/93/YT/I/SC 1-122. Frascati.
  - Price K.E.: “Hierarchical Matching Using Relaxation“. *Computer Vision, Graphics, and Image Processing*, Volume 34, pp 66-75, 1986.
  - Puget P., Skordas T.: “An Optimal Solution for Mobile Camera Calibration“. *Proceedings of the First European Conference on Computer Vision*, Antibes, France, pp. 187 – 198, 1990.
  - Shadbolt, C.H., A study of the effects of geology on mining subsidence in the East Pennine coalfield, PhD, University of Nottingham, 1987
  - Scharstein D., Szeliski R.: “A Taxonomy and Evaluation of Dense Two-Frame Stereo Correspondence Algorithms“. *International Journal of Computer Vision*, Volume 47, Issue 1-3, pp. 7 – 42, 2002.
  - Schenk T.: “Fotogrametria Digital. Volumen 1“. Marcombo, S.A. and Institut Geografic de Catalunya, Barcelona, Spain, 2002.
  - Schüler t.: On ground-based GPS tropospheric delay estimation. Institute of Geodesy and Navigation. University FAF Munich Germany 2001.
  - Shinagawa Y.: “Unconstrained Automatic Image Matching Using Multiresolutional Critical-Point Filters“. *IEEE Transactions on Pattern Analysis and Machine Intelligence*, Volume 20, Issue 9, pp. 994 – 1010, 1998
  - Spreckels, V.; Musiedlak, J.: Linie oder Punkt zu Flaeche? Messkonzepte bei der Ueberwachung des Grubenwasseranstiegs am Beispiel des ehemaligen BW Westfalen. In: Schriftenreihe des Institutes fuer Markscheidewesen und Geodaesie an der Technischen Universitaet Bergakademie Freiberg, Heft 2008-1. 9. Geokinematischer Tag, May 8-9, 2008, Freiberg, Germany, pp. 251-264.
  - Spreckels, V.; Walter, D.; Wegmueller, U.; Deutschmann, J.; Busch, W.: Nutzung der Radarinterferometrie im Steinkohlenbergbau. In: *Allgemeine Vermessungs-Nachrichten*, AVN 7/2008, Wichmann Verlag, Heidelberg, Germany, ISSN 0002-5968, pp. 253 - 261.
  - Spreckels, V.; Musiedlak, J.: Messkonzept zur Überwachung der Tagesoberfläche mittels hochpräziser Satellitengeodäsie und Radarinterferometrie. In: Schriftenreihe des Institutes fuer Markscheidewesen und Geodaesie an der Technischen Universitaet Bergakademie Freiberg, Heft 2010-1. 11. Geokinematischer Tag, 6.-7. Mai 2010, Freiberg, S. 259-271.
  - Swanson R A, EF Holton, E Holton 2005 *Research in Organisations: foundations and methods of enquiry* chapter 8 multivariate research methods Bk Berrett-Koehler Publishers, Inc. San Francisco.
  - Thin GT, Pine RJ and Trueman R., “Numerical Modelling as an Aid to the Determination of the Stress Distribution in the Goaf Due to Longwall Coal Mining“. *Int. J. Rock Mech Min. Sci.*, vol.30, no.7, pp.1403-1409, 1993.
  - Tsai R.: “An Efficient and Accurate Camera Calibration Technique for 3D Machine
  - Tubby, JE and Farmer IW, “Stability of Undersea Workings at Lynemouth and Ellington Collieries“. *The Mining Engineer*, August 1981, pp87-96
  - Usai, S. and Hanssen, R., 1997, Long time scale InSAR by means of high coherence features. *Proceedings of the Third ERS Symposium*, Florence, Italy - <http://florence97.ers-symposium.org/data/usai/index.html> .
  - Vasile G., Trouve E., Ciuc M, and Buzuloiu V.: General adaptive neighbourhood technique for improving SAR interferometric coherence and phase estimation. *J. Opt. Soc. Am.* 1455, 2004
  - Walter, D.; Kamphans, K.; Busch, W.; Spreckels, V.: Einsatz der Radarinterferometrie im Rahmen eines GIS-basierten Montoringssystems zur Analyse bergbaulicher Bodenbewegungen. In: Schriftenreihe des Institutes fuer Markscheidewesen und Geodaesie an der Technischen Universitaet Bergakademie Freiberg, Heft 2008-1. 9. Geokinematischer Tag, May 8-9, 2008, Freiberg, pp. 75-90

- Walter, D.; Wegmueller, U.; Spreckels, V.; Busch, W. (2008): Application and evaluation of ALOS PALSAR data for monitoring of mining induced surface deformations using interferometric techniques. In: Proceedings of ALOS PI Symposium 2008. Rhodes, Nov. 03-07, 2008, ESA SP-664 (CD-ROM). ESA Publications Division, European Space Agency, Noordwijk, The Netherlands.
- Walter, D.; Wegmüller, U.; Spreckels, V.; Hannemann, W.; Busch, W.: Interferometric monitoring of an active underground mining field with high-resolution SAR sensors. In: ISPRS Hannover Workshop 2009, WG I/2, I/4, IV/2, IV/3, VII/2, Hannover, Germany, June 2 - 5, 2009.
- Wegmueller, U.; Walter, D.; Spreckels, V.; Werner, C.: Evaluation of TerraSAR-X DINSAR and IPTA© for ground-motion monitoring. In: Proceedings of 3rd TerraSAR-X Science Team Meeting, Nov. 25-26, 2008, DLR, Oberpfaffenhofen, Germany.
- Wegmueller, U.; Walter, D.; Spreckels, V.; Werner, C.: Nonuniform Ground Motion Monitoring With TerraSAR-X Persistent Scatterer Interferometry. In: IEEE Transactions on Geoscience and Remote Sensing, Vol. 48., No. 2, 2010, pp. 895 - 904
- Wu B., Yeung M., Hara Y. and., Kong J. A. InSAR height inversion by using 3-d phase projection with multiple baselines. Progress In Electromagnetics Research, 2009
- Xu G.: GPS theory, algorithms and applications. Springer-Verlag, Berlin 2003.
- Yillasenor J., Zebker H. 1992: Temporal decorrelation in repeat-pass radar interferometry. Proceedings of IGARSS '92.
- Zabih R., Woodfill J.: "Non-parametric Local Transforms for Computing Visual Correspondence". Proceedings of European Conference on Computer Vision, Stockholm, Sweden, pp.151-158, 1994,
- Zitnick C.L., Kanade T.: "A Cooperative Algorithm for Stereo Matching and Occlusion Detection". IEEE Transactions on Pattern Analysis and Machine Intelligence, Volume 22, Issue 7, Washington, United States, 2000.

## 5. GLOSSARY

### 5.1. ABBREVIATIONS

Abbrev	Description
2D	Two dimensional
2000 GK 6	Polish Gauß-Krüger coordinate system, 6 <sup>th</sup> meridian strip
3D	Three dimensional
ArcGIS	A suite consisting of a group of geographic information system (GIS) software products produced by ESRI.
ASAR	Advanced Synthetic Aperture Radar
BLH	Geographic coordinates (latitude, longitude, ellipsoidal height)
BLOB	Binary Large Object
DXF	AutoCAD Drawing Interchange Format (ASCII), by Autodesk.
DWG	AutoCAD Drawing Format (binary), by Autodesk.
ENVISAT	Environmental Satellite, European Space Agency (ESA)
FLAC	Fast Lagrangian Analysis of Continua
Flac	Mining Software by Itasca Consulting Group Inc.
GeoMon-DB	RAG's Geometric Monitoring Point Database
GRP	Glass reinforced plastic
GSI	Geological strength index
H1	Hypothesis 1
H2	Hypothesis 2
IPTA	Interferometric Point Target Analysis (©Gamma Remote Sensing)
KT	A type of fully threaded rockbolt used in the UK
l/s	litres per second
L/G	Left hand gate
m	metres
mm	millimetres
MPa	Mega Pascals
PS	Persistent Scatterer
PSI	Persistent Scatterer Interferometry
R/G	Right hand gate
RFCS	Research Fund for Coal and Steel
SEH	Subsidence Engineers Handbook
SFS	Shaft Stability Sensor
SG-ROW	Local coordinate system used in Polish mines
SHE	Short Elliott Hendrickson Inc. - Consulting Firm, inter alia Mining Services

### 5.2. SYMBOLS USED IN EQUATIONS

Symbol	Meaning	Dimensions
$c$	Kinematic model parameter representing the speed of the point's subsidence	[1/year]
$d$	most likely aggregate tensile strain (derived from SEH)	
$E_k$	Energy of the $k^{\text{th}}$ bump	[J]
$E_0$	Reference energy	[J]
$h$	distance to overlying water source (or surface)	metres
$k$	the minimum sample number	
$m$	extraction height	metres
$N$	the number of covariates (the number of independent variables)	
$p$	the smallest of the proportions of negative or positive cases in the population	
$R$	rank sum of data	
$R$	Curvature radius	km
$T$	inclination	mm/m
$Tensstr$	Tensile strain	mm/m
$S$	maximum subsidence	metres
$w$	longwall panel width	metres
$Z$	significance indicator	

Symbol	Meaning	Dimensions
$\mu$	mean	
$\sigma^2$	variance	
$\bar{U}$	vector of rock mass displacement	m
$\{u, v\}$	horizontal components of the $\bar{U}$ vector at (X,Y) plane	m
$w$	vertical component of the $\bar{U}$ vector	m
$d\bar{U}$	The vector field displacement function growth	m
$\varepsilon$	horizontal deformation	mm/m
$\varepsilon_{dop}[x_i]$	allowable resistance on deformation of $x_i$ object	mm/m
$\varepsilon[\omega_i]$	value of surface deformation at sub area $\omega_i$ - zone of the object location	mm/m
$\sigma$	Electrical conductivity	S m <sup>-1</sup>
$\Delta\theta$	Circumferential Stress	MN/m <sup>2</sup>
$\Delta r$	Radial Stress	MN/m <sup>2</sup>
$w(x, y)$	Subsidence at a point of x, y co-ordinates	[mm]
$r$	The radius of the zone of mining influence on surface	[m]
$W_{max}$	The maximum value of surface subsidence	[mm]
$W(t)$	Trajectory of the point's subsidence	[m]
$W^k$	Asymptotic value of the point's subsidence after the assumed k <sup>th</sup> period of mining	[mm]

## 6. APPENDICES

### 6.1. MONITORING AND CONTROL OF SUBSIDENCE EFFECTS ON SURFACE.WP2

#### 6.1.1. Geometrical monitoring tools

Due to the extension of this appendix and the limited extension of the final report, an independent document called “Analysis of satellite radar images of the mining area monitored in task 2.2” has been completed.

#### 6.1.2. Seismicity monitoring tools

Due to the extension of this appendix and the limited extension of the final report, an independent document called “The work accomplished in task 2.2” has been completed.

#### 6.1.3. Field trials of shaft fill stability sensor

This appendix gives further details of the results of the field trials that were carried out for the shaft fill stability sensor in task 2.3.

##### 6.1.3.1. Sensor re-design work

It had already been established, earlier in the project, that to achieve the lowest power consumption it would be preferable to replace the originally-envisaged Hall-effect sensors by magnetic reed switches. However it was soon realised, during tests, that the contact bounce time of reed switches was not conducive to operation above a few tens of hertz. A second problem was that the frictional retarding device proved to be difficult to set up correctly. It was also observed that the initial prototype, which had been designed specifically with long-term environmental and biological protection in mind, was time-consuming to manufacture where evaluation of multiple prototypes was envisaged.

As a result of the initial trials and for the reasons given above, it was decided to re-design the sensor specifically to make a cheaper version that could be used with early trials of the data logger. The mark II prototype would specifically not be environmentally or biologically protected, but would address the problems of reed bounce and frictional retardation of the spool (Figure 6.1.3.1-1)

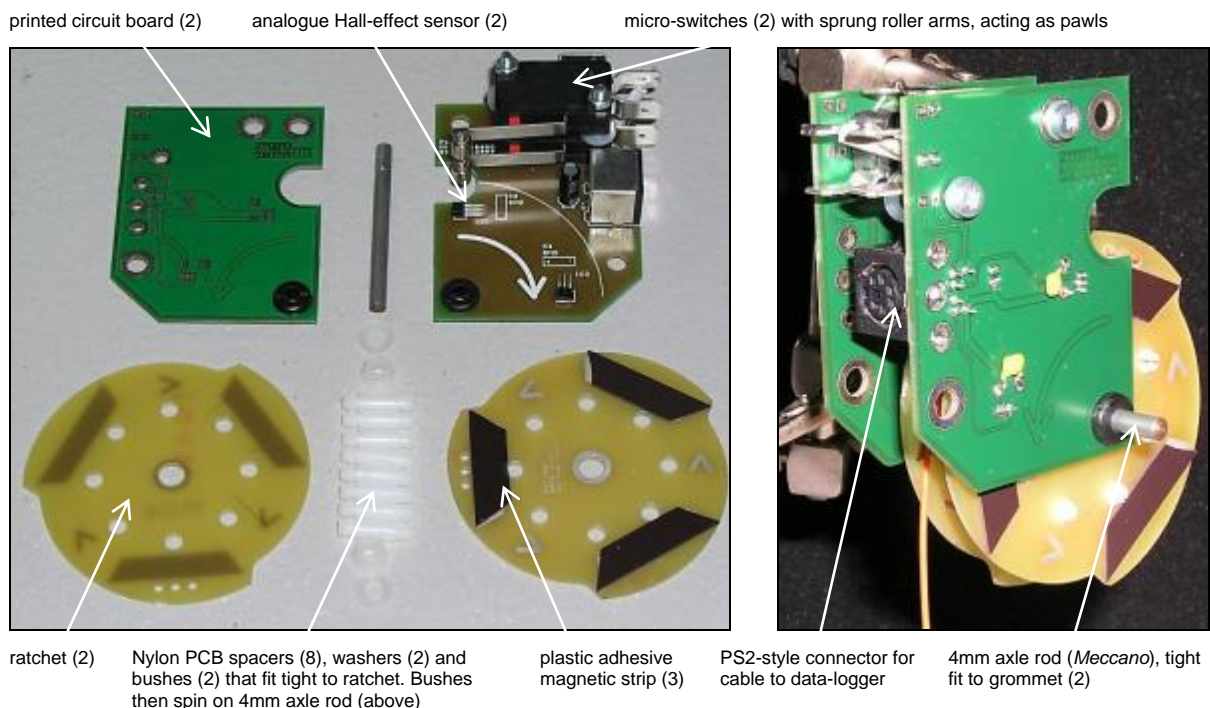


*Figure 6.1.3.1-1 : Mark II shaft fill sensor showing separate parts and assembled unit*

A novel feature of the new design was that it used a combination of Hall sensors and mechanical switches to address the twin problems of contact bounce and polling current. It also differed from the mark I in that the Hall sensors were analogue devices, calibrated in software, because this allowed more latitude over the choice of magnets. Thus, the mark II used a cheap plastic magnetic sheet, cut to size, rather than a high-performance magnet of specific dimensions, as was used in the mark I prototype. A second feature of the new design was that it used a pawl and ratchet to achieve retardation of the spinning spool, because this allowed a more controllable retarding force. A further novel feature was that the pawl arms (two are required for quadrature detection) were the sprung contacts of two micro-switches, with the switches providing the signal to energise the sensing microprocessor. The assembly was constructed from a four-PCB sandwich, held together with plastic clips and comprised cheap, easily assembled parts that would allow several prototypes to easily be constructed. It is shown in the (Figure 6.1.3.1-2). Because the device worked on different principles to the original prototype it helped to provide valuable experimental results to aid the production of the environmental version.



*Figure 6.1.3.1-2 : Assembly for investigating very slowly-moving shaft fill*

### **6.1.3.2. Further Details of System Elements**

These sections expand on the outline given in the main text.

#### **6.1.3.2.1. Data Logger**

Initial trials concentrated on verifying the software framework for the logger. Of primary importance was the concept of an activity logger. For ease of debugging, it was considered useful to be able to view the GPRS modem's responses to commands and to inspect the data received from the web server; in addition to accessing the logged parameters of shaft-fill stability, temperature and so on. However, an early field deployment made such a task difficult, as the remote data logger needed to be considered as inaccessible – the only communication being via the web server. A scheme was therefore developed to address this difficulty, for which the key element was an activity log file within the data logger, which was uploaded to the web server periodically. A further important aspect of the operation was for the web server to be able to send a revised program to the logger and to have it re-boot into the new code. This was intended to allow field trials to continue despite what could have been extensive revisions to the operation of the logger, without the need for an engineer to visit the remote site.

#### **6.1.3.2.2. Telemetry transmitter**

Software development was undertaken prior to an integrated field trial and concentrated mainly on the testing of the communications protocols. Because the equipment under development required such low-power operation it was necessary to design it using OEM (original equipment manufacturer) modules (e.g. a GPRS modem) and this required an understanding of low-level communications protocols. These are specified in documents that are available from ETSI at [portal.etsi.org/Docbox/Catalog/The\\_ETSI\\_Standards\\_Catalogue.html](http://portal.etsi.org/Docbox/Catalog/The_ETSI_Standards_Catalogue.html). In particular these include those listed below.

- **ETSI TS 100 901** V7.4.0 (1999-12). *Technical Specification: Digital cellular telecommunications system (Phase 2+); Technical realization of the Short Message Service. (GSM 03.40 version 7.4.0 Release 1998)*

- **ETSI TS 100 900 V7.2.0 (1999-07). *Technical Specification: Digital cellular telecommunications system (Phase 2+); Alphabets and language-specific information. (GSM 03.38 version 7.2.0 Release 1998).*** (The title of this document is misleading – it is useful primarily because it contains a helpful summary of the ‘SMS Data Coding Scheme’ and the ‘Cell Broadcast Data Coding Scheme’)

#### **6.1.3.2.3. Web server**

Operation of the web server was initially simulated using synthesised data. Programs running on one web server simulated the operation of the remote data-logger by sending daily HTTP requests containing small amounts of data to a second web server which stored these in a database. The issues of scalability are discussed below, under ‘network capability’.

It was originally envisaged that the data would be stored in a relational database such as MySQL, which is a popular ‘structured query language’ (SQL) database, available under a GNU General Public License. (MySQL is named after the original developer’s daughter, My). Such a database would be useful when the data is collected from perhaps thousands of sensors over a prolonged period of time. However, during the initial system development there was no advantage to using MySQL and so, instead, the database was managed initially as a simple text file and then as a simple key/value-pair database using the Berkeley-style Database Abstraction Layer (DBA) class in PHP, available at [pear.php.net/package/DBA](http://pear.php.net/package/DBA). From such a database, the data could easily be made accessible by a number of display routines. Initially, these were based on those that were originally developed as part of the RFCS RAINOW project.

The concept of uploading the logger data and then separately parsing it and translating it into the form required for the database may, at first sight, appear to be cumbersome. However, this process was arrived at after consideration of several possible schemes, because it breaks the project down into modules that could be developed separately.

#### **6.1.3.2.4. Battery Life**

It had been estimated, during the design stage, that the mean current consumption of the Hall-effect sensors and sensing electronics would be 10 mA. This, together with a computing cycle of 100  $\mu$ s and a polling frequency of 16 Hz (as required by the shaft-fill sensor), would result in a mean battery current of 140 mAh/year. It had also been estimated that the GPRS transmitter might require 100 mA for 1 minute per day, i.e. 600 mAh/year. However, the originally-envisaged polled Hall-effect sensor was replaced, during the development process, by a magnetic reed switch controlling an interrupt input of a microprocessor. In this way, almost the entire 140 mAh/year of this part of the circuit could be saved.

In practical experiments, the reed switch sensor was replaced by a small timer (driven by an independent battery) that woke the microprocessor every hour. The temperature data was logged and transmitted by GPRS. Instead of the long-life lithium-iron-disulphide (LiFeS<sub>2</sub>) batteries that had been proposed for the field unit, rechargeable low self-discharge, ‘hybrid’ NiMH cells were used, with a quoted capacity of 2.1 Ah. With 24 data transmissions per day, the mean current consumption should therefore have been around 14.4 Ah/year, and the NiMH cells were predicted to last for around eight weeks.

The experiments undertaken indicated a slightly lower lifetime of around six weeks, but it was difficult to establish whether this was due to the batteries having a lower capacity than stated, or the mean current of the GPRS module being higher, or the transmission time being longer than predicted. One of the obstacles was that, due to the protocol negotiations within the GPRS module, its current consumption can fluctuate; and it is certainly possible that acquiring network access may be a lengthier process at certain times of day. Amongst software revisions being considered for future development is therefore an ability for the logger to report the duration of each transmission.

Despite the above problems, it is possible to draw the conclusion given in the main text, namely that the current consumption of the logger, reporting its status once every two days, would be around 400 mAh/year, so a ‘twin’ set of LiFeS<sub>2</sub> cells should last for 15 years, which is their recommended lifetime. It should be noted that, because the cells are small and cheap, there is really no practical limit

to the number of sets that can be used as a power source if a more frequent data transmission is required. (In the event of an incident, data transmission is immediate, of course). 400 mAh/year at 12 V is only 500 mW so a relatively small (say 5 W; 300 mm square) solar panel might suffice but – as noted earlier in the project – the use of even a small solar panel considerably increases the manufacturing and installation costs.



European Commission

**EUR 25097 — Prediction and monitoring of subsidence hazards above coal mines  
(Presidence)**

*C. Herrero, A. Muñoz, J. C. Catalina, F. Hadj-Hassen, R. Kuchenbecker, V. Spreckels, J. Juzwa,  
S. Bennett, M. Purvis, D. Bigby, D. Moore*

Luxembourg: Publications Office of the European Union

2012 — 131 pp. — 21 × 29.7 cm

Research Fund for Coal and Steel series

ISBN 978-92-79-22246-7

doi:10.2777/3356

ISSN 1831-9424



## HOW TO OBTAIN EU PUBLICATIONS

### **Free publications:**

- via EU Bookshop (<http://bookshop.europa.eu>);
- at the European Union's representations or delegations. You can obtain their contact details on the Internet (<http://ec.europa.eu>) or by sending a fax to +352 2929-42758.

### **Priced publications:**

- via EU Bookshop (<http://bookshop.europa.eu>).

### **Priced subscriptions (e.g. annual series of the *Official Journal of the European Union* and reports of cases before the Court of Justice of the European Union):**

- via one of the sales agents of the Publications Office of the European Union ([http://publications.europa.eu/others/agents/index\\_en.htm](http://publications.europa.eu/others/agents/index_en.htm)).

Mining subsidence engineering is one of the most important topics in relation to coal mining. Although its occurrence, prediction and control are well known, this project will apply various innovative techniques to an old problem (photogrammetry, InSAR, GPS, seismic tools, SFS).

Geology is a major factor in surface subsidence. Empirical predictions are inaccurate where experience is lacking and geology unusual. Geomechanical subsidence modelling can account for geology but requires anisotropic solutions to reproduce subsidence profiles. Four items have been developed in relation to the prediction of subsidence caused by underground infrastructures: two in relation to shafts (telemetry and instrumentation for fill stability, and the laser-scanner techniques for surveys); another in relation to a survey methodology using numerical modelling for infrastructure roadway, and the last one in relation to the effect of mine water on concrete and other materials.

A 4D database, called GeoMond-DB has been developed to manage subsidence hazards on the surface, working with data from Germany, Poland and Spain. A methodology based on geomechanical models to establish a prevision of surface and subsidence was carried out and validated. Specially, the consistency of FLAC 3D was checked to evaluate subsidence and the tensile strain on the surface.

In conclusion, the techniques employed in this research represent a significant advance on the current situation in forecasting and control of subsidence. Therefore, although some of the investigated techniques must still be refined, it can be said that the results of this research project will have a positive effect in the monitoring of the subsidence in the coal basins of the EU and some outcomes, such as the technique of monitoring the movements of the ground with a GPS and vibrating sensors, could be exported outside the EU.